Reduced Graphene Oxide-Nanocellulose composite development for supercapacitor application

Master's Thesis

Yu Zou

Supervisors:

Dr. Lokesh Kesavan,
Prof. Carita Kvarnström

Materials Chemistry Research Group
Department of Chemistry

Contents

ACKNOWLEDGEMENT 4
1. ABSTRACT 5
2. INTRODUCTION 6
2.1. Graphene Oxide (GO) 6
2.2. Reduced Graphene Oxide (rGO) 7
2.3. Cellulose Nanofibers (CNF) 8
2.4. rGO-CNF composite in literature 9
2.5. Supercapacitor 9
2.6. The objective 11
2.7. Electrochemistry 11
2.8. Ultraviolet light (UV) 12
2.9. Cyclic Voltammetry (CV) 13
3. EXPERIMENTAL SECTION 14
3.1. Materials 14
3.2. Preparation of cellulose nanofibers 14
3.3. Preparation of rGO 14
Reduction by $NaBH_4$ 14
Open air system reduction (Beaker) 15
Closed system reduction (Rotavapor - RB flask) 16
3.4. Sonochemical synthesis of rGO: CNF composites 18
Preparation of rGO: CNF 90:10 composite 19
Preparation of rGO: CNF 70:30 composite 19
Preparation of rGO: CNF 50:50 composite 19
Preparation of rGO: CNF 30:70 composite 19
Preparation of rGO: CNF 10:90 composite 19
Preparation of rGO: CNF film (for freestanding electrode) 20
3.5. Materials characterization 21
UV-visible spectroscopy analyses 21
4-probe conductance tests 21
3.6. Electrochemistry measurements 22
Cyclic voltammetric (CV) tests of bare graphite sheets 22
Cyclic voltammetric (CV) tests of rGO: CNF-coated graphite sheets 23

Galvanostatic Charging-Discharging tests for rGO**s** & rGO: CNF modified graphite sheets 24
Problem solving 25
4. RESULTS AND DISCUSSION 26
4.1 UV-Vis spectroscopic identification of rGO 26
4.2 Electrochemical performance of plain rGOs & rGO: CNF composites (CV, GCD) 29
5. CONCLUSION AND PROSPECTS 39
APPENDIX 40
REFERENCES 77

ACKNOWLEDGEMENT

Herein I greatly thank Dr. Lokesh Kesavan and Prof. Carita Kvarnström for supervising me in my whole project and especially Dr. Lokesh during my difficult periods. I also appreciate the help from Sachin Kochrekar and Roni Hentula, who have made this project go smoothly. Besides, all the people in the laboratory helped me to find the chemicals and supported the daily operations.

1. ABSTRACT

The energy problem requires new technologies that move away from non-renewable fossil energy sources. Because of these needs, new energy storage technologies should also be improved. New technologies should not only eliminate fossil energy sources but also utilize solar, wind, or wave energy. Therefore, supercapacitors are a good tool for energy storage. Reduced graphene oxide (rGO) is one of the best ideal materials for supercapacitors. On the other hand, cellulose, the most abundant natural polymer, also needs attention for its effective utilization and value addition by material chemists. Cellulose nanofibers (CNF) can be composed with rGO to make thin films with huge bulk capacitance. CNF can improve the mechanical properties and facilitate the formation of rGO-based thin films as it helps to securely fix the rGO particles without losing their electrical conductivity. The results show that the quality of the films depends not only on the ratio of rGO to cellulose but also on the quality of the rGO formed during the reduction. The mechanistic properties of the film were significantly enhanced when cellulose was mixed with rGO dispersions. The basis of this study was to find the periods for good reduction of GO (30 min, 1 h, 2 h, 3 h, and 6 h, respectively) and to test the electrical conductivity of rGO, rGO: CNF composites at different ratios.

2. INTRODUCTION

2.1. Graphene Oxide (GO)

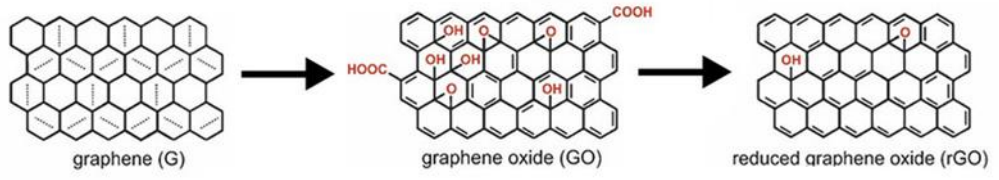

Figure.1. Structure of GO & rGO

Graphene oxide (GO) has emerged as a revolutionary material for the new century, with countless applications ranging from electronics to energy storage. This two-dimensional carbon-based material derived from graphene has unique properties that make it an ideal candidate for various technological advances. One of the most promising applications of graphene oxide is in the field of supercapacitors because of its excellent properties that help enhance energy storage capacity. Special attention is paid to its role in advancing supercapacitor technology in current research. Graphene oxide is essentially a graphene derivative with a single layer of carbon atoms arranged in a hexagonal lattice (Fig. 1) [1]. Graphene oxide is formed by introducing oxygen-containing functional groups, such as epoxides, hydroxyl, and carboxyl groups, into the graphene structure.

Graphene oxide is highly functionalized due to the presence of oxygen-containing groups. This functionalization gives graphene oxide a hydrophilic nature, allowing it to dissolve better in aqueous solutions. Like graphene, graphene oxide has a very high surface area. This property is critical for its use in supercapacitors, as it provides a large contact area for the electrolyte ions, facilitating a fast charging and discharging process. Although the introduction of oxygen functional groups reduces the conductivity, graphene oxide still maintains a reasonable level of conductivity. This conductivity promotes efficient electron transfer within the supercapacitor electrodes, reducing internal resistance and improving overall performance. Graphene oxide possesses good mechanical strength. This property contributes to the structural integrity of supercapacitor devices. Graphene oxide has good electrochemical stability, ensuring the long-term performance and durability of supercapacitor devices [2].

Graphene oxide has become a key material for advancing supercapacitor technology. While the integration of graphene oxide in supercapacitors has shown promising results, there are still challenges and areas for improvement. Although graphene oxide has fairly high electrical

conductivity, further efforts are needed to enhance its conductivity. Strategies such as additional reduction processes or hybridization with other conductive materials could be explored to improve overall performance. The scalability and cost-effectiveness of graphene oxide in the production of large-scale supercapacitor applications remain important considerations. Research into scalable production methods and cost reductions are critical for the widespread adoption of graphene-based supercapacitors. Ensuring the long-term stability and durability of graphene oxide-based supercapacitors is crucial for practical applications. Research should continue to address factors such as electrode degradation and electrolyte compatibility to extend the lifetime of these energy storage devices. Tailoring the properties of graphene oxide for specific supercapacitor applications is an area of ongoing research. Fine-tuning the pore structure, functionalization and composite formulations will enable GO-based supercapacitors to meet different technical requirements.

2.2. Reduced Graphene Oxide (rGO)

Reduced graphene oxide (rGO), a two-dimensional nanomaterial derived from graphene oxide, has emerged as a promising material for revolutionizing supercapacitor (SC) technology due to its excellent performance and versatile characteristics. Reduced graphene oxide is usually derived from graphene oxide (GO) by a reduction process. Graphene oxide is obtained from the oxidation of natural graphite to give materials containing oxygen-containing functional groups such as epoxides, hydroxyl, and carboxyl groups. Reduction of graphene oxide involves the removal or reduction of these oxygen functional groups, leading to the formation of graphene oxide. Common reduction methods include chemical reduction using hydrazine or hydrothermal reduction. $NaBH_4$ reduction has also been used for the synthesis of reduced graphene oxide-silver nanocomposites for photocatalytic degradation of Pb ions in aqueous solutions. In addition, $NaBH_4$ has been used as a reducing agent for the preparation of trimetallic alloy catalysts on n-doped reduced graphene oxide (NrGO) for direct ethanol fuel cell (DEFC) anodes. $NaBH_4$ was also used as a reducing agent for the preparation of reduced graphene oxide (rGO) using environmentally friendly banana extract.

Compared to conventional energy storage systems, rGO-based energy storage systems have superior energy and power densities and are well suited for applications requiring rapid energy bursts or high-power output. While the production of reduced graphene oxide has shown promising results on a laboratory scale, scalability remains a challenge. The development of cost-effective and scalable synthesis methods is essential for the widespread commercial

application of rGO-based supercapacitors. Although rGO-based supercapacitors offer high power density, efforts are still underway to increase their energy density. Strategies include combining other advanced materials, and hybrid structures, and optimizing electrode design to strike a balance between power and energy density. Among these, the environmental impact of the reduced graphene oxide synthesis process must be considered. Many reduction methods involve the use of potentially hazardous and environmentally unfriendly chemicals. Research is now exploring green synthesis methods using environmentally benign reducing agents to alleviate these concerns.

2.3. Cellulose Nanofibers (CNF)

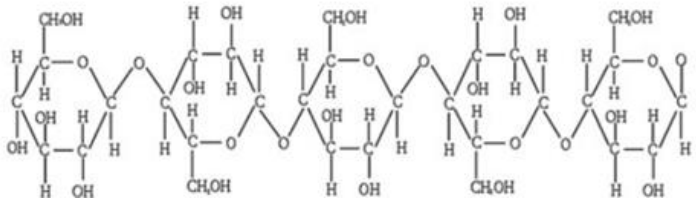

Figure.2. Structure of cellulose[3, 4]

Cellulose is the most popular and common natural biopolymer (Fig. 2) [3, 4] available on earth. It is a unique, sustainable, and functional material because of its low-cost, hierarchical fibrous structures, high surface area, thermal stability, hydrophilicity, biocompatibility, and mechanical flexibility. These special advantages make cellulose ideal for use in sustainable and flexible energy storage, for example: supercapacitors. Cellulose is commonly obtained from wood, hemp, algae, and bacteria. Hence, it is also one of the most important renewable materials. It can form a strong, stable, stiff-chain molecular structure because of its inherent hydrophilicity. It also has mechanical flexibility characteristics, and its fibers can form a 3D hierarchical structure. In battery making, cellulose paper-based electrodes have become a popular topic in order to have lightweight, sustainable, electric energy storage (EES)[5].

The poor electrical conductivity and low surface capacitance of cellulose-based materials limit their practical application in supercapacitors. To overcome these limitations, researchers have developed a composite modification of cellulose to improve the electrical conductivity and capacitance of cellulose-based materials. The composites obtained in this case exhibit better electrical conductivity and enhanced capacitance, making them ideal for supercapacitor electrodes. In this way compared to conventional energy storage systems, cellulose-based

energy storage systems offer superior energy and power densities, making them ideal for applications that require rapid energy bursts or high-power output[6,7].

2.4. rGO-CNF composite in literature

The quest for efficient energy storage solutions has led to the exploration of advanced materials and composites for supercapacitors. rGO and cellulose composites are promising materials for SC technology due to their excellent performance and versatility. The composites obtained using the Chemical Vapor Deposition (CVD) method exhibit improved electrical conductivity and enhanced capacitance, making them ideal for SC electrodes. The combination of cellulose-based materials with flexible electrolytes and membranes further expands their application in SCs. SCs based on graphene oxide and cellulose composites offer superior energy and power densities compared to conventional energy storage systems, making them ideal for applications requiring fast energy bursts or high-power output. The abundant availability and cost-effectiveness of reduced graphene oxide and cellulose make them viable alternatives to the expensive and resource-intensive materials used in current SC technologies. The combination of reduced graphene oxide (rGO) and cellulose in composites offers a compelling avenue for improving the performance of supercapacitors. This paper focuses on fine-tuning the performance of rGO-cellulose composites for specific supercapacitor requirements. This includes optimizing the ratio of rGO to cellulose, exploring the reduction time of rGO at different times, and its effect on the performance of the composites[8, 9, 10].

2.5. Supercapacitor

Over the past two decades, with the development of portable electronic systems, researchers have begun to focus on developing equally versatile energy storage devices. Supercapacitors offer better energy density, power density, and cycle life than regular batteries and conventional capacitors. As the next generation of products, supercapacitors have high sustainability requirements, including low-cost, lightweight, and environmentally friendly materials. Although there are few research articles on cellulose-based energy-related devices, there is still little attention paid to cellulose-based supercapacitors. Supercapacitors (Fig. 3)[11] consist of two electrodes separated by an electrolyte, and they store energy through charge separation at the electrode-electrolyte interface. Supercapacitors work very similarly to conventional capacitors. A conventional capacitor consists of two metal plates called electrodes with a layer of dielectric material sandwiched between them.

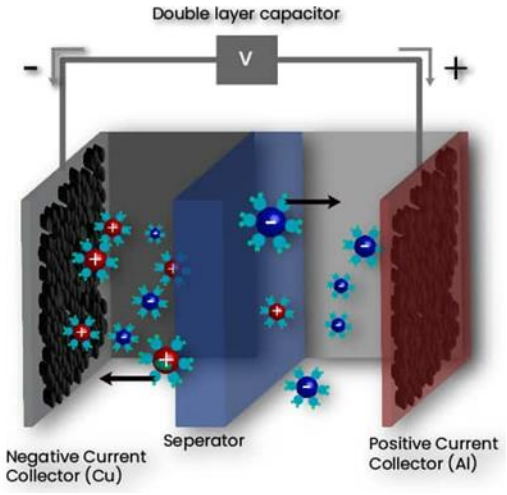

Figure.3. Structure of supercapacitor

When an electric potential E (volts) is applied, electrons gather at one of the two electrodes, thus storing charge. Supercapacitors have several advantages over conventional batteries, including high power density, fast charging and discharging, and long cycle life. They are also more environmentally friendly than batteries because they contain no toxic chemicals or heavy metals. Ultracapacitors have a wide range of applications, including electric vehicles, renewable energy systems, consumer electronics, and aerospace. Researchers are exploring a variety of materials and designs to improve the performance and reduce the cost of supercapacitors, such as graphene, carbon nanotubes, and metal oxides. One of the characteristics of supercapacitors is their high-power density. Supercapacitors store and release energy through the physical separation of charges, which enables them to provide rapid bursts of energy. This characteristic makes them ideal for applications that require fast energy bursts, such as electric vehicles (EVs) and regenerative braking systems. The development of new materials and designs is expected to further improve the performance and reduce the cost of supercapacitors, making them a more viable alternative to conventional batteries in the future. Therefore, the primary task and goal of this project is to explore the use of cellulose as an auxiliary material for building supercapacitor composites[12].

2.6. The objective

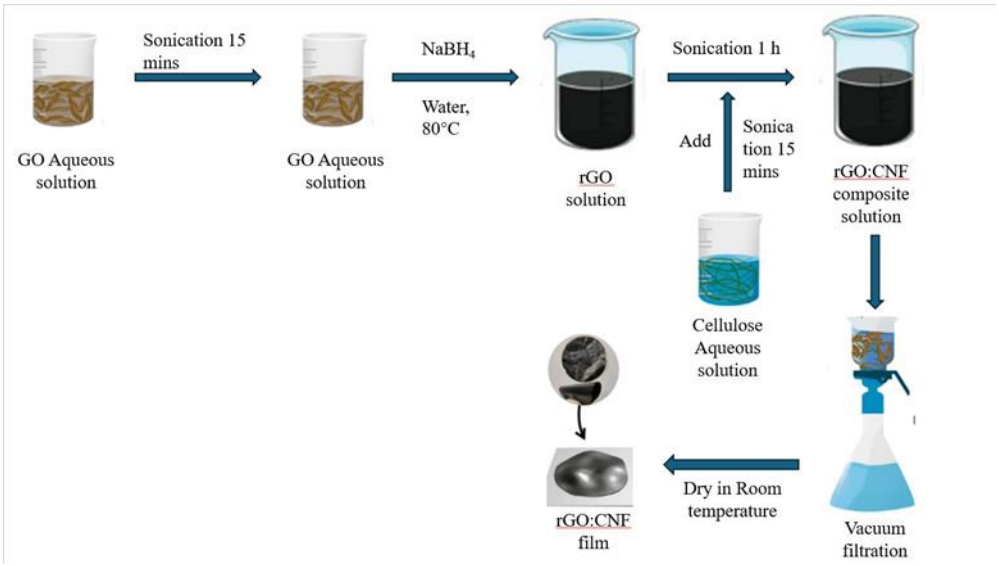

Figure.4. Idea of the project

The experiment (Fig. 4) aims to ensure that the reduced graphene oxide (rGO) effectively integrates with cellulose through sonication. It is essential to carefully determine the ratio of rGO to cellulose to demonstrate the electrical capacity of the composite. The goal is to minimize the amount of rGO used in the composite while maintaining the same level of electrical conductivity, thereby creating an eco-friendly material for supercapacitors.

2.7. Electrochemistry

Electrochemistry is the study of what causes electrons (currents) to move in chemical reactions and vice versa. The movement of electrons is called an electric current and is the result of a redox reaction. This may be due to the transfer of electrons from one element to another. Electrochemistry can be used in physical, chemical, and biological sciences. It is an important area of research in modern studies and has been studied since 1793. It is a fundamental area of research with many applications in various fields including energy storage, corrosion protection, and electroplating. Scientists discovered that chemical energy can be converted into electrical energy, which led to the discovery of the first battery. Electrical energy can also be converted into chemical energy. Essentially, electrochemistry is the reaction of chemical substances at the interface between an electronic conductor and an ionic conductor. Electrodes are typically made of metal or semiconductor materials and ionic conductors, while an aqueous or organic solvent that can supply the ions is called an electrolyte. An electrochemical cell

consists of two electrodes, an anode, and a cathode, separated by an electrolyte. The anode is the electrode where oxidation occurs, while the cathode is the electrode where reduction occurs. The two electrodes are connected by a wire that allows electrons to flow from the anode to the cathode. The nature of these two electrodes determines the performance of an electrochemical cell. Anode and cathode materials must be carefully selected to ensure that they are compatible with the electrolyte and can withstand the operating conditions of the cell. The anode material must be able to readily release electrons, while the cathode material must be able to readily accept electrons. The choice of electrode material also affects the voltage and current output from the battery[13].

Electrochemistry is used as a core technology when cleaner technologies are required for energy consumption and conversion. Platinum, for example, is used as an electrode material because it is an electrocatalyst that improves the efficiency of hydrogen oxidation and oxygen reduction. Electrochemistry has played an important role in the development of supercapacitors, which are energy storage devices capable of storing and releasing electrical energy quickly and efficiently[14].

2.8. Ultraviolet light (UV)

Ultraviolet (UV) light is a type of electromagnetic radiation with wavelengths shorter than visible light but longer than X-rays. UV light has a wide range of applications in various fields such as chemistry, biology, and medicine. One of the most common applications of UV light in chemistry is UV-visible spectroscopy, which is used to analyze the electronic structure of molecules. UV-visible spectroscopy is based on the principle that when a molecule absorbs UV or visible light, one of its electrons jumps from a lower energy molecular orbital to a higher energy molecular orbital. By measuring the amount of light absorbed by a sample at different wavelengths, chemists can determine the electronic structure of the sample and determine the presence of certain functional groups.

UV light is widely used in chemistry for a variety of purposes, including the analysis of compounds and the study of chemical reactions[15]. UV-Vis spectroscopy is an analytical tool for detecting chromophores in compounds by monitoring the wavelength of the absorption spectrum. It has been used in a variety of applications including, archaeological studies, food quality control, photocatalytic activity, fingerprinting, color change in gemstones, wine analysis and stability studies.

2.9. Cyclic Voltammetry (CV)

Cyclic voltammetry (CV) is an electrochemical technique for measuring the current, and it can show the linearly cycled potential sweep of redox-active solution for two or more set values. CV was discovered first in 1938 by Randles, and it is a widely used approach for getting qualitative knowledge of electrochemical reactions. CV can easily calculate the influence of media in the redox process and is considered a reliable approach for example: diffusion properties, analyte concentration, and so on[16].

CV is a powerful and popular electrochemical technique commonly used to study the reduction and oxidation processes of molecular substances. It provides information about the electron transfer processes that occur during oxidation and reduction reactions.CV is widely used in chemistry for a variety of purposes, including the analysis of compounds and the study of chemical reactions. One of the most common applications of CV in chemistry is UV-visible spectroscopy, which is used to analyze the electronic structure of molecules. By measuring the amount of light absorbed by a sample at different wavelengths, chemists can determine the electronic structure of the sample and determine the presence of certain functional groups.CV has also been used in the development of supercapacitors, which are energy-storage devices that store and release electrical energy quickly and efficiently. Researchers have developed various strategies to improve the performance of supercapacitors by altering the characteristics of the electrodes, including the use of CV. In summary, cyclic voltammetry is a powerful electrochemical technique with a wide range of applications in various fields such as chemistry and supercapacitor technology.CV is widely used in chemistry for a variety of purposes including the analysis of compounds and the study of chemical reactions[17].

3. EXPERIMENTAL SECTION

3.1. Materials

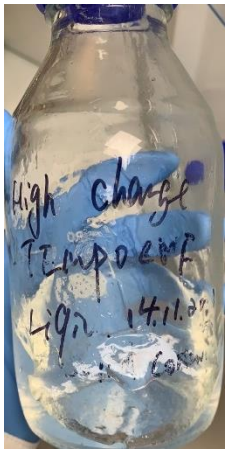

Figure. 5. High-charge cellulose

High-charge cellulose hydrogel solution (Fig. 5) with a concentration of 0.93 wt% dry weight of cellulose has been used throughout the experiments. This TEMPO-oxidized cellulose nanofiber hydrogel is obtained from our collaborator at Åbo Akademi University. Other chemicals and equipments are DI water, Millipore membrane filters (0.1 µm VCTP), $NaBH_4$ (Aldrich), H_2SO_4 (2.5 M, Fluka), Nafion™ 117 containing solution, Graphite sheets (Grafoil), centrifuge tubes (SARSTEDT), sonication equipment (VWR), UV equipment (Agilent Technologies), heating plate with temperature measuring probe, rotation evaporation equipment, 4-probe conductometer equipment (KEITHLEY), centrifuge machine (Biofuge stratas), high-speed centrifuge machine (SIGMA), heating oven, filtration equipment, glass vials, and Vaseline (under high-temperature performance).

3.2. Preparation of cellulose nanofibers

Cellulose nanofibers were obtained from TEMPO-oxidization of pulp fires and then redispersed in water as a colorless hydrogel by our collaborators. This was supplied to us, and then we utilized it without pre-treatment.

3.3. Preparation of rGO

Reduction by $NaBH_4$

$NaBH_4$ was found to be a promising graphene oxide reducing agent, which can reduce the band gap of GO to 2.30 eV and has higher carbon-carbon bond recovery compared to other reducing agents. Reduction of graphene oxide with $NaBH_4$ has been shown to have more homogeneous properties than graphene oxide. We have reduced the GO dispersion in an open-air system and a closed-system methods (Table. 1) as described below.

rGO Sample number	Volume of GO dispersion /ml	GO amount /mg	Volume of $NaBH_4$ dispersion /ml	Amount of $NaBH_4$ /mg	Reduction time /h	Total amount of rGO /ml	Reduction system	Adding NaOH
001	10	50	100	378.3	0.5	50	Open air (Beaker)	1. Yes 2. No
002	20	100	200	756.6	0.5	100	Open air (Beaker)	No
003	10	50	100	378.3	1	50	Closed	No
004	20	100	200	756.6	1	100	Closed	No
005	20	100	200	756.6	1	100	Closed	No
006	20	100	200	756.6	1	100	Closed	No
007	20	100	200	756.6	1	100	Closed	No
008	20	100	200	756.6	3	100	Closed	No
009	20	100	200	756.6	0.5, 1, 2, 3, 6	100	Closed	No
010	20	100	200	756.6	6	100	Closed	No

Table 1. Preparation of rGOs by $NaBH_4$ reduction

Figure. 6. Magnetically stirring heating plate with temperature probe

Figure. 7. Heating plate shows temperature and stirring speed control knobs

Open air system reduction (Beaker)

10 ml of aqueous GO dispersion (5 mg/ml) solution was added to a beaker containing 100 ml of DI water, followed by the addition of 378.3 mg of $NaBH_4$ (dissolved in 100 ml H_2O) to it. This mixture was heated at 80 °C for 1 hour on a magnetically stirring hot plate (Fig. 6, 7). The temperature was monitored on a digital display after dipping a (metal rod-like) temperature probe in the reaction mixture. To achieve 80 °C inside the reaction mixture, the hot plate has to be kept at 170-180 °C. A magnet stirrer bar with a speed of

1200 rpm can generate enough vortex on the liquid surface. This is how the first 50 mg rGO batch was made (rGO Sample number 001: Table 1).

In the next experiment, we doubled all the precursor materials to form a 100 mg rGO batch (rGO Sample number 002: Table 1). After the reduction was complete, the samples were neutralized to pH 7 by washing with plenty of DI water, and by adopting centrifugation. We kept the product's pH, i.e., rGO dispersion always at 7, before proceeding to characterization and electrochemical tests.

Closed system reduction (Rotavapor - RB flask)

Figure. 8. Rotavapor machine

In the case of closed-system reduction RB flask connected to a rotary vapor system (Fig. 8) was employed. The water rotavapor machine has a cooling system located under the table, from which the cold water is pumped to the condenser unit of the Rotavapor and then back to the cooling unit. A vacuum pump system is connected to the condenser outlet of the rotavapor machine which helps in evacuating the air from the RB flask. Another large flask is placed on the side of the condenser unit to collect the evaporated water. With this system, the temperature can be more precisely controlled, but the stirring speed is slower compared to an open system (Beaker).

Figure. 9. RB flask immersed in water

Figure. 10. Three-neck RB flask with closed valve

In a typical experiment, the calculated amount of GO dispersion was added to one-necked RB flasks (Fig. 9) (samples 003-008) or triple-necked flasks (samples 009-010) (Fig. 10) and then the measured amount of $NaBH_4$ solution (1: 7.57 wt GO: $NaBH_4$) was added to the flask followed by a make-up volume of H_2O (100 ml). During the reduction process, we made sure that the water level in the rotavapor bath stayed higher than the water level inside the RB flask, to ensure that the liquid mixture was sufficiently heated (Fig. 9). When using a three-necked RB flask (Fig. 10), both necks should be closed with a rubber septum, and it is always good to evacuate for 30

minutes, in the beginning, to remove any dissolved and atmospheric oxygen from the reaction mixture. Then the valve between the RB flask and Rotavapor was closed before injecting the $NaBH_4$ solution through the septum followed by rotation. The rotation speed of the three-neck RB flask should be maintained at approximately 80 rpm to prevent the bath water from splashing around.

Finally, the heating was started and kept at 80 °C for 1 hour for both one-neck and three-neck RB flask experiments to complete the $NaBH_4$-mediated reduction of GO dispersion. When the reaction was over, the reaction mixture was contracted to 50 ml by evaporating the water for another 1 one hour and then cooled down to room temperature. All glass connections between the RB flask, the nozzle, and the rotary evaporator should be coated with Vaseline petroleum jelly to get the vacuum sealing. The outer part of the glass connections should be secured with plastic clips to prevent the flask from falling into the bathtub, throughout the experiments.

Figure. 11. Centrifuge machine

Figure. 12. High-speed centrifuge machine

The final reaction mixture (rGO dispersion in H_2O at pH 9) was washed with plenty of DI water through centrifugation, bringing the pH down to 7. The low-speed centrifuge machine (Fig. 11) was used for the first step of the neutralization process, with a maximum speed of 5000 rpm. Each round typically takes 20-30 minutes. The internal chamber temperature was set to 10 °C to prevent deformation at the bottom of the centrifuge tubes. The high-speed centrifuge machine (Fig. 12) was used immediately after each round with the low-speed centrifuge. The rotation speed was set to 7000-8000 rpm, with a temperature of 5 °C, and each round lasted 5 minutes. The washing was done in 30 mg rGO installments in DI water.

3.4. Sonochemical synthesis of rGO: CNF composites

rGO sample used	Ratio rGO: CNF	Volume of rGO dispersion /ml	rGO amount /mg	Volume of cellulose solution /ml	Cellulose amount /mg	Final Concentration of composite mg/ml
001	70:30	20	20	5	8.57	0.9
002	50:50	2	2	2	2	0.2
004	90:10	30	30	3	3.3	1
	50:50	15	30	15	30	1
005	90:10	30	30	3	3.3	1
	50:50	20	30	10	30	1
006	90:10	30	30	3	3.3	1
	50:50	20	30	10	30	1
007	30:70	30	30	20	70	0.6

Table 2. rGO: CNF composites prepared via Sonochemical method.

Figure. 13. VWR Sonication equipment

Different ratios of rGO: CNF composite were prepared (Table 2) as follows. The calculated amounts of as synthesized rGO dispersion solution and cellulose hydrogel solution were ultrasonicated (Fig. 13) separately in 25 ml conical flasks for 15 minutes at a temperature range of 20-22 °C. Then the cellulose solution was transferred to rGO containing conical flask by rinsing it with a small amount of water. This mixture of rGO and CNF having a total volume of 30 ml was then sonicated for 1 hour at a temperature range of 20-25 °C. The sonication bath filled with water was used throughout the experiment and the conical flask was made sure that it was immersed inside the water level. To maintain the temperature of the bath during sonication, small pieces of ice were added to the water. These prepared composites were then collected and stored in large centrifuge tubes. The final concentration of the composite was 1 mg/ml in 30 ml solution.

Preparation of rGO: CNF 90:10 composite

rGO Samples 004, 005, and 006 (30 mg from 100 mg batch) were used to prepare a 90:10 ratio of rGO: CNF composite by the above-mentioned common procedure.

Preparation of rGO: CNF 70:30 composite

rGO Sample 001 (50 mg batch) was the sole sample used (20 mg) to prepare a 70:30 ratio composite by the above-mentioned common procedure.
There were two variations of rGO Sample 001 synthesized: one sample from a neutral (pH - 6) synthesis medium and another sample from a NaOH spiked medium (pH – 10). By increasing the Bronsted basicity (- OH) in the graphene oxide (GO) solution, the removal of oxygen-containing function groups from GO can be facilitated, thus the formation of rGO can be catalyzed.

Preparation of rGO: CNF 50:50 composite

rGO Samples 004, 005, and 006 (100 mg batches) were used (30 mg each) to make 50:50 composites by using the above-mentioned common procedure.

rGO Sample 002 was only left with 2 mg in stock, which was used for 50:50 composite making. Because of less rGO used from sample 002 and more water medium present in the mixture, the concentration of rGO in the composite decreased to 0.2 mg/ml.

Preparation of rGO: CNF 30:70 composite

rGO Sample 007 (100 mg batch) was the only sample used (30 mg) to prepare a 30:70 ratio of composite by the above-mentioned common procedure.

Preparation of rGO: CNF 10:90 composite

No experiments were carried out to prepare this ratio as the CV and GCD results of all previous ratios indicated that the amount of rGO present in those composites, was sufficient enough to receive electro-response.

Preparation of rGO: CNF film (for freestanding electrode)

Figure. 14. Vacuum filtration equipment

Figure. 15. Pressure gauges connect between pipes

Various ratios of rGO: CNF composite hydrogel solution were subjected to vacuum filtration to convert the hydrogel into a thin film. The vacuum filtration equipment (Fig. 14) consists of a glass crucible-like container with an inbuilt sintered silicon filter at the bottom. This portion was connected to a collector conical flask through glass joints. Two rubber rings were placed between the bottom of the glass crucible and the conical flask. A metal clip secures tightly the holder and the flask together to prevent leakage. The conical flask was connected sideways to a plastic pipe, which was further attached to the vacuum pump through a pressure gauge (Fig. 15) to facilitate suction.

Figure. 16. rGO: CNF 90:10 free-standing film

After the filtration of water from rGO: CNF composite hydrogel solution, we were able to see a thin, black, circular film-like layer on the sintered filter. This layer was allowed to dry overnight at room temperature so that it could be peeled off easily the next day morning. The best thin film formation result was achieved with rGO: CNF 90:10 ratio composite (prepared from rGO sample 004). Lower volumes (5 ml) of composite solutions resulted in brittle films, whereas higher volumes (13 ml) yielded a strong, flexible thin film (Fig. 16). The strong, flexible thin films were cut into two slides of 1 cm width (Fig. 16). These cut slide films were considered to be free-standing electrodes.

3.5. Materials characterization

UV-visible spectroscopy analyses

The UV-Vis instrument (Fig. 17) was used to characterize the as-formed rGO to confirm the GO dispersion was reduced by our synthesis method. A small quartz cuvette was used to hold the sample in a water mixture. The product rGO dispersion of 45 µl and 90 µl were separately taken in cuvettes (Fig. 18) and then made up to 3 ml volume each. Because the concentration of as prepared rGO dispersion was very high, hence the UV-Vis rays were unable to pass through the dispersion, resulting in no absorption peaks found except huge noises in the spectrum. So, the concentration was diluted by adding extra DI water to the cuvette. Then the survey scan was performed from 200 to 800 nm wavelength range, to detect the characteristic absorption peaks corresponding to GO and rGO. The samples are arranged in an order (high to low) based on peak intensities in Table S1 (Appendix).

Figure. 17. UV instrument

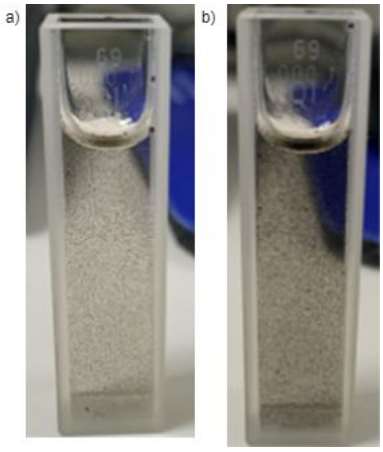

Figure. 18. a) 45µl composite in 3 ml b) 90µl composite in 3 ml

4-probe conductance tests

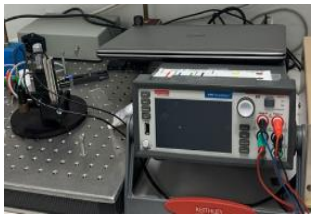

Figure. 19. 4-probe electro-conductance instrument

The flexible, thin films made from rGO: CNF composite hydrogel were investigated for a 4-probe electrical conductance measurement using a conductometer, connected to a computer (Fig. 19). This technique is commonly used to characterize the electrical properties of materials, especially thin films and semiconductors. The 4-probe method is superior to the 2-probe method because it eliminates the resistance of the measurement leads, providing more accurate results. The test consists of passing a known current through two external probes and measuring the voltage difference between two internal probes to calculate the resistance. It is commonly used in the semiconductor industry and materials science research.

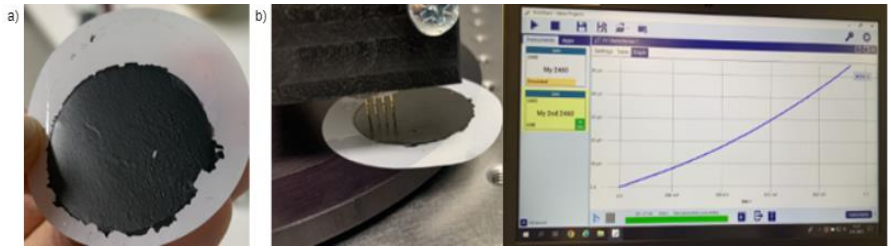

Figure. 20. a) rGO: CNF 90:10/ 5 ml/ 100 mg rGO
b) rGO: CNF 90:10/ 13 ml/ 100 mg rGO/ 4-probe conductance

Figure 20 shows how the films were studied for 4-probe conductance measurement. Figure. 20 a, shows the film made from 5ml of the composite dispersion (prepared from sample 004) via vacuum filtration. This film did not exhibit any conductivity (indirectly understood from the I-V characteristic curve). Then a thicker film was made from 13 ml of the same composite material and the results showed a good I-V response (Fig. 20.b). This means that the thicker film is conductive and can be used for supercapacitor (SC) development.

3.6. Electrochemistry measurements

Cyclic voltammetric (CV) tests of bare graphite sheets

The CV measurement was carried out using a two-electrode system with the electrolyte being 1 M H_2SO_4. For this, two graphite flakes (grafoil sheets) were used as base electrode materials. Initially, bare graphite sheets were tested as blanks for comparison with all other rGOs and composite-casted sheets. The dimensions of the grafoil sheets were 1 cm wide and 4.8 cm long. A ruler was used to measure out an area of 1 cm^2 at one end of the grafoil sheet in its vertical position, and then cellophane tape was applied just above the marked area. The same tape is required on the back of the test section. Then the other end of the grafoil sheets were attached to the alligator clips of the Working Electrode (W.E) and Counter Electrode (C.E) lines while measuring CV.

The CV test for blank, plain rGO & rGO: CNF midified electrodes was run for 3 cycles for every set of conditions. There were 4 different conditions: i). 50 mV/s in the range of 0 to 1 V, ii). 50 mV/s in the range -0.5 to +0.5 V, iii). 100 mV/s in the range of 0 to 1 V, and iv). 100 mV/s in the range -0.5 to +0.5 V, all in 1 M H_2SO_4.

Cyclic voltammetric (CV) tests of rGO: CNF-coated graphite sheets

Plain rGOs and rGO: CNF composites were tested by coating on two graphite flakes electrodes through drop-casting of the as-synthesized materials on grafoil sheets. The drop casting was done, by first taking two petri dishes of different sizes and inverting the smaller dish into the concave portion of the bigger dish. Graphite sheets were bound with tape on the back of a smaller petri dish so that the test surface would face upward. This arrangement was needed to have a movable flat surface and prevent any accidental dripping of the sample dispersion outside the marked area on the electrodes.

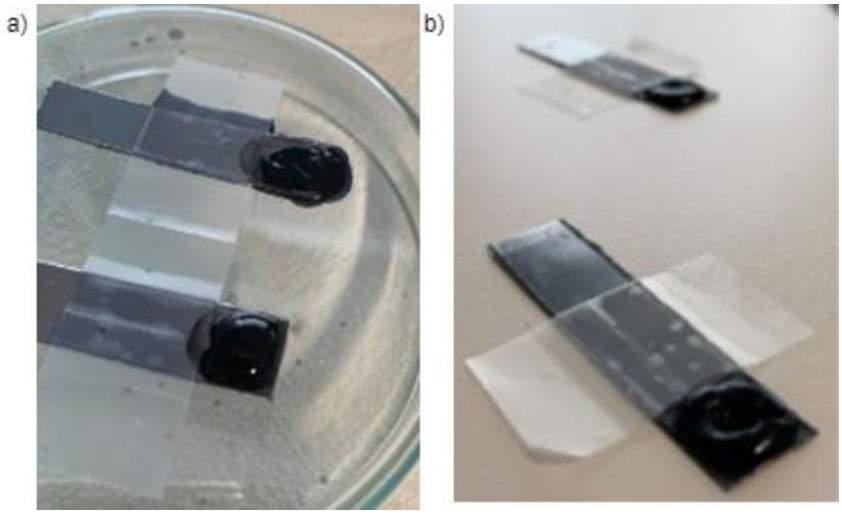

Figure. 21. a) rGO: CNF 90:10 dispersion overflowing b) neutral rGO drying at room temperature

Once the graphite sheets were prepared, 1 ml dispersion (containing 1 mg of solid) of plain rGO or the composite was dropped on the marked area. This volume was dropped in 10 installments using a 100 µl pipette. These drops will form a huge bubble with high surface tension on the marked area of the electrode. This tension will cause the bursting of the bubble and its overflow out of the marked area. It is important to note that care must be taken not to let the drop, flow out of the marked testing area while dropping (Fig. 21.a). Therefore, for each 100 µl drop of the composite or rGO on the sheet, the sheet was kept in the center of the heating oven (Fig. 22) at 120 °C for 3-5 minutes to dry up the water with some wetness left on the electrode. (The oven was preheated to reach the required temperature before starting the process). The next 100 µl of composite material was added to the same marked area (as evenly as possible) before the previous coating was completely dried. Finally, 10 µl of nafion was added on the wet sheet as covering, or 10 µl of nafion was already mixed in the dispersion and sonicated for 30 minutes, before drop

Figure. 22. Heating oven

casting. After the whole process, all sheets were dried overnight (Fig. 21.b) at room temperature before going for CV measurements.

Galvanostatic Charging-Discharging tests (GCD) for plain rGO & rGO: CNF modified graphite sheets

GCD test was done for the above-coated sheets (e.g., Fig. 21.b), which were tested for CV measurement already. These sheets are now assumed to be supercapacitors. During GCD measurements, the sheets were subjected to five different current densities: 1 mA/cm^2, 2 mA/cm^2, 5 mA/cm^2, 10 mA/cm^2 and 20 mA/cm^2. The potential ranges were: 0 to 1 V and -0.5 to +0.5 V as in the case of CV measurements. After 5 times of cyclic measurements, the last cycle from each test was collected and analyzed. The calculated results can be found in the Table. S2.

The areal capacitance can be calculated by the following equation:

$$Areal\ capacitance = \frac{2 \times I_a \times \Delta t}{(\Delta V - IR)} = \frac{2 \times I_a \times \Delta t}{\Delta V_r}$$

In the equation, I_a (A/cm^2) refers to current density, Δt (s) refers to discharging time, and IR refers to the voltage drop caused by the internal resistance in the system which is to be deducted from the discharging voltage (V).

The Gravimetric specific capacitance can be calculated with the following equation.

$$C_p = \frac{I \times \Delta t}{m \times \Delta V}$$

In this equation, I (A) is the discharge current, Δt (s) is the discharging time, m (g) is the mass of the working electrode and ΔV (V) is the discharge voltage.

Problem Solving:

1. During the electrode fabrication process, drop casting should be done very carefully so that the dispersion drops which forms a big bubble on the marked area of the graphite sheet, does not burst and leak outside of the marked area. One way to stop this problem is to rub and roughen the surface of the test area of the graphite flake using sandpaper and then start doing drop casting. Because the smooth and shiny surface of the graphite sheet always causes a high-tension bubble on it.

2. The finger-pressing force on the crocodile clips to hold and dip the modified graphite sheets into the electrolyte liquid, should be very well controlled. More force will cause graphite sheets to break and fall inside the electrolyte liquid.

3. In hindsight, the optimal reduction time for GO seems to be just 1 hour. The longer hour reduction reaction has yielded only the poor quality rGO (less electrocapacitive). The reason behind this may be that the rGO particles which formed after 1 hour will grow larger in size during the course of the further reaction time. This can be avoided so that the smaller particles can easily mix with cellulose while composite making.

4. rGO: CNF composite thin films were easy to prepare with a low volume of composite hydrogel solution. Because they produce films with very few stacked layers, hence the wastewater can easily pass through them under high vacuum pressure. With high volumes of composite hydrogel solution, the film gets thicker and then it is harder for wastewater to pass through (or not at all), even under high vacuum pressure. Thicker films may need to be under high vacuum for more than a day to remove all the water from the composite hydrogel. If the volume is high, sometimes it may not be possible at all to remove the water completely. Also, the dried rGO is highly hydrophobic, hence we should not allow rGO to dry while it is on the filter membrane. Because the water in the successive aliquots of composite solution cannot mix with rGO and pass through the filter at all if the previous aliquot of rGO is already dried. So, care must be taken, while considering the volume for vacuum filtration.

4. RESULTS AND DISCUSSION

4.1 UV-Vis spectroscopic identification of rGO

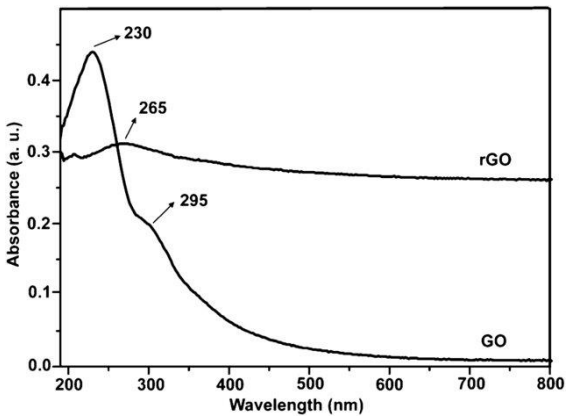

Figure. 23. UV-vis spectra of rGO and GO[1]

After completing every synthesis experiment, the dispersions of rGOs and various ratios of rGO: CNF composites were investigated for UV-Vis spectroscopy. A model UV spectrum for GO (230nm, 295 nm) and rGO (265 nm) is given in the figure. 23. UV-Vis measurements were performed for all synthesized rGOs, before they were ultilized for composite synthesis (with CNF).

Figure 24 shows the comparison of UV spectrums of all rGO dispersions (Samples 004-010) at two different concentrations (C): 45 µl in 3 ml H_2O and 90 µl in 3 ml H_2O.

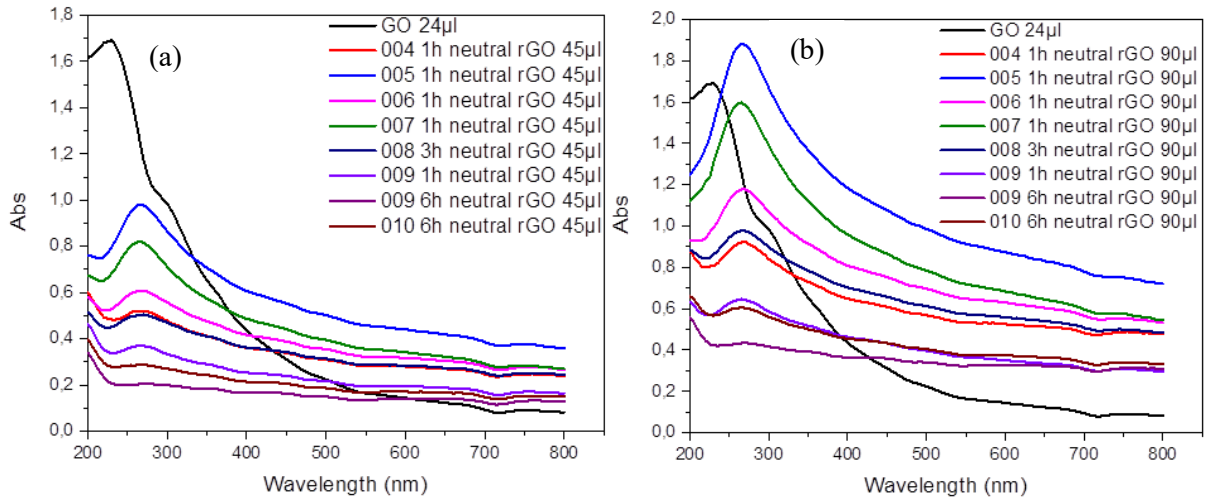

Figure. 24. UV-Vis spectrums of rGO samples (004-010) a) 45 µl in 3 ml H_2O b) 90 µl in 3 ml H_2O c) All 45 µl rGO UV d) All 90 µl rGO UV

The GO precursor dispersion (24 µl in 3 ml H_2O) showed its characteristic peaks at 230 nm and 295 nm (black spectral line), whereas rGOs showed its only characteristic peak at 265 nm in all samples confirming its formation after the reduction process (Fig. 24 a). 90 µl rGO solutions of all samples showed higher absorbance (A) than 45 µl rGO solutions ($A \propto C$) (Fig. 24 b). rGO samples (004-008 prepared from 1-3 h reduction have shown higher absorbance

than samples (009, 010) prepared from longer hour (6 h) reduction. This may be due to rGO particles growing gradually to reaction time. The absorbance intensity was highest for sample 005 rGO.

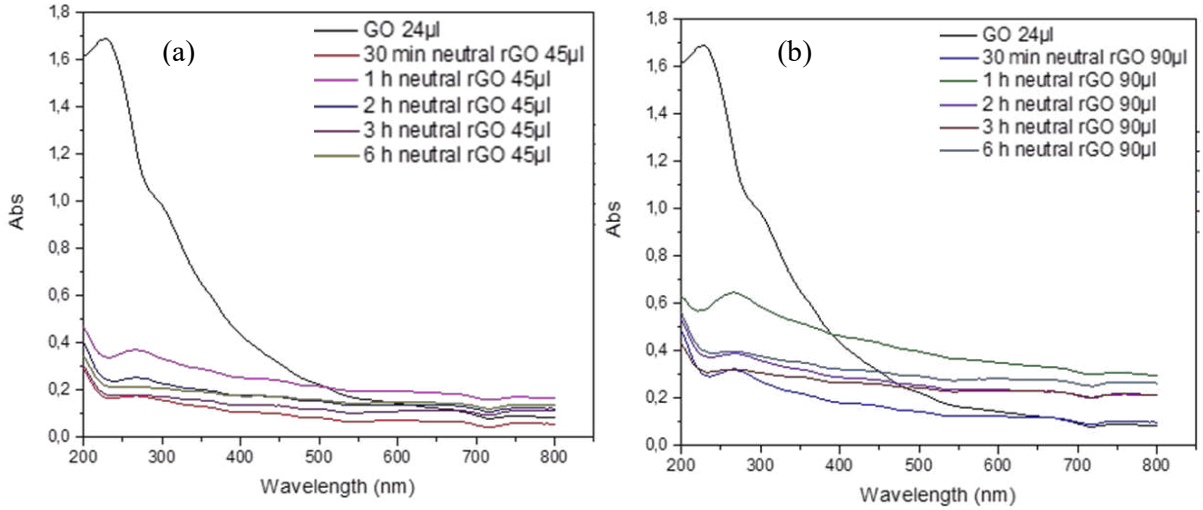

Figure. 25. UV spectrums of rGO (009) samples collected periodically in a 6h reaction a) 45 µl in 3 ml H_2O b) 90 µl in 3 ml H_2O.

Figure 25 shows UV-Vis spectrums for rGO (009) sample aliquots collected at different time intervals in a single experiment (6h reaction). This again confirms that the sample collected at 1 h showed better absorbance response than all other samples, proving longer reaction time is detrimental to the quality of rGO in terms of particle size, and shorter reaction time (30 minutes) was not sufficient enough to reduce rGO completely. From these results, it is clear that the optimal reduction time for GO was 1 h under $NaBH_4$ wet chemical conditions.

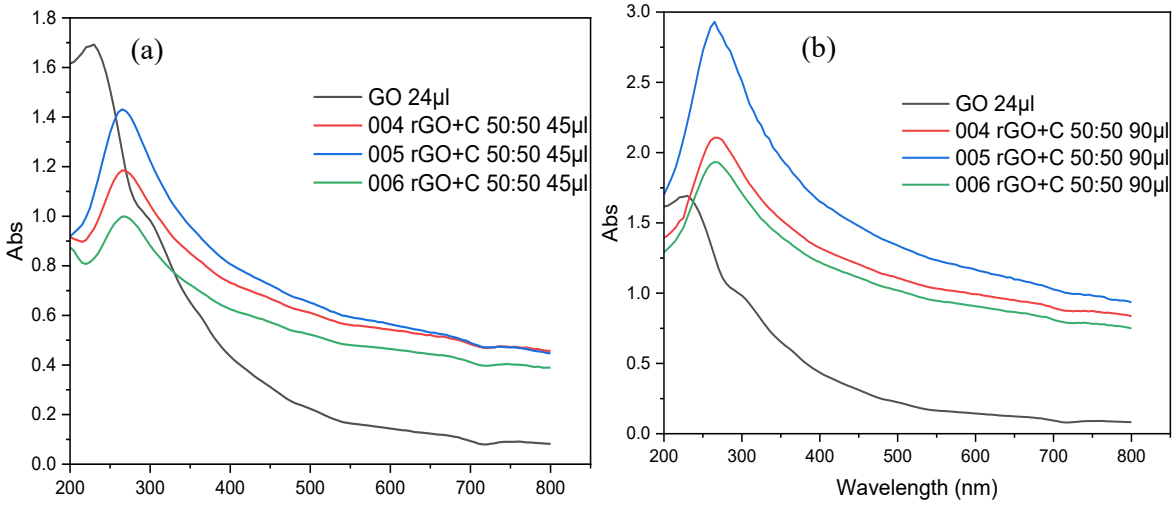

Figure. 26. UV-Vis spectrums of samples (004, 005, 006) rGOs: CNF 50:50, a) 45 µl in 3 ml b) 90 µl in 3 ml. (In 'rGO+C', the 'C' refers to CNF)

Further, rGO: CNF (50:50, 90:10) and rGO: CNF (70:30) composites derived from rGO samples (004, 005, 006) and (007) respectively, were picked for UV-Vis spectroscopy to make sure the rGO didn't undergo any change during sonication treatment with cellulose hydrogel solution. The selection of composites was based on the best UV-Vis responsive rGO samples used for composite making, as we know from figure 24 that samples (004, 005, 006, 007) have shown highly intense absorbance.

Figures 26 and 27, show that the rGOs didn't undergo any chemical change and lost their characteristic UV-Vis absorbance (at 265 nm) even after being composed with cellulose hydrogel. The absorbance intensity was highest for the composite made from sample 005 as in the case of plain rGO sample 005, whereas samples 004 and 006 have shown intensity interchangeably to their plain rGO counterparts, in all cases (Fig 26 a, b., Fig 27 a, b). This was an interesting observation.

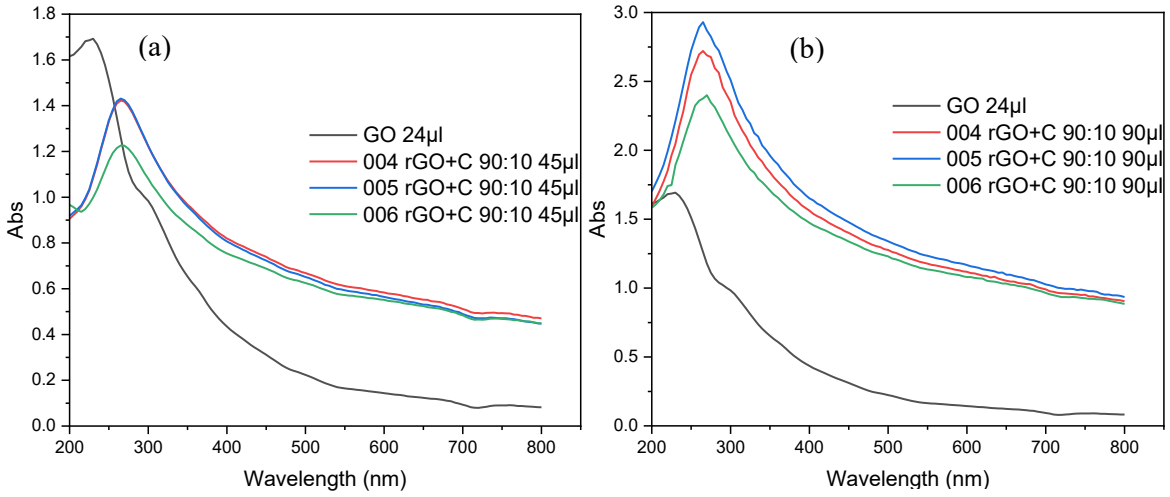

Figure. 27. UV-Vis spectrums of samples (004, 005, 006) rGOs: CNF 90:10, a) 45 µl in 3 ml b) 90 µl in 3 ml. (In 'rGO+C', the 'C' refers to CNF)

Figure 28 shows that the sample (007) rGO, prepared from a neutral pH condition was better than the one prepared from an alkaline condition based on the intensity of the absorbance peak at 265 nm. The idea was to increase the Bronsted basicity, so that it would neutralize the acidic groups (-OH, -COOH) on the carbon skeleton of GO. But the result was not as expected. Then we compared the plain rGO and the composite in the same graph. Surprisingly, the rGO: CNF 30:70 composite showed a better absorbance intensity response (at 265 nm) than its plain rGO counterpart.

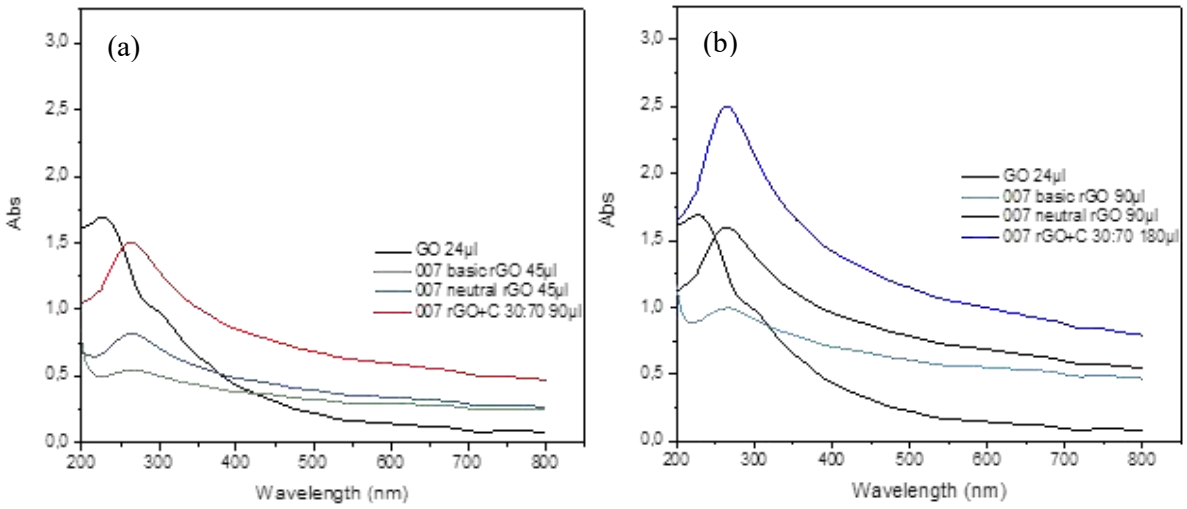

Figure. 28. UV-Vis spectrums of the sample (007) rGO as alkaline, neutral and rGO: CNF 30:70 composite. a) 45 µl in 3 ml b) 90 µl in 3 ml. The concentration of rGO in the composite was shallow (0.6 mg/ml), hence the volume of the composite was doubled to 90 µl, 180 µl. (In 'rGO+C', the 'C' refers to CNF)

Table. S1 shows the order of plain rGO & rGO: CNF composite sample IDs in terms of high to low UV-Vis absorbance intensities.

Thus, we infer from UV-Vis spectroscopic data that to synthesize rGO the optimal reduction time for GO was 1 h at neutral pH, under $NaBH_4$ wet chemical conditions. All the rGO: CNF composites irrespective of their ratios, proved that the chemical nature of rGO was intact in them even after sonicating with cellulose hydrogel.

4.2 Electrochemical performance of plain rGOs & various ratios of rGO: CNF composites (CV, GCD)

There were 10 samples (Sample IDs 001-010) of rGO prepared (Table 1) by $NaBH_4$ induced reduction of GO. In general, these were repeating the same reaction except for a few changes, like batch sizes and operation modalities (e.g., pH, time duration). These 10 rGOs were further composed with cellulose (TEMPO oxidized, highly charged) in different ratios to yield various rGO: CNF composites. All these plain rGOs and composites were investigated for capacitance measurement studies under CV and GCD conditions. Freshly prepared 1 M H_2SO_4 was used as the electrolyte in all the experiments.

The unmodified graphite flakes' electrodes were initially tested as blank electrodes under CV, GCD conditions in 1 M H_2SO_4. The scan rates were 50 mV and 100 mV, and the scan ranges were from -0.5 V to +0.5 V and from 0 V to 1 V (Fig S1). The same conditions were followed

for rGO modified and rGO: CNF composite modified electrodes. The photographs of modified electrodes, CVs, and GCDs were given in the supporting information section as an appendix (Fig. S2- S37).

Sample IDs	Scan rate at current density 1 mA/cm^2	C_A F/cm^2	C_P F/g
Blank	-0.5 to +0.5V	7.99×10^{-2}	0
Blank	0 – 1 V	4.27×10^{-2}	0

Table. 3. Areal capacitance and gravimetric-specific capacitance for blank graphite flakes' electrodes.

The calculated values of areal capacitance (C_A) and gravimetric-specific capacitance (C_P) for blank electrodes are shown in Table 3. The results show that the electrodes possess very basic capacitance values.

Next, 001 rGO (50 mg batch, 0.5 h reduced) and its derivative 001 rGO: CNF composite was not tested for their electrochemical performance. Because of a few shortcomings. First of all, the 001 rGO was prepared under two different conditions; a). without NaOH (non-alkaline) b) with NaOH (alkaline), during its synthesis. The first sample; non-alkaline 001 rGO was initially added to cellulose hydrogel (CNF) to develop the composite. However, it did not mix well with cellulose, as rGO particles got separated from the cellulose phase and stuck to the walls of the reaction flask. This could be because that we did not wash the rGO with deionized water to neutralize its pH to 7, before adding cellulose to it. The fact is that after $NaBH_4$'s utilization in the reduction process, its by-product $NaBO_2$ will still be present in the medium, which will raise the pH to 10. This high pH was found to be unfavorable for rGO to mix with cellulose easily. Based on this enlightenment, we did not attempt to make a composite from the second sample; alkaline rGO (NaOH spiked).

Therefore, the 002 rGO sample (100 mg batch, 30 min reduced) was first neutralized to pH 7 by continuous washing/centrifugation/decantation with DI and then composed with cellulose to get desired rGO: CNF composites. These were tested for their electrochemical performance (Fig S2, S3). The calculated values of areal capacitance and gravimetric-specific capacitance are shown in Table 4. The results show that the addition of cellulose to rGO (50:50) was beneficial as it increased the capacitance values largely (x3 times C_A & x6 times C_P). This

proves that our aim of composing cellulose with rGO is justified. Thus, cellulose act as a supporting medium for rGO particles for their better dispersion and anchoring on graphite flake electrode surface. Practicality-wise, care must be taken for the level of finger press on crocodile clips while dipping graphite flak electrode in the electrolyte. Excess of pressing might lead to the breaking of graphite electrodes.

rGO Sample IDs	rGO:CNF Ratio	Total material concentration mg/ml	Scan range at current density 1 mA/cm^2	rGO mass /mg	C_A F/cm^2	C_P F/g
002	100:0	1(Cover)	-0.5 to +0.5 V	2	158.4	39.6
002	100:0	1(Cover)	0 - 1 V	2	126.18	31.545
002	50:50	1(Cover)	-0.5 to +0.5 V	1	492.34	246.17
002	50:50	1(Cover)	0 - 1 V	1	381.46	190.73

Table 4. Areal capacitance and gravimetric-specific capacitance for 002 rGO & its composites.

Another notable point is that 002 rGO: CNF composite underwent total of 2 h of sonication, when compared with all other composite making procedure. (The reason was accidental because the composite was sonicated for 1 hour first and then left overnight undisturbed before being tested for electrochemistry. The next day, there was some phase separation between rGO and cellulose; hence another 1-hour sonication was applied to the composite mixture). (002 rGO: CNF was the most active supercapacitor material, possibly due to longer sonication time before drop casting.)

Next, the 003 rGO sample (50 mg batch, 1 h reduced) was again not tested for its electrochemical performance, because of the following reasons. Usually, we neutralize the product rGO dispersion to pH 7 and keep the rGO in water (30 ml), in a centrifuge tube as a storage container. This neutral rGO dispersion will be directly used for drop casting on electrodes for its electrochemical performance studies. However, we took a different approach for 003 rGO. What we did was, we dried the neutral rGO dispersion in an oven to remove the water completely to get solid flakes of rGO (50 mg) (Fig. S4 a). Then, we tried to smash or grind these rGO flakes (10 mg) to redisperse them in water again. But the rGO flakes were not crushable proving its mechanical strength. We tried different solvents like ethanol, and acetone, to redisperse the rGO flakes (Fig. S4 b), but no dispersion was achieved. Thus, we couldn't get rGO dispersion again from 003 rGO for further drop casting on electrodes. So, the rGO: CNF

composite was also not made. Thus, it was clear that neutral rGO dispersion must not be dried and kept as it is in the original aqueous medium for further use.

Further to check the reproducibility of 002 rGO, other rGOs and composites' samples (004-010) were tested for their performances, one by one. 004 rGO sample (100 mg batch, 1 h reduced) and its composites (50:50, 90:10) (Fig. S5) were investigated for their capacitance performances (Fig. S6-S10) and shown in Table 5. The 50:50 composite has shown 1.4 times (40%) increase in C_A for and C_P at -0.5 to +0.5 V concerning plain rGO (2 mg). However, the 0-1 V scan range showed decreased values for the 50:50 composite. The 90:10 composite has shown 1.9 times (88%) increase in C_A, C_P at -0.5 to +0.5 V, and 1.3 times (33%) increase in C_A, C_P at 0-1 V.

rGO Sample IDs	rGO:CNF Ratio	Total material concentration mg/ml	Scan range at current density 1 mA/cm^2	rGO mass /mg	C_A F/cm^2	C_P F/g
004	100:0	1(Cover)	-0.5 to +0.5 V	2	101.64	25.41
004	100:0	1(Cover)	0 - 1 V	2	110.46	27.615
004	50:50	1(Cover)	-0.5 to +0.5 V	1	141.3	35.325
004	50:50	1(Cover)	0 - 1 V	1	79.14	19.785
004	50:50	2(Cover)	-0.5 to +0.5 V	2	238.52	29.815
004	50:50	2(Cover)	0 - 1 V	2	156.1	19.5125
004	90:10	1(Cover)	-0.5 to +0.5 V	1.8	191.02	47.755
004	90:10	1(Cover)	0 - 1 V	1.8	147.38	36.845
004	90:10	1 (ink)	-0.5 to +0.5 V	1.8	230.94	57.735
004	90:10	1 (ink)	0 - 1 V	1.8	160.16	40.04

Table 5. Areal capacitance and gravimetric-specific capacitance for 004 rGO & its composites

In order to improve the capacitance, we have taken two approaches 1). increasing the loading of 50:50 composite on the electrode (4 mg) 2). Adding Nafion (covering) to the fresh drop casted 90:10 composite on the electrode. The results show that doubling the amount of composite on a graphite sheet in the same 1 cm^2 area, increased the C_A 1.7 times (69%) at -0.5 to +0.5 V and 2 times (97%) at 0-1 V. Whereas C_P did not improve as expected. This reveals that not all the added rGO was taking part in the charging-discharging process, whereas area coverage by rGO on the electrode surface was improved. Further, composites with the same

ratio (90:10) and same loading (2 mg) were compared to evaluate the effects of Nafion coating from this sample. Adding Nafion on the 90:10 composite modified electrode has improved the C_A, C_P 1.2 times (21%) at -0.5 to +0.5 V and 1.1 times (9%) at 0-1 V. However, the Nafion-coated electrodes took a slightly longer time to dry sufficiently. 1 mA/cm² current density under GCD condition was providing the best results all along.

We have also made a film from 004 rGO: CNF ratio 50:50 composite hydrogel solution by vacuum filtration, to produce a free-standing electrode. However, the film was so thin and light, that it was impossible to dip it in the electrolyte vertically. Thus, the film was floating on the electrolyte liquid surface. Hence, no CV, or GCD results could be obtained for the stand-alone film.

Next, the 005 rGO sample (100 mg batch, 1 h reduced) and its composites (90:10, 50:50) (Fig. S11) were investigated for their capacitance performances (Fig. S12-S14) and shown in Table 6. The 90:10 composite has shown 1.3 times (33%) increase in C_A and C_P at both ranges; -0.5 to +0.5 V, 0-1 V, concerning plain 005 rGO (2 mg). Whereas the 50:50 composite has shown 1.85 times (85%) increase in C_A and C_P at both the ranges; -0.5 to +0.5 V, 0-1 V, concerning plain 005 rGO (2 mg).

rGO Sample IDs	rGO:CNF Ratio	Total material concentration mg/ml	Scan range at current density 1 mA/cm²	rGO mass /mg	C_A F/cm²	C_P F/g
005	100:0	1(Cover)	-0.5 to +0.5 V	2	109.94	27.485
005	100:0	1(Cover)	0 - 1 V	2	95.96	23.99
005	90:10	1(Cover)	-0.5 to +0.5 V	1.8	146.5	36.625
005	90:10	1(Cover)	0 - 1 V	1.8	127.18	31.795
005	50:50	1(Cover)	-0.5 to +0.5 V	1	203.06	50.765
005	50:50	1(Cover)	0 - 1 V	1	131.4	32.85
005	50:50	1 (ink)	-0.5 to +0.5 V	1	152.08	38.02
005	50:50	1 (ink)	0 - 1 V	1	98.16	24.54

Table 6. Areal capacitance and gravimetric-specific capacitance for 005 rGO & its composites

Further, composites with the same ratio (50:50) and different ratios (90:10) were compared to evaluate the effects of Nafion coating versus inking for this sample. But this time the results were not improving, as it improved in the case of 004 rGO: CNF 90:10 composite.

Further 006 rGO sample (100 mg batch, 1 h reduced) and its composites (50:50, 90:10: with/without Nafion ink) (Fig. S15) were investigated for their capacitance performances (Fig. S16-S19) and shown in Table 7. The 50:50 composite hasn't shown any improvement in terms of C_A and C_P values at both the ranges; -0.5 to +0.5 V, 0-1 V, concerning plain 006 rGO (2 mg). Whereas 50:50 composite with Nafion as ink delivered an increase of 1.5 times (53%) in C_A and C_P values, at the range, -0.5 to +0.5 V, concerning plain 006 rGO (2 mg). But it did not show any improvement at 0-1 V range.

006 rGO: CNF 90:10 composite has shown 1.5 times (47%) increase in C_A and C_P at -0.5 to +0.5 V and 1.4 times (43%) increase in C_A and C_P at 0-1 V range, concerning plain 006 rGO (2 mg). Whereas 90:10 composite with Nafion as ink delivered an increase of 1.4 times (44%) in C_A and C_P values, at -0.5 to +0.5 V range, and 1.3 times (28%) increase at 0-1 V range, concerning 90:10 composite without Nafion ink. Hence, composing rGO with cellulose proved to be advantageous in terms of capacitance. Also, the Nafion based catalyst ink drop casting improved the results significantly.

rGO Sample IDs	**rGO:CNF Ratio**	**Total material concentration mg/ml**	**Scan range at current density 1 mA/cm^2**	**rGO mass /mg**	**C_A F/cm^2**	**C_P F/g**
006	100:0	1(Cover)	-0.5 to +0.5 V	2	86.24	21.56
006	100:0	1(Cover)	0 - 1 V	2	76.64	19.16
006	50:50	1(Cover)	-0.5 to +0.5 V	1	85.2	21.3
006	50:50	1(Cover)	0 - 1 V	1	51.5	12.875
006	50:50	1 (ink)	-0.5 to +0.5 V	1	130.26	32.565
006	50:50	1 (ink)	0 - 1 V	1	76.56	19.14
006	90:10	1(Cover)	-0.5 to +0.5 V	1.8	126.54	31.635
006	90:10	1(Cover)	0 - 1 V	1.8	109.96	27.49
006	90:10	1 (ink)	-0.5 to +0.5 V	1.8	182.78	45.695
006	90:10	1 (ink)	0 - 1 V	1.8	140.54	35.135

Table 7. Areal capacitance and gravimetric-specific capacitance for 006 rGO & its composites.

Our next idea was to decrease the amount of rGO in the composite to rGO: CNF 30:70 ratio. So, we prepared this composite from 007 rGO sample (100 mg batch, 1 h reduced). If the decrease in rGO amount doesn't affect the conductivity & capacitance, only less amount of

rGO is sufficient for future developments. Also, an alkaline 007 rGO sample was tested to see if the pH value affected the result.

rGO Sample IDs	rGO:CNF Ratio	Total material concentration mg/ml	Scan range at current density 1 mA/cm^2	rGO mass /mg	C_A F/cm^2	C_P F/g
007 (alkaline)	100:0	1(Cover)	-0.5 to +0.5 V	2	82.22	20.555
007 (alkaline)	100:0	1(Cover)	0 - 1 V	2	67.1	16.775
007 (non-alkaline)	100:0	1(Cover)	-0.5 to +0.5 V	2	128.64	32.16
007 (non-alkaline)	100:0	1(Cover)	0 - 1 V	2	98.94	24.735
007 (n-a)	30:70	1(Cover)	-0.5 to +0.5 V	0.6	54.08	13.52
007 (n-a)	30:70	1(Cover)	0 - 1 V	0.6	19.66	4.915
007 (n-a)	30:70	1 (ink)	-0.5 to +0.5 V	0.6	56.4	14.1
007 (n-a)	30:70	1 (ink)	0 - 1 V	0.6	20.06	5.015

Table 8. Areal capacitance and gravimetric-specific capacitance for 007 rGO & its composites.

007 rGO samples (alkaline, non-alkaline) and their composites (30:70: with/without nafion ink) (Fig. S20) were investigated for their capacitance performances (Fig. S21-S23) and shown in Table 8. The alkali mediated rGO synthesis yielded a poor quality rGO as the C_A and C_P values dropped down 1.6 times (56%) at -0.5 to +0.5 V range and 1.5 times (47%) at 0-1 V range, concerning non-alkali mediated rGO product (2 mg). Thus, it was clear that the addition of NaOH-like alkaline solution in the synthesis of rGO is a futile exercise under our reduction conditions. Therefore, rGO must always be kept at pH 7 before going for composite making.

The 007 rGO: CNF 30:70 composite showed poor performance in terms of capacitance values (C_A, C_P), concerning 007 rGO (2 mg). So, it is proved that the 90:10, and 50:50 ratios were better than the 30:70 ratio. Hence, the optimal minimum amount of rGO in the composite should not fall under 50%.

Further, the 30:70 composite with Nafion as the ink has slightly improved the C_A and C_P values, at -0.5 to +0.5 V, 0-1 V ranges, concerning the 30:70 composite without Nafion as ink (2 mg).

The next trials were to see whether prolonged durations (3 - 6 h) of reduction could help in producing more capacitive rGO or not. So far, in the previous trials, the common reduction period was about 0.5 to 1 hour. Also, we looked into the advantage of drying the drop casted electrodes inside the oven (120 °C, 1h) rather than drying it outside at room temperature (RT).

rGO Sample IDs (Reduced for 3 h)	**rGO:CNF Ratio**	**Total material concentration mg/ml**	**Scan range at current density 1 mA/cm^2**	**rGO mass /mg**	**C_A F/cm^2**	**C_P F/g**
008 (RT dried)	100:0	1(Cover)	-0.5 to +0.5 V	2	136.84	34.21
008 (RT dried)	100:0	1(Cover)	0 - 1 V	2	104.34	26.085
008 (Oven)	100:0	1(Cover)	-0.5 to +0.5 V	2	150.34	37.585
008 (Oven)	100:0	1(Cover)	0 - 1 V	2	108.18	27.045

Table 9. Areal capacitance and gravimetric-specific capacitance for 008 rGOs.

008 rGO samples (RT-dried, Oven-dried) (Fig. S24) were investigated for their capacitance performances (Fig. S25, S26) and shown in Table 9. The oven-dried rGO showed a 10 % increase in C_A and C_P values in -0.5 to +0.5 V range and 4% increase in 0-1 V range, concerning RT dried rGO product (2 mg). Thus, oven-dried rGO was slightly performing better than rGO dried at room temperature. Capacitance-wise, 008 rGO (from 3h reduction) was on par with 002 rGO (0.5 h reduced), but slightly better than 004-007 rGO (1 h reduced) samples. Thus, a longer reduction of GO did not improve the capacitance of rGO to a significant level. This is also supported by the UV-Vis result where we found that the absorbance intensities for 3h, and 6h reduced GO samples were less than it was for 1h reduced sample. So, we believe that the longer reaction time at 80 °C, could have caused an increase in particle size of rGO, thus ending up with no big improvement in capacitance.

The next inquiry was what if the reduction time is extra longer and what the performances of periodically collected samples will be. This way we can understand what is happening to the rGO during the reaction.

rGO Sample IDs (Reduction time)	rGO:CNF Ratio	Total material concentration mg/ml	Scan range at current density 1 mA/cm^2	rGO mass /mg	C_A F/cm^2	C_P F/g
009 (0.5 h)	100:0	1(Cover)	-0.5 to +0.5 V	2	26.5	6.625
009 (0.5 h)	100:0	1(Cover)	0 - 1 V	2	16.52	4.13
009 (1 h)	100:0	1(Cover)	-0.5 to +0.5 V	2	83.32	20.83
009 (1 h)	100:0	1(Cover)	0 - 1 V	2	59.72	14.93
009 (2 h)	100:0	1(Cover)	-0.5 to +0.5 V	2	68.48	17.12
009 (2 h)	100:0	1(Cover)	0 - 1 V	2	40.94	10.235
009 (3 h)	100:0	1(Cover)	-0.5 to +0.5 V	2	62.68	15.67
009 (3 h)	100:0	1(Cover)	0 - 1 V	2	46.14	11.535
009 (6 h)	100:0	1(Cover)	-0.5 to +0.5 V	2	50.3	12.575
009 (6 h)	100:0	1(Cover)	0 - 1 V	2	32.08	8.02
009 (6 h)	100:0	1 (Cover)	-0.5 to +0.5 V	2	58.18	14.545
009 (6 h)	100:0	1 (Cover)	0 - 1 V	2	30.1	7.525
009 (6 h)	100:0	1 (ink)	-0.5 to +0.5 V	2	141.46	35.365
009 (6 h)	100:0	1 (ink)	0 - 1 V	2	96.1	24.025

Table 10. Areal capacitance and gravimetric-specific capacitance for 009 rGOs.

009 rGO (100 mg batch) from the reduction of GO for 6h in 3 necked RB flask, was collected periodically at 0.5, 1, 3, and 6 h using a syringe through the septum-locked side neck of the RB flask and then investigated (Fig. S27) for capacitance performances (Fig. S28-S34) as shown in Table 10. The results show that the capacitance values (C_A, C_P) increase for the samples between 0.5 h and 1 h and then linearly decrease concerning time (2 h,3 h, 6 h) at both the scan ranges: -0.5 to +0.5 V & 0 - 1 V. This confirms that the optimum reduction time for GO was 1 h under our wet chemical conditions.

Table 10 also compares the data of 009 rGO (6 h) with 009 rGO (6 h, Nafion coated) and 009 rGO (6 h, Nafion ink). Of these three samples, one next showing higher capacitance than the previous one sequentially, at 0.5 to +0.5 V. Whereas at 0-1 V, first two samples show almost similar values, but the third one showed higher value (C_A, C_P) than all. This indicates that the addition of Nafion either in the form of a final coating or catalyst ink improves the performance of the drop-casted rGO material. However, it should be made sure that Nafion itself should not artificially contribute to the capacitance value in the future.

Then the final experiment was the synthesis of 010 rGO in a direct 6-hour reduction period under a fully closed system without any periodical sample collection. Because it was believed that in the 009 rGO synthesis, the periodical collection of samples using a syringe through the septum-locked side neck of the three-necked flask might have caused the air/oxygen entry into the RB flask, resulting in the poor reduction of GO at 2 h, 3 h, 6 h. So, 010 rGO synthesis was done for 6h straight without any disturbance. The synthesized (100 mg batch, 6 h reduced) 010 rGO drop casted electrodes dried at room temperature or in the oven. Then investigated (Fig, S35) for capacitance performances (Fig. S36, S37) as shown in Table 11. The results show the capacitance values (C_A, C_P) were lesser than what we got for 009 rGO at 6h, in both the scan ranges: -0.5 to +0.5 V & 0 - 1 V. So, we concluded that longer hour reduction of GO was not favorable to the production of good capacitive rGO.

rGO Sample IDs (Reduced for 6 h)	**rGO:CNF Ratio**	**Total material concentration mg/ml**	**Scan range at current density 1 mA/cm^2**	**rGO mass /mg**	**C_A F/cm^2**	**C_P F/g**
010 (RT dried)	100:0	1 (ink)	-0.5 to +0.5 V	2	105.78	26.445
010 (RT dried)	100:0	1 (ink)	0 - 1 V	2	83.3	20.825
010 (Oven)	100:0	1 (ink)	-0.5 to +0.5 V	2	86.26	21.565
010 (Oven)	100:0	1 (ink)	0 - 1 V	2	71.24	17.81

Table 11. Areal capacitance and gravimetric-specific capacitance for 010 rGOs.

There were also some practical issues while doing 010 rGO synthesis. The reduction was started only after degassing the RB flask content for 30 minutes under high vacuum suction followed by closing the valve between the flask and condenser unit to avoid any air leak into the flask. As there was low pressure inside the flask, a little mishap happened because of the H_2 generation by $NaBH_4$ dissolution. The septum in the side neck was popped out because of the H_2 pressure, allowing the entry of air into the flask, at the very beginning of the experiment. This could have also caused the lower performance of 010 rGO than we expected.

5. CONCLUSION AND PROSPECTS

The presented research topic on 'rGO: CNF composite for supercapacitor application' delivered experimental results which clearly show that a). Graphene oxide (GO) can be reduced by $NaBH_4$ very efficiently in less time (1- 3 h), b) the as-synthesized rGO can be composed with cellulose nanofibers (CNF) under ultrasonic wet chemical conditions easily without any laborious steps, c) the addition of non-conducting CNF improves the capacitance properties of rGO without spoiling its conductivity, d) CNF can act as a supporting/anchoring substrate for rGO particles to develop free-standing thin film electrodes in future. From the capacitance measurements studies, it has been found that the 002 rGO: CNF (50:50) composite was performing better with C_A = 492.34 F/cm^2 & C_P = 246.17 F/g, as against the plain 002 rGO which exhibits the capacitance values 158.4 F/cm^2, 39.6 F/g only, respectively. Thus, it confirms that our way of making rGO: CNF composites could yield more capacitance if the reaction/ operation conditions are finetuned further.

APPENDIX

Supporting Information (SI)

UV-vis	Amount	Order of sample IDs in terms of high to low absorbance intensities (Peak height)
rGO	45 µl	005>007>006>004>008>009(1h)>010>009(6h)
	90 µl	005>007>006>008>004>009(1h)>010>009(6h)
rGO-CNF 50:50	45 µl	005>004>006
	90 µl	
rGO-CNF 90:10	45 µl	005>004>006

Table. S1. UV-Vis spectroscopic data

rGO Sample IDs	rGO:CNF Ratio	Total material concentration mg/ml	Scan range at current density 1 mA/cm^2	rGO mass /mg	C_A F/cm^2	C_P F/g
Blank	0	0	-0.5 to +0.5 V	0	7.99×10^{-2}	0
Blank	0	0	0 - 1 V	0	4.27×10^{-2}	0
002	100:0	1(Cover)	-0.5 to +0.5 V	2	158.4	39.6
002	100:0	1(Cover)	0 - 1 V	2	126.18	31.545
002	50:50	1(Cover)	-0.5 to +0.5 V	1	492.34	246.17
002	50:50	1(Cover)	0 - 1 V	1	381.46	190.73
004	100:0	1(Cover)	-0.5 to +0.5 V	2	101.64	25.41
004	100:0	1(Cover)	0 - 1 V	2	110.46	27.615
004	50:50	1(Cover)	-0.5 to +0.5 V	1	141.3	35.325
004	50:50	1(Cover)	0 - 1 V	1	79.14	19.785
004	50:50	2(Cover)	-0.5 to +0.5 V	2	238.52	29.815
004	50:50	2(Cover)	0 - 1 V	2	156.1	19.5125
004	90:10	1(Cover)	-0.5 to +0.5 V	1.8	191.02	47.755

004	90:10	1(Cover)	0 - 1 V	1.8	147.38	36.845
004	90:10	1 (ink)	-0.5 to +0.5 V	1.8	230.94	57.735
004	90:10	1 (ink)	0 - 1 V	1.8	160.16	40.04
005	100:0	1(Cover)	-0.5 to +0.5 V	2	109.94	27.485
005	100:0	1(Cover)	0 - 1 V	2	95.96	23.99
005	90:10	1(Cover)	-0.5 to +0.5 V	1.8	146.5	36.625
005	90:10	1(Cover)	0 - 1 V	1.8	127.18	31.795
005	50:50	1(Cover)	-0.5 to +0.5 V	1	203.06	50.765
005	50:50	1(Cover)	0 - 1 V	1	131.4	32.85
005	50:50	1 (ink)	-0.5 to +0.5 V	1	152.08	38.02
005	50:50	1 (ink)	0 - 1 V	1	98.16	24.54
006	100:0	1(Cover)	-0.5 to +0.5 V	2	86.24	21.56
006	100:0	1(Cover)	0 - 1 V	2	76.64	19.16
006	50:50	1(Cover)	-0.5 to +0.5 V	1	85.2	21.3
006	50:50	1(Cover)	0 - 1 V	1	51.5	12.875
006	50:50	1 (ink)	-0.5 to +0.5 V	1	130.26	32.565
006	50:50	1 (ink)	0 - 1 V	1	76.56	19.14
006	90:10	1(Cover)	-0.5 to +0.5 V	1.8	126.54	31.635
006	90:10	1(Cover)	0 - 1 V	1.8	109.96	27.49
006	90:10	1 (ink)	-0.5 to +0.5 V	1.8	182.78	45.695
006	90:10	1 (ink)	0 - 1 V	1.8	140.54	35.135
007 (alkaline)	100:0	1(Cover)	-0.5 to +0.5 V	2	82.22	20.555
007 (alkaline)	100:0	1(Cover)	0 - 1 V	2	67.1	16.775
007 (non-alkaline)	100:0	1(Cover)	-0.5 to +0.5 V	2	128.64	32.16
007 (non-alkaline)	100:0	1(Cover)	0 - 1 V	2	98.94	24.735
007 (n-a)	30:70	1(Cover)	-0.5 to +0.5 V	0.6	54.08	13.52
007 (n-a)	30:70	1(Cover)	0 - 1 V	0.6	19.66	4.915
007 (n-a)	30:70	1 (ink)	-0.5 to +0.5 V	0.6	56.4	14.1
007 (n-a)	30:70	1 (ink)	0 - 1 V	0.6	20.06	5.015
008 (RT dried)	100:0	1(cover)	-0.5 to +0.5 V	2	136.84	34.21
008 (RT dried)	100:0	1(cover)	0 - 1 V	2	104.34	26.085

008 (Oven)	100:0	1(cover)	-0.5 to +0.5 V	2	150.34	37.585
008 (Oven)	100:0	1(cover)	0 - 1 V	2	108.18	27.045
009 (0.5 h)	100:0	1(cover)	-0.5 to +0.5 V	2	26.5	6.625
009 (0.5 h)	100:0	1(cover)	0 - 1 V	2	16.52	4.13
009 (1 h)	100:0	1(cover)	-0.5 to +0.5 V	2	83.32	20.83
009 (1 h)	100:0	1(cover)	0 - 1 V	2	59.72	14.93
009 (2 h)	100:0	1(cover)	-0.5 to +0.5 V	2	68.48	17.12
009 (2 h)	100:0	1(cover)	0 - 1 V	2	40.94	10.235
009 (3 h)	100:0	1(cover)	-0.5 to +0.5 V	2	62.68	15.67
009 (3 h)	100:0	1(cover)	0 - 1 V	2	46.14	11.535
009 (6 h)	100:0	1(cover)	-0.5 to +0.5 V	2	50.3	12.575
009 (6 h)	100:0	1(cover)	0 - 1 V	2	32.08	8.02
009 (6 h)	100:0	1(cover)	-0.5 to +0.5 V	2	58.18	14.545
009 (6 h)	100:0	1(cover)	0 - 1 V	2	30.1	7.525
009 (6 h)	100:0	1 (ink)	-0.5 to +0.5 V	2	141.46	35.365
009 (6 h)	100:0	1 (ink)	0 - 1 V	2	96.1	24.025
010 (RT)	100:0	1 (ink)	-0.5 to +0.5 V	2	105.78	26.445
010 (RT)	100:0	1 (ink)	0 - 1 V	2	83.3	20.825
010 (Oven)	100:0	1 (ink)	-0.5 to +0.5 V	2	86.26	21.565
010 (Oven)	100:0	1 (ink)	0 - 1 V	2	71.24	17.81

Table S2. Areal capacitance and gravimetric-specific capacitance for rGOs & its composites.

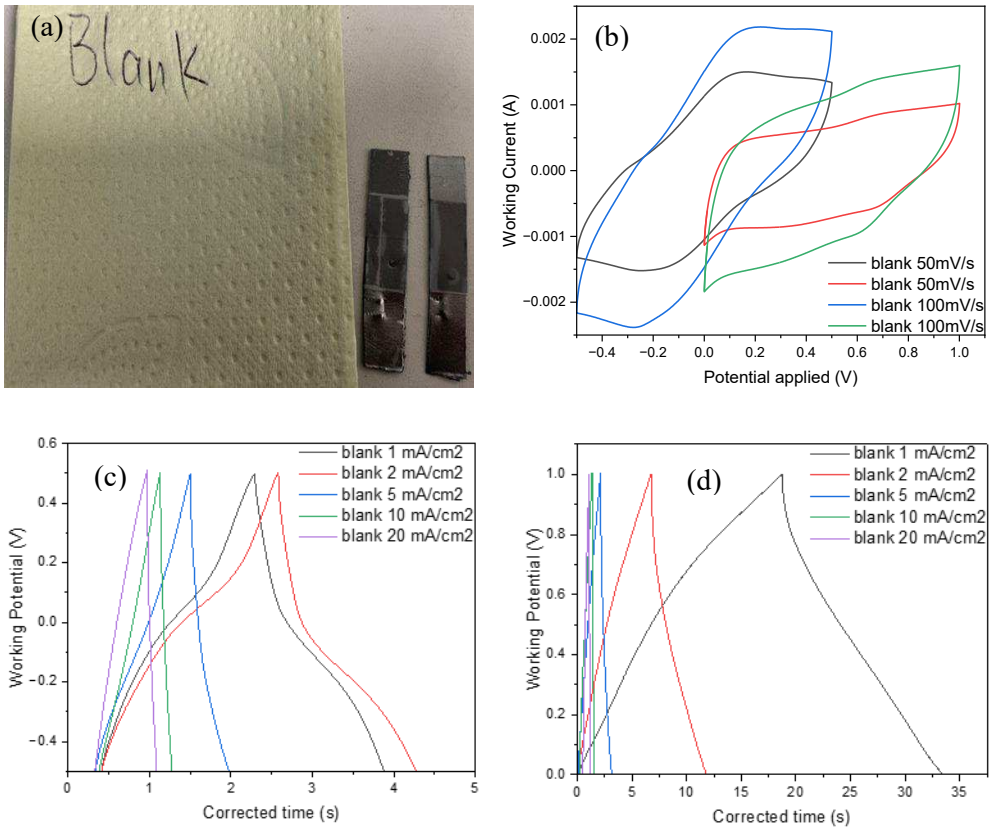

Figure. S1. a) Blank electrodes (unmodified graphite flakes) b) CV test of blank electrodes c) GCD test of blank electrodes, -0.5 to +0.5 V d) GCD test of blank electrodes, 0 to 1 V

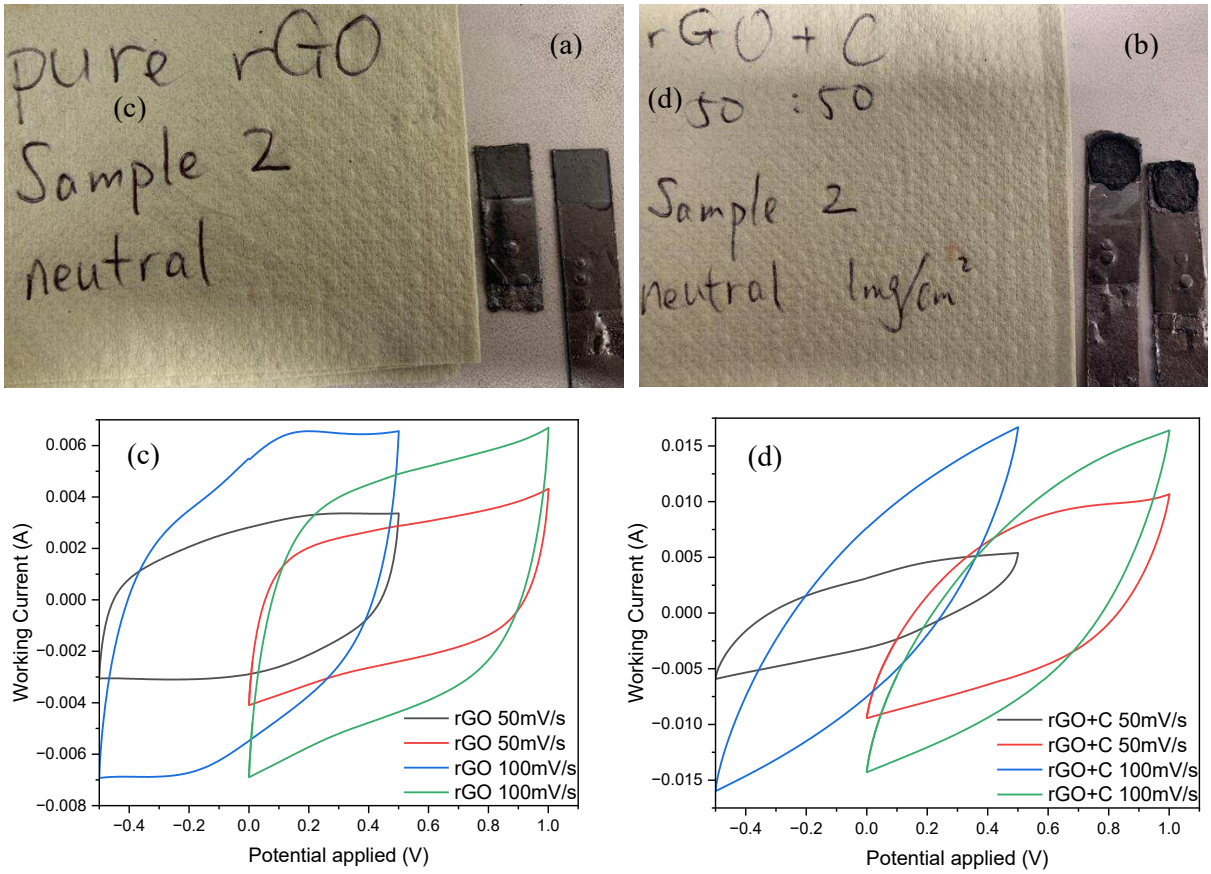

Figure. S2. a) 002 rGO on graphite b) 002 rGO: CNF (50:50) on graphite c) CVs of 002 rGO d) CVs of 002 rGO: CNF 50:50. (All fabrications have Nafion covering)

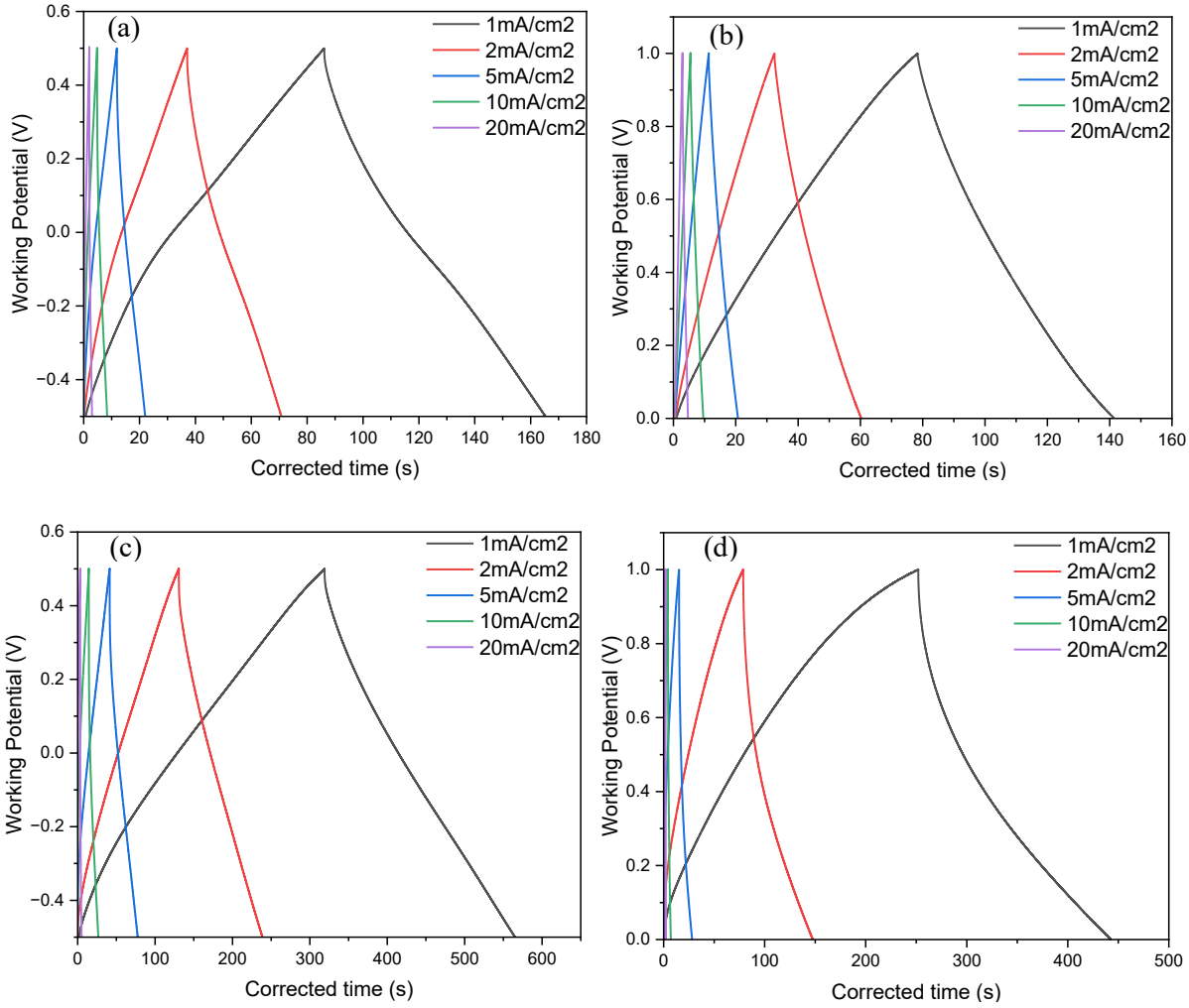

Figure. S3. GCDs of 002 rGO a) -0.5 to +0.5 V b) 0 to 1 V; GCDs of 002 rGO: CNF (50:50) c) -0.5 to +0.5 V d) 0 to 1 V

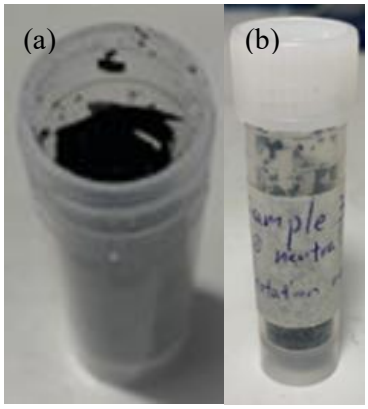

Figure. S4. a) Dried 003 rGO b) Storage for 003 rGO

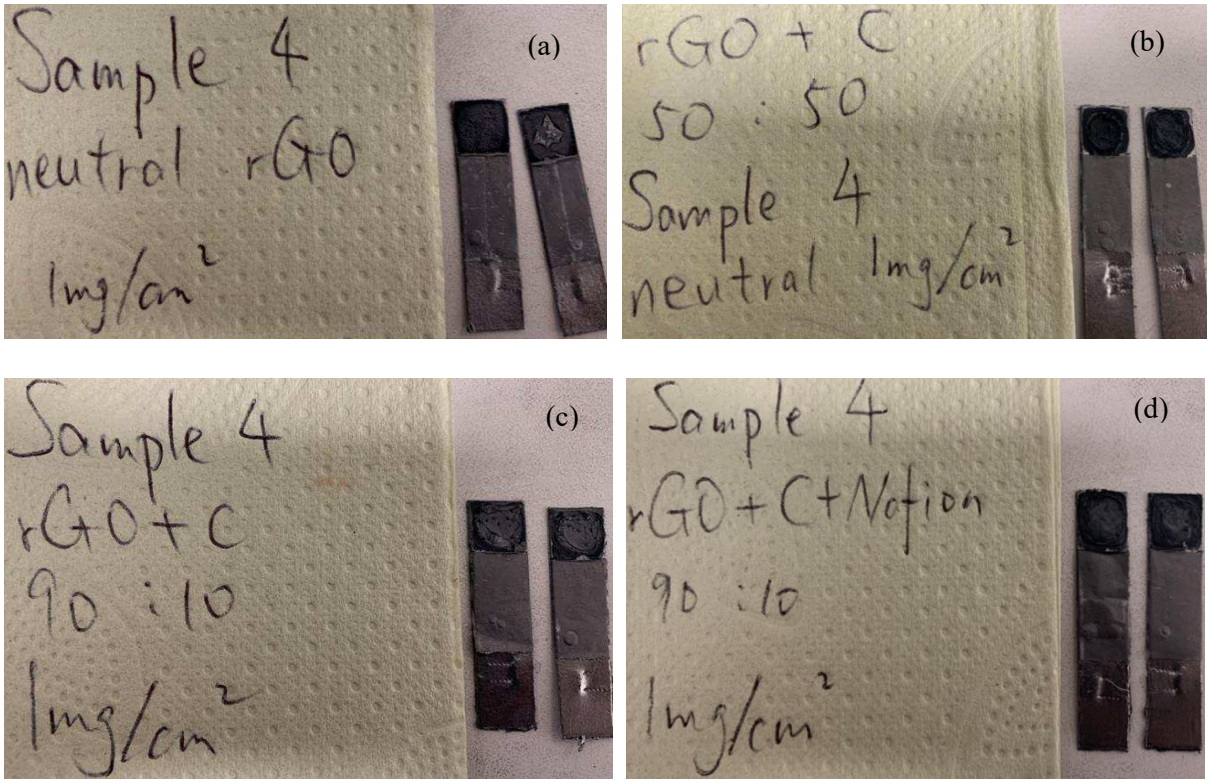

Figure. S5. a) 004 rGO on graphite b) 004 rGO: CNF (50:50) on graphite c) 004 rGO: CNF (90:10) on graphite. (a, b, c fabrications have Nafion covering). d) 004 rGO: CNF (90:10) on graphite / Nafion ink

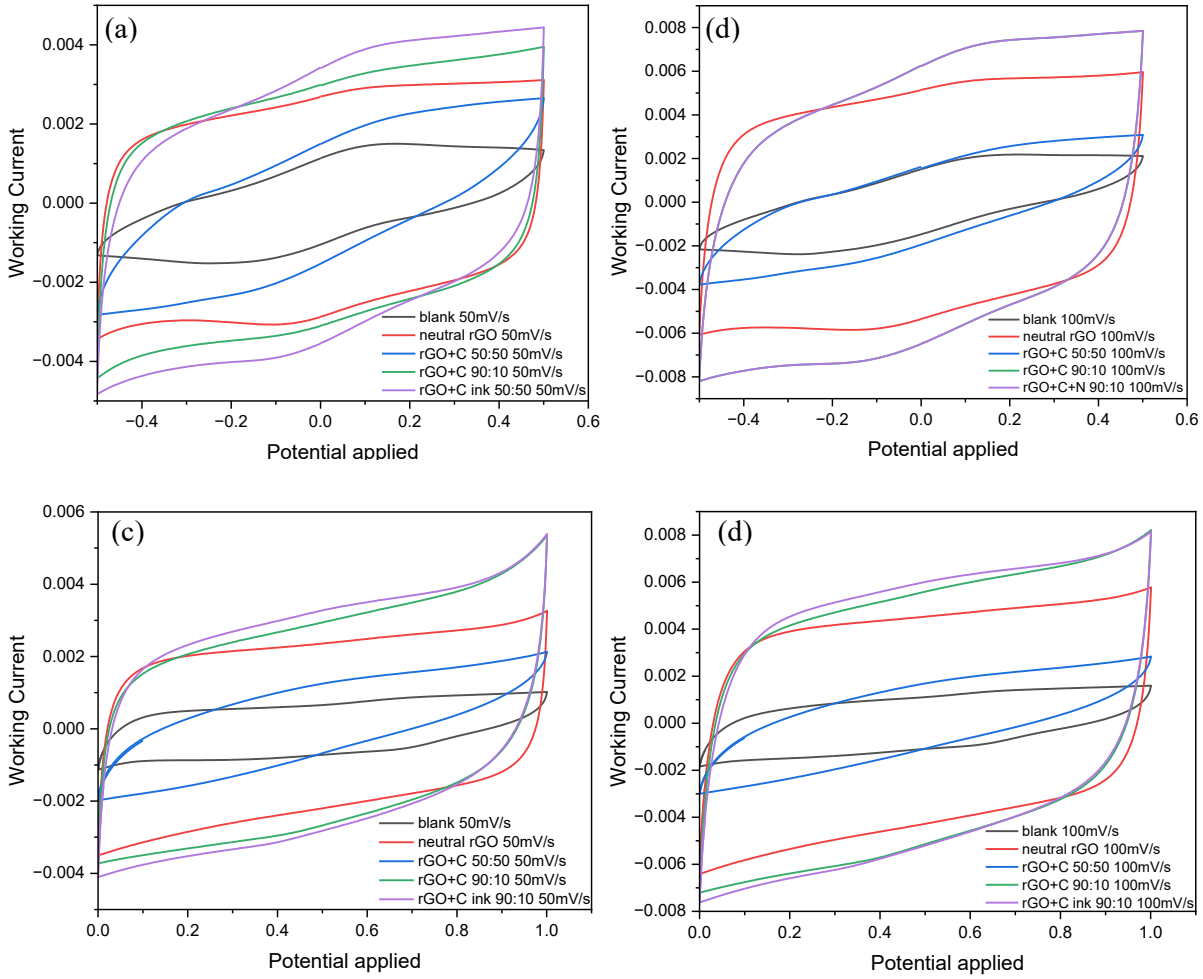

Figure. S6. Comparison of CVs of 004 rGO on graphite, 004 rGO: CNF (50:50) on graphite, 004 rGO: CNF (90:10) on graphite a) 50 mV/s, -0.5 to +0.5 V b) 100 mV/s, -0.5 to +0.5 V c) 50 mV/s, 0 to 1 V d) 100 mV/s, 0 to 1 V.

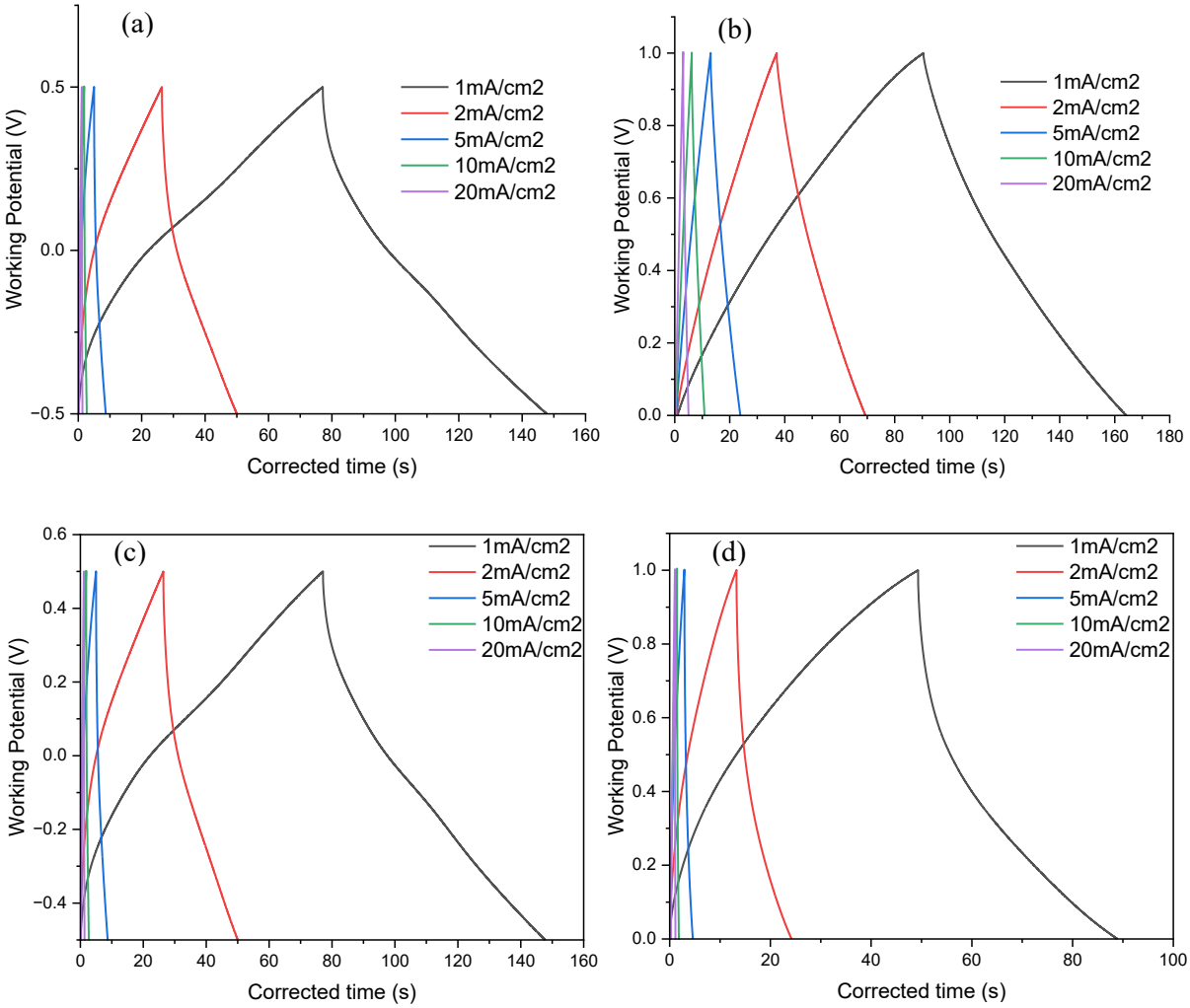

Figure. S7. GCDs at different current densities: for 004 rGO on graphite a) -0.5 to +0.5 V b) 0 to 1 V; for 004 rGO: CNF (50:50) on graphite c) -0.5 to +0.5 V d) 0 to 1 V.

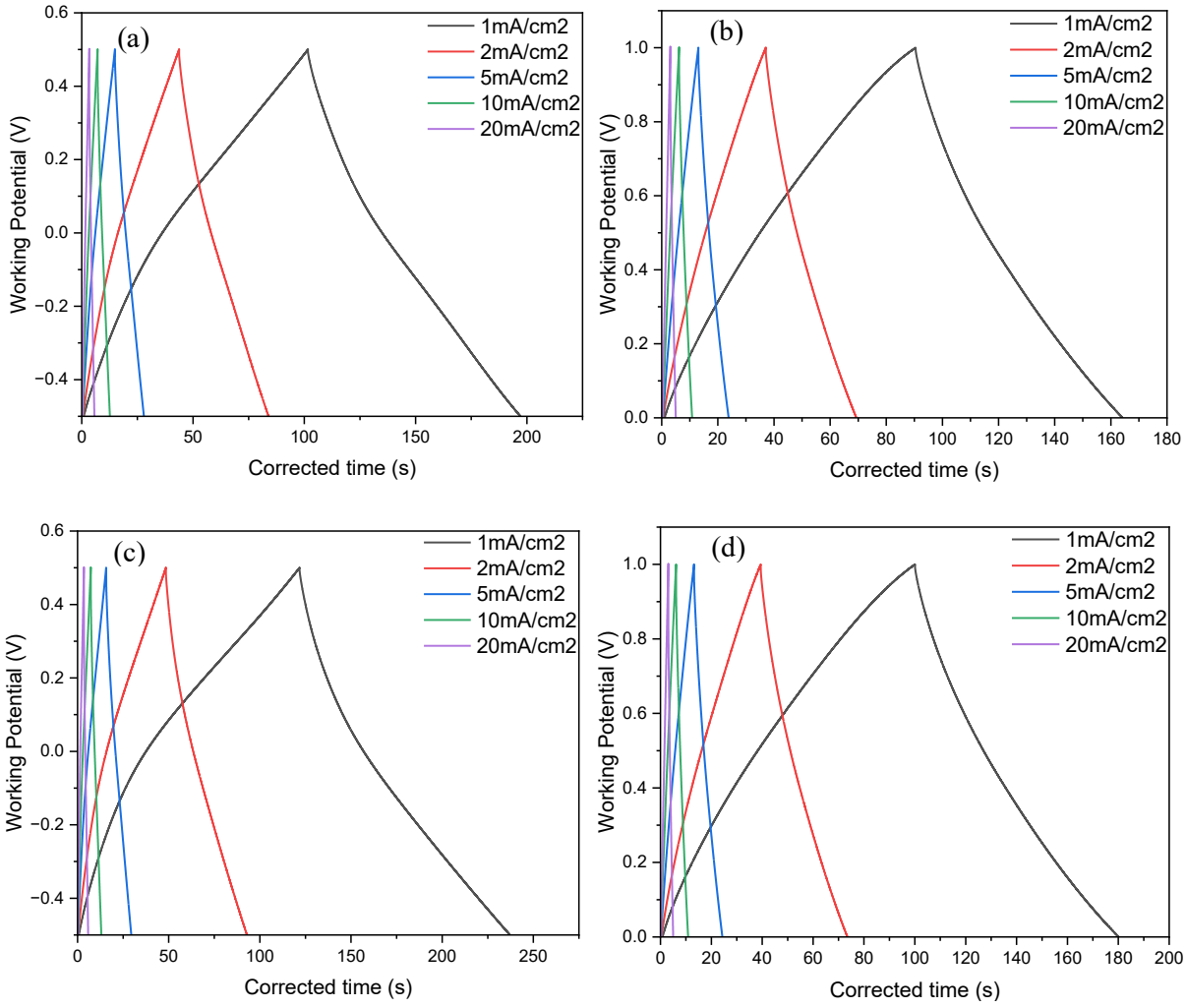

Figure. S8. GCDs at different current densities for 004 rGO: CNF (90:10) on graphite: No Nafion a) -0.5 to +0.5 V b) 0 to 1 V; Nafion covering c) -0.5 to +0.5 V d) 0 to 1 V.

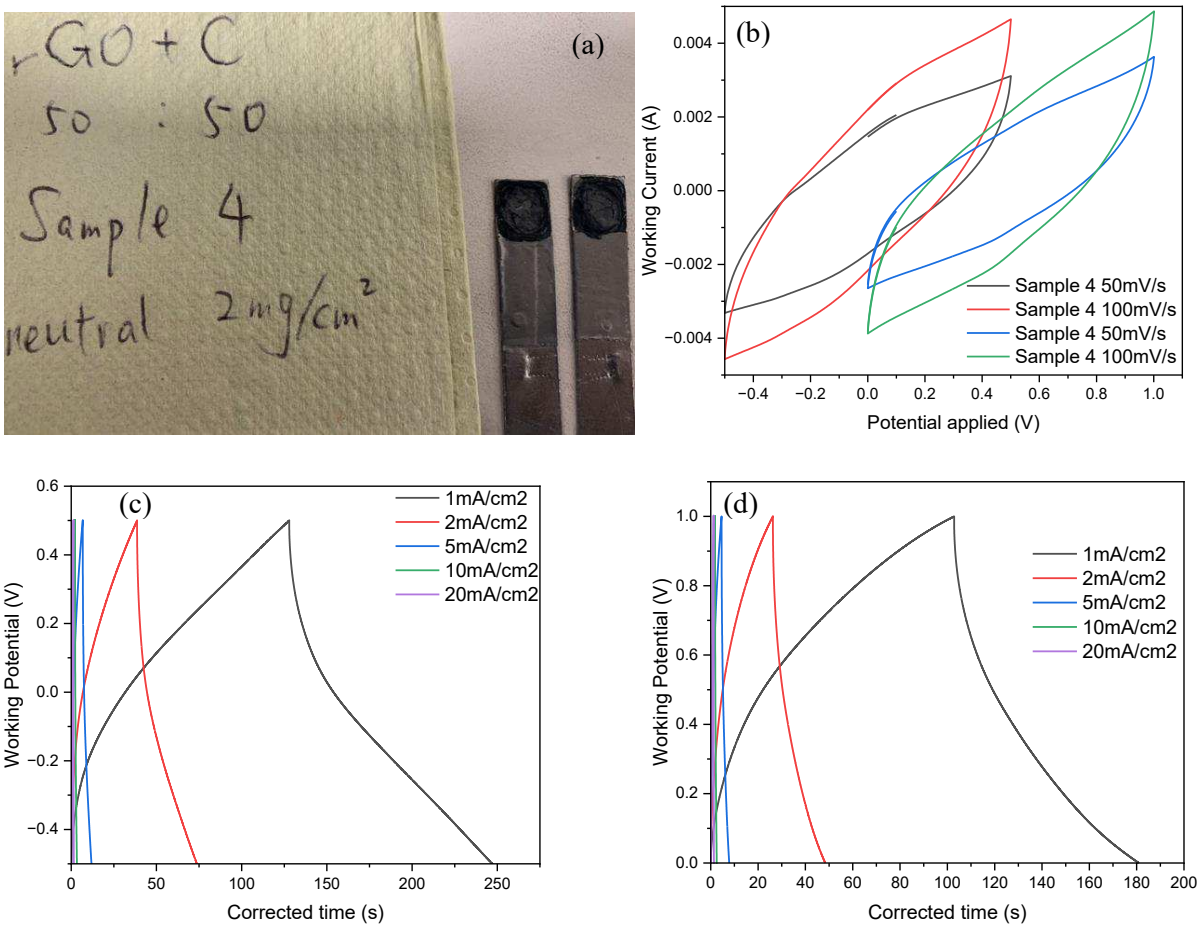

Figure. S9. a) 004 rGO: CNF (50:50) on graphite / 2 mg (Nafion covering) b) CVs. GCDs at c) -0.5 to +0.5 V d) 0 to 1 V

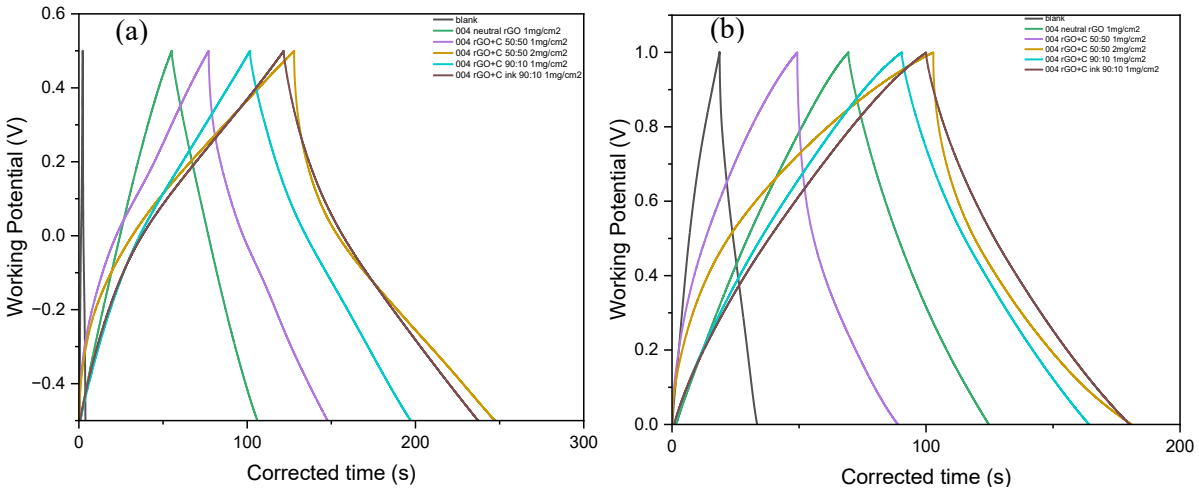

Figure. S10. GCDs of 004 rGO, 004 rGO: CNF (50:50) / 1mg, 2 mg and (90:10) / 1mg a) -0.5 to +0.5 V b) 0 to 1 V

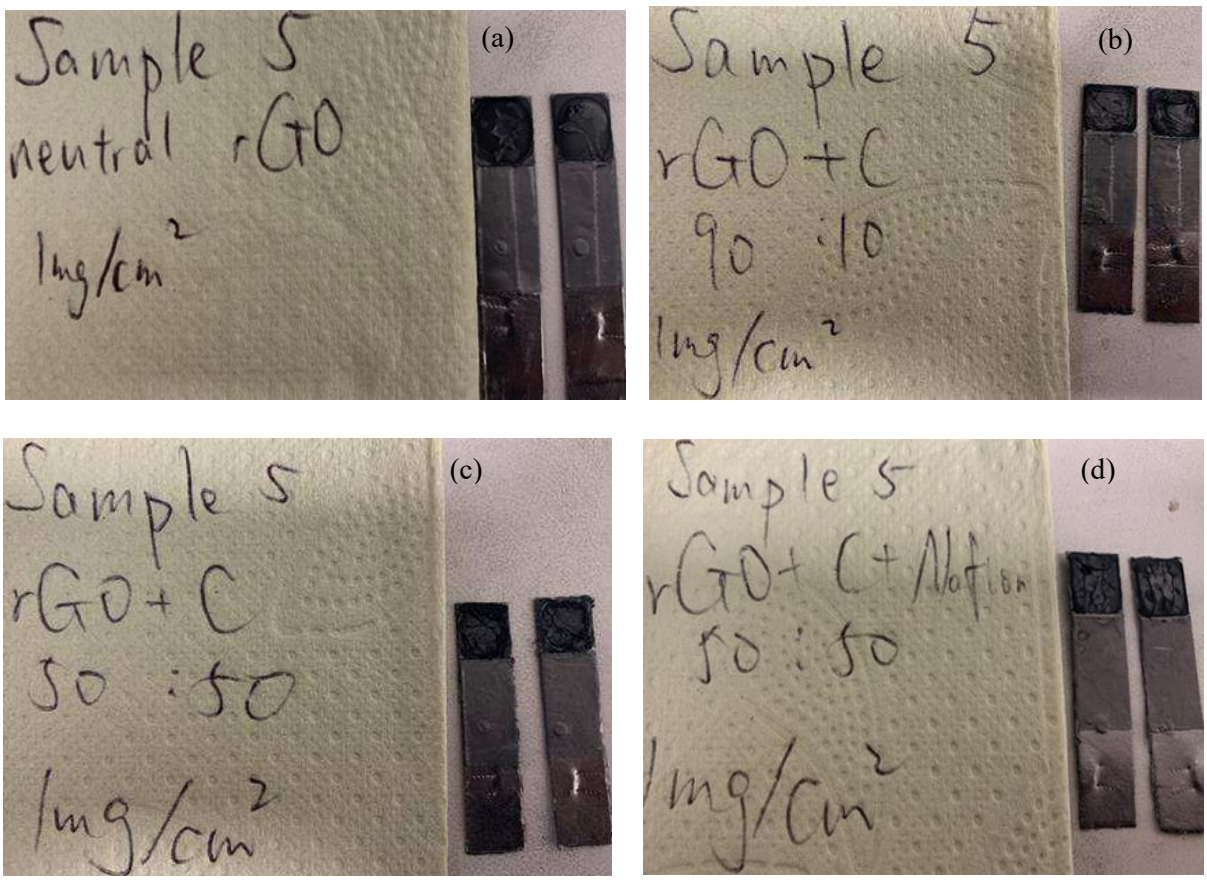

Figure. S11. a) 005 rGO on graphite b) 005 rGO: CNF (90:10) on graphite c) 005 rGO: CNF (50:50) on graphite (a, b, c have Nafion covering) d) 005 rGO: CNF (50:50) on graphite / Nafion ink

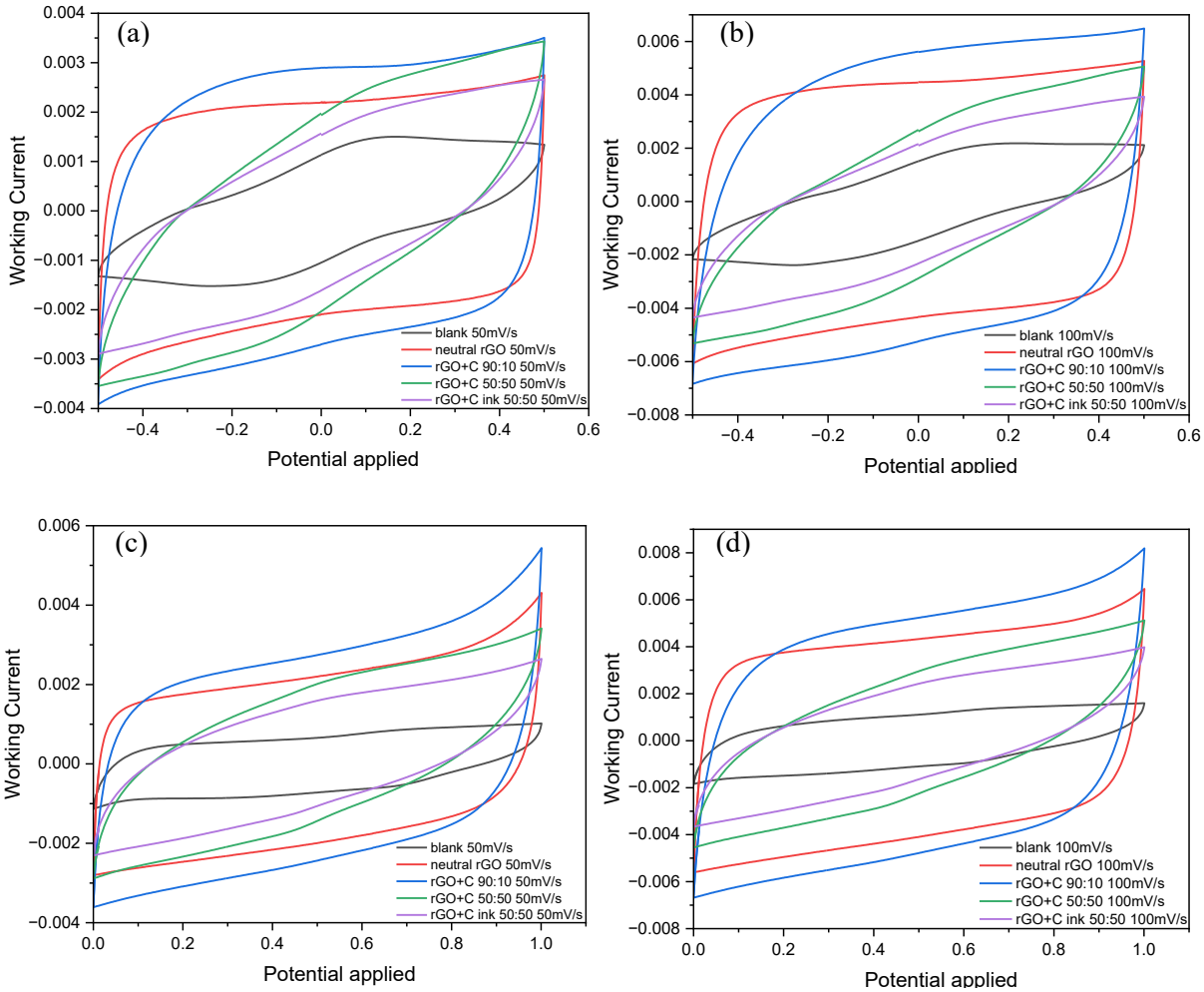

Figure. S12. Comparison of CVs of 005 rGO on graphite, 005 rGO: CNF (50:50) on graphite, 005 rGO: CNF (90:10) on graphite a) 50 mV/s, -0.5 to +0.5 V b) 100 mV/s, -0.5 to +0.5 V c) 50 mV/s, 0 to 1 V d) 100 mV/s, 0 to 1 V.

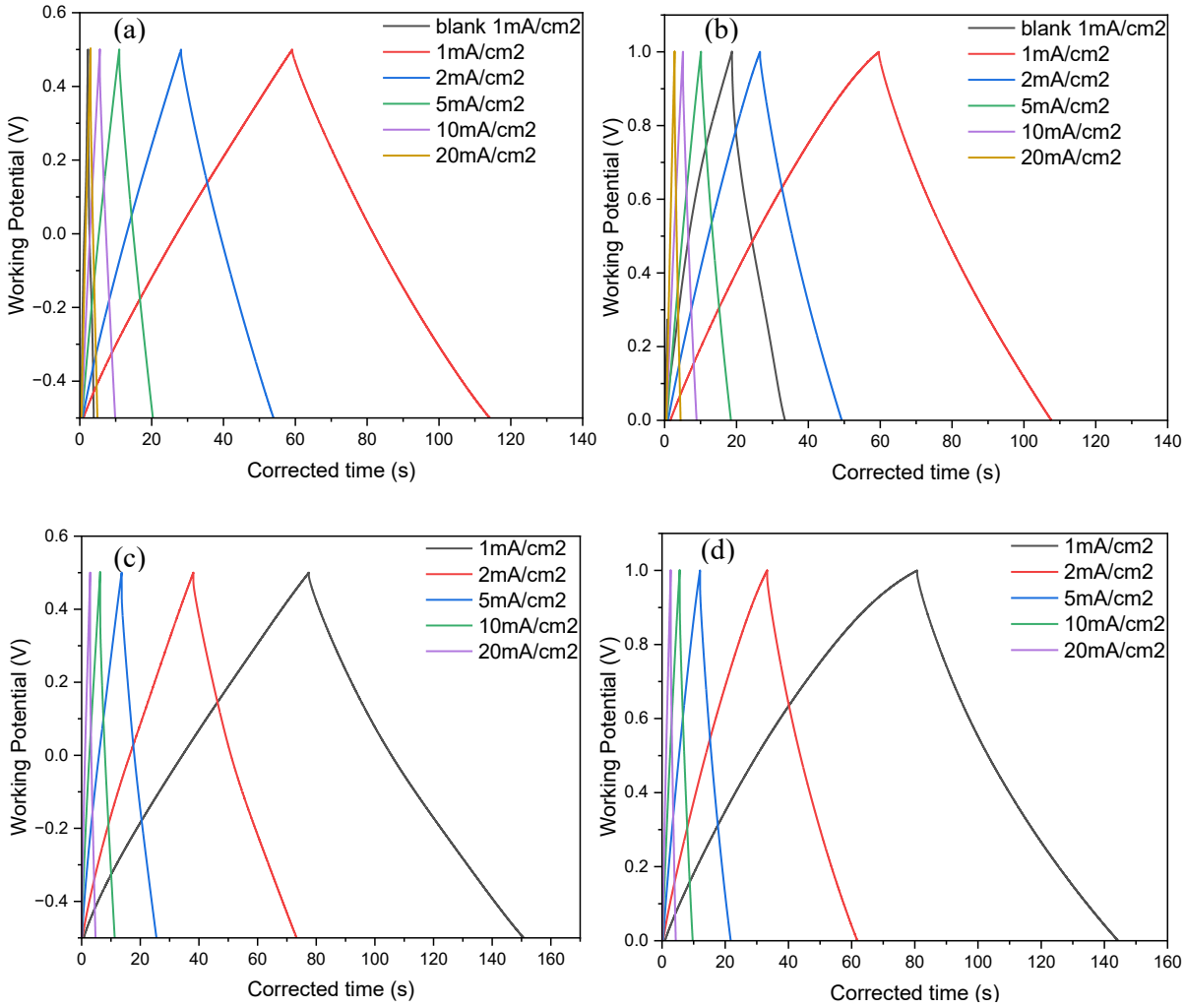

Figure. S13. GCDs at different current densities: for 005 rGO on graphite a) -0.5 to +0.5 V b) 0 to 1 V; for 005 rGO: CNF (90:10) on graphite c) -0.5 to +0.5 V d) 0 to 1 V

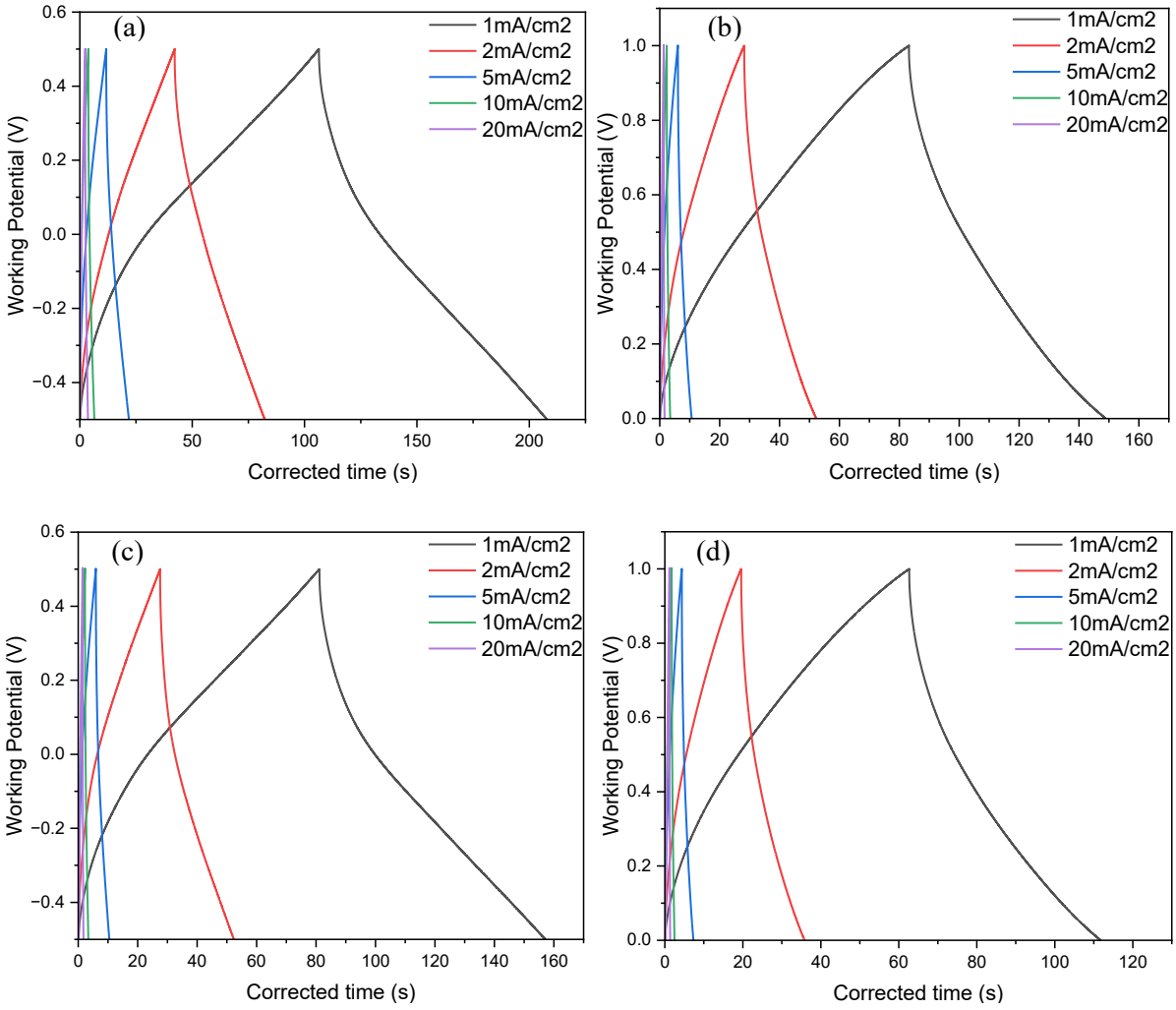

Figure. S14. GCDs at different current densities for 005 rGO: CNF (50:50) on graphite: Nafion covering a) -0.5 to +0.5 V b) 0 to 1 V; Nafion ink c) -0.5 to +0.5 V d) 0 to 1 V

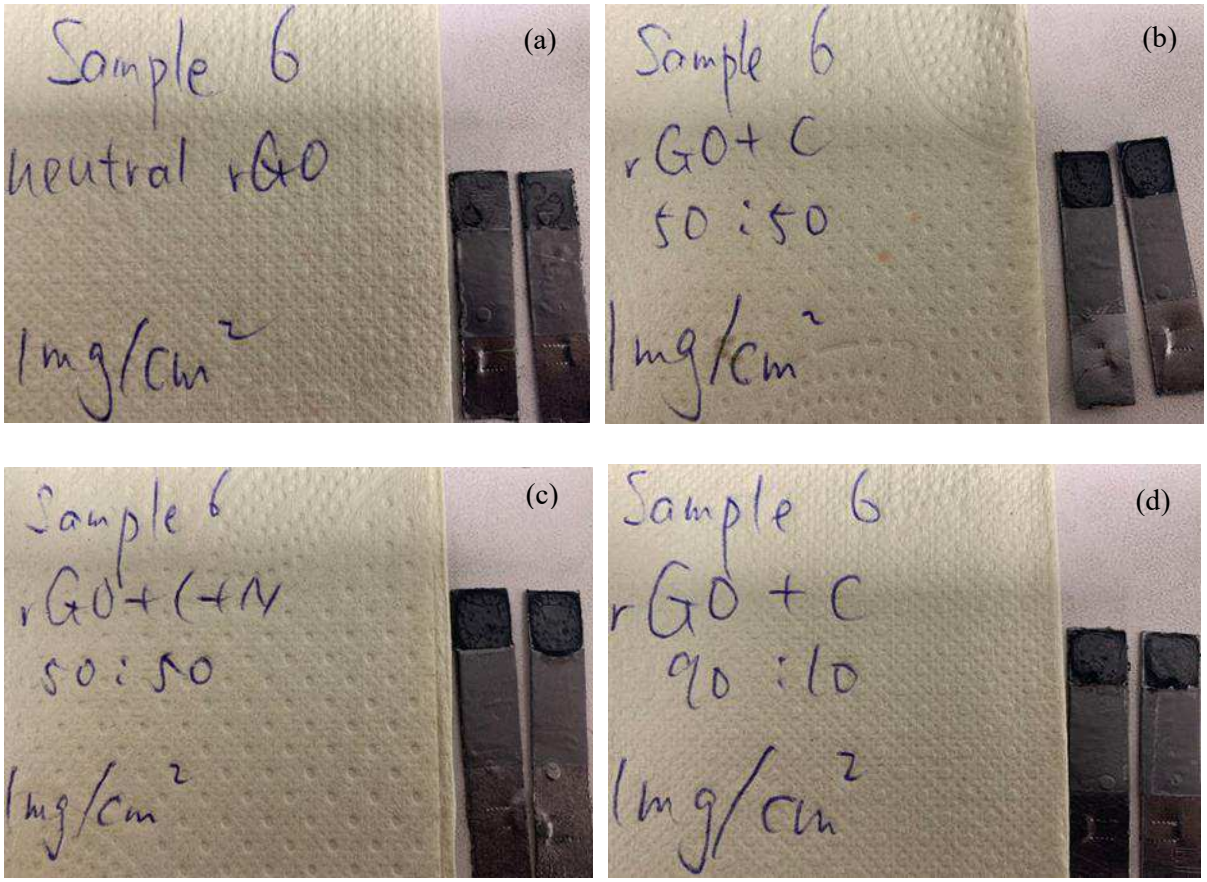

Figure. S15. a) 006 rGO on graphite, b) 006 rGO: CNF (50:50) on graphite. (a, b have Nafion covering). c) 006 rGO: CNF (50:50) on graphite / Nafion ink d) 006 rGO: CNF (90:10) on graphite (Nafion covering)

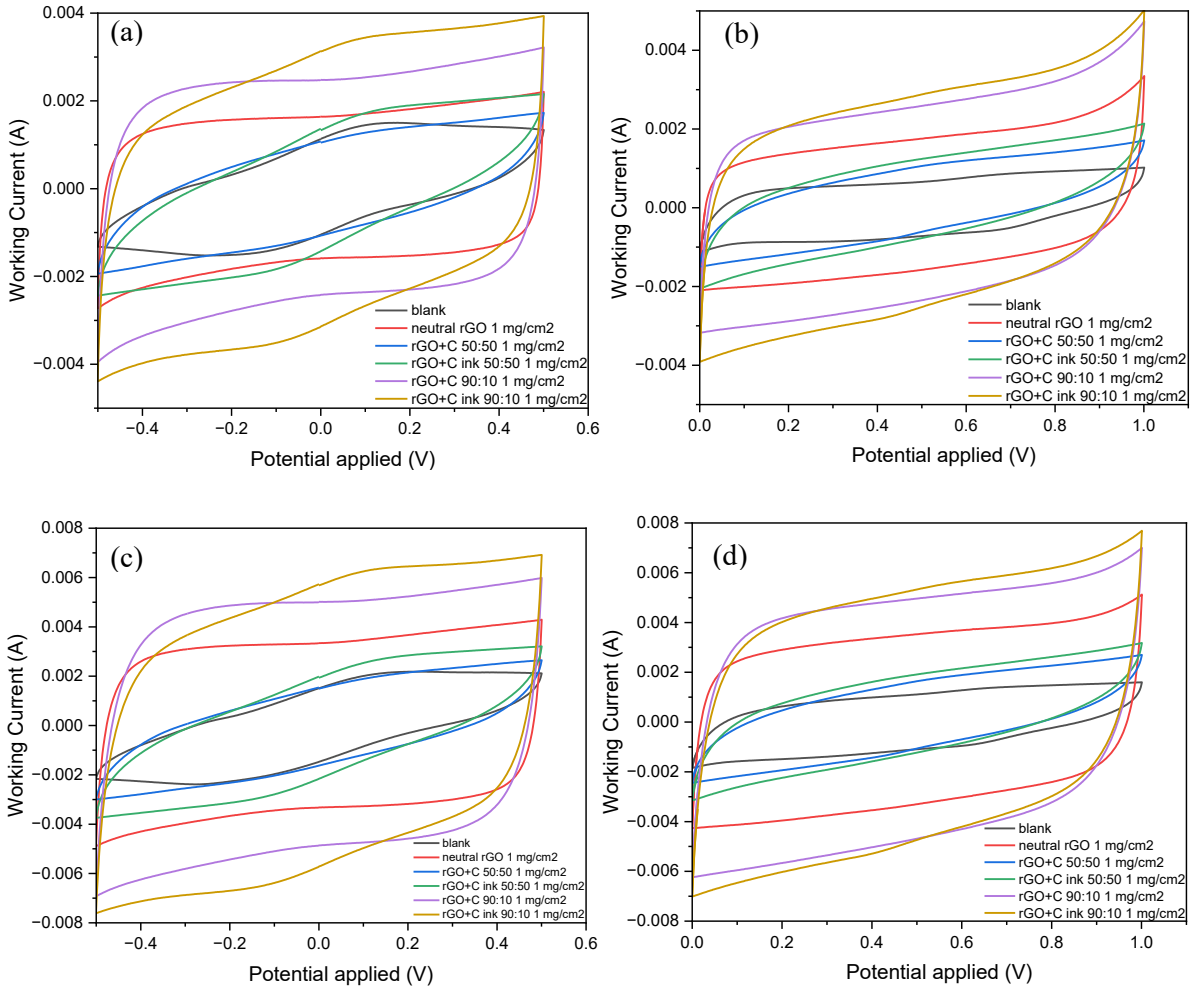

Figure. S16. Comparison of CVs of 006 rGO on graphite, 006 rGO: CNF (50:50) on graphite, 006 rGO: CNF (90:10) on graphite a) 50 mV/s, -0.5 to +0.5 V b) 50 mV/s, 0 to 1 V c) 100 mV/s, -0.5 to +0.5 V d) 100 mV/s, 0 to 1 V.

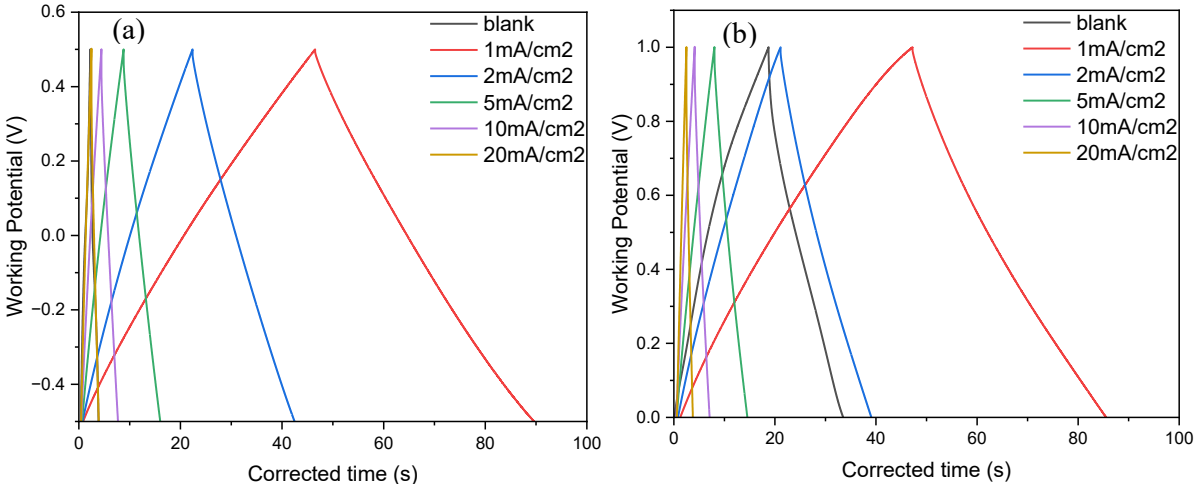

Figure. S17. GCDs at different current densities for 006 rGO on graphite a) -0.5 to +0.5 V b) 0 to 1 V

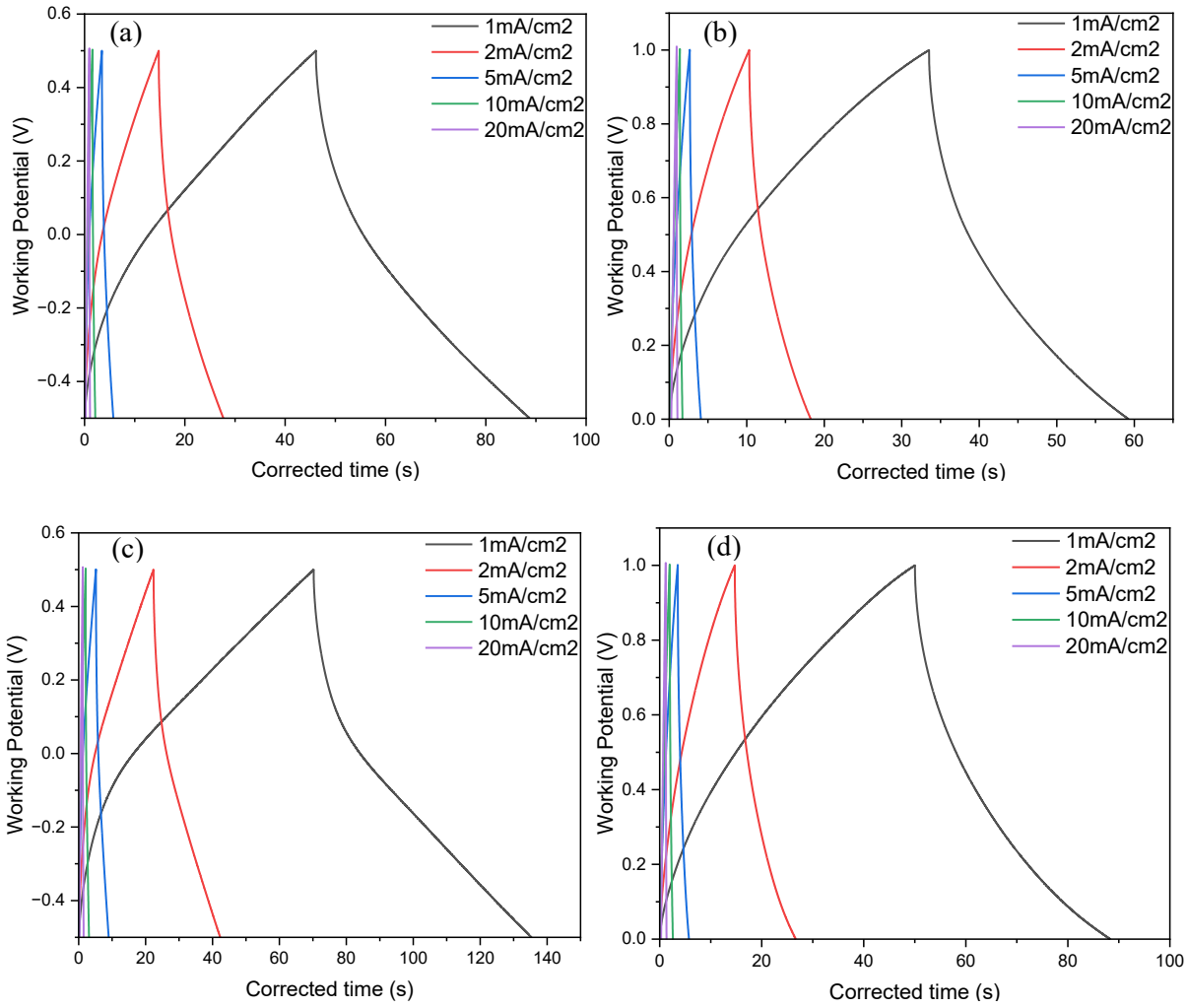

Figure. S18. GCDs at different current densities for 006 rGO: CNF (50:50) on graphite: Nafion covering a) -0.5 to +0.5 V b) 0 to 1 V; Nafion ink c) -0.5 to +0.5 V d) 0 to 1 V

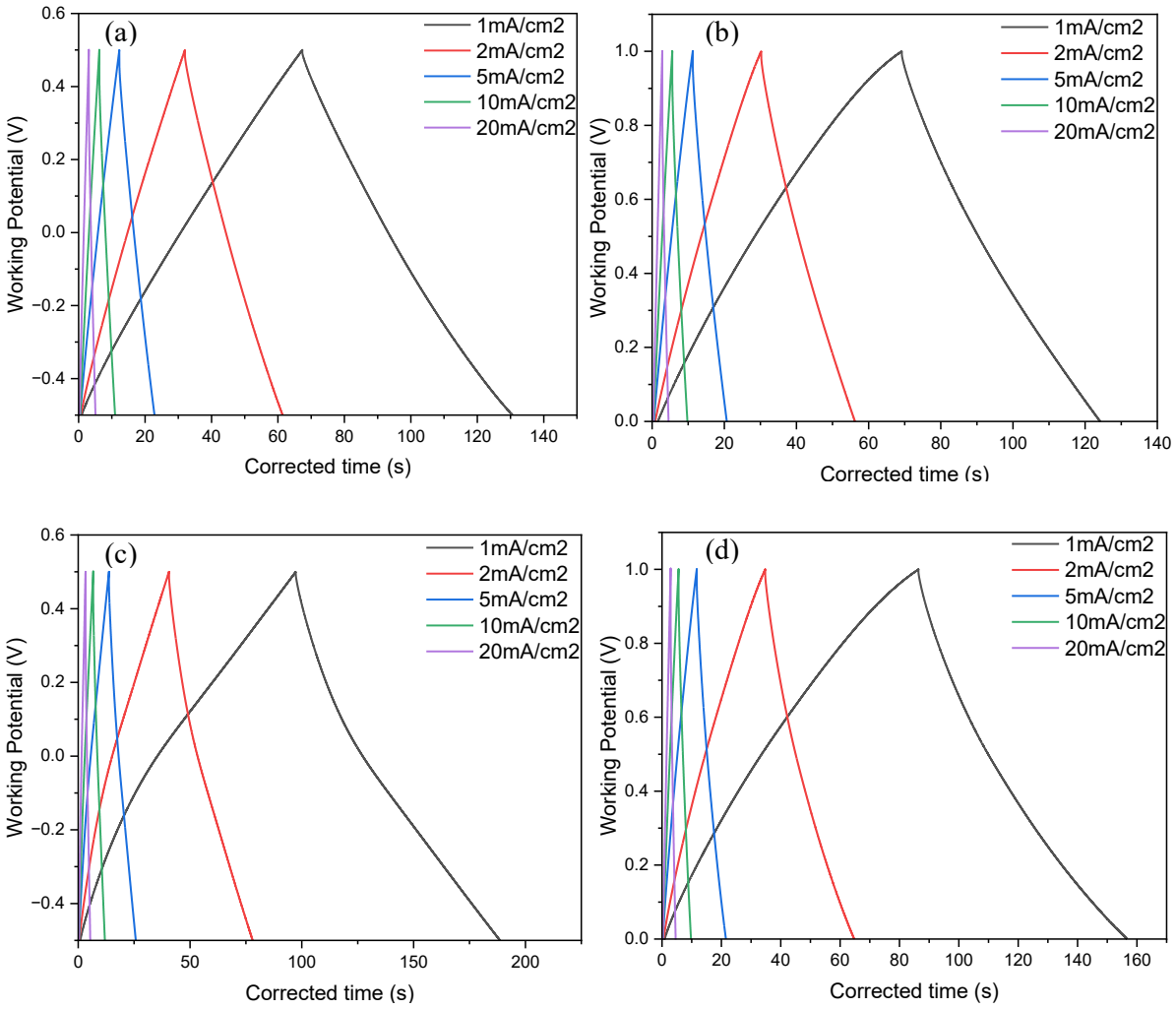

Figure. S19. GCDs at different current densities for 006 rGO: CNF (90:10) on graphite: Nafion covering a) -0.5 to +0.5 V b) 0 to 1 V; Nafion ink c) -0.5 to +0.5 V d) 0 to 1 V

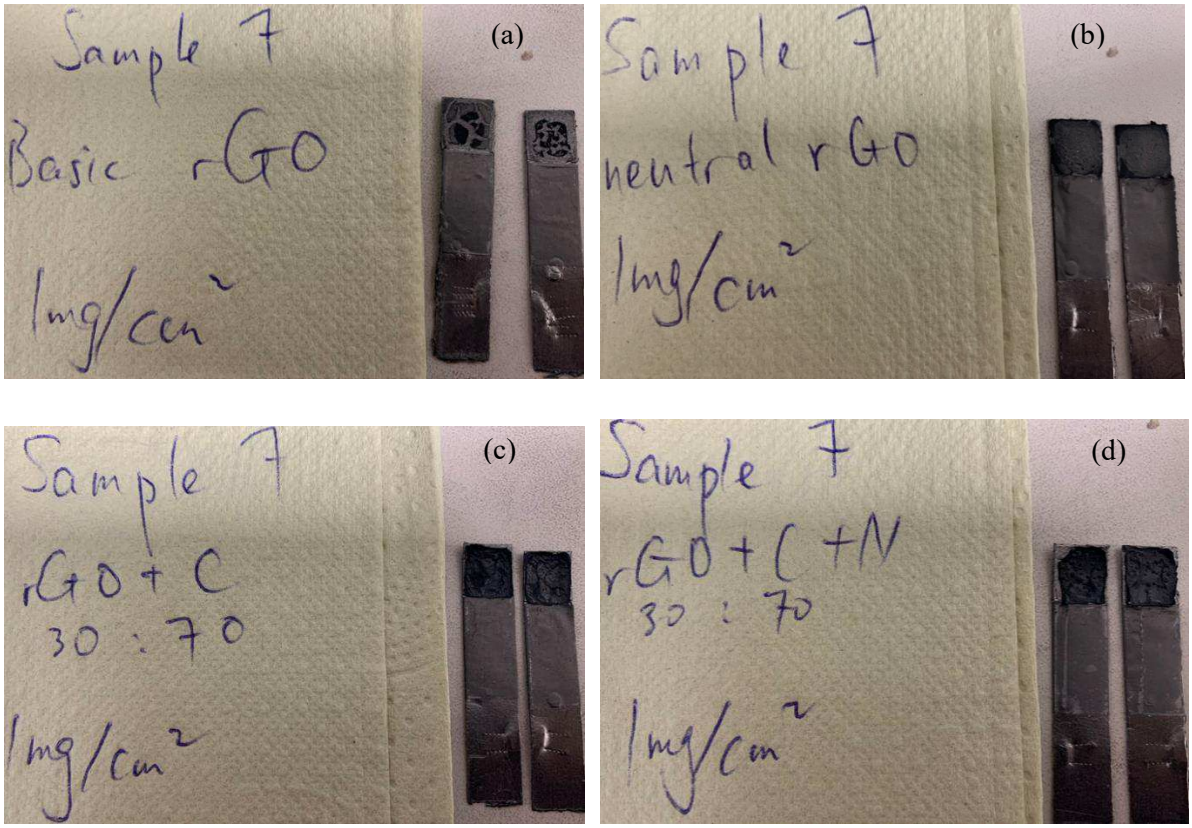

Figure. S20. 007 rGO on graphite: a) alkaline b) non-alkaline (a, b, have Nafion covering); non-alkaline 007 rGO: CNF (30:70) on graphite: c) Nafion covering d) Nafion ink

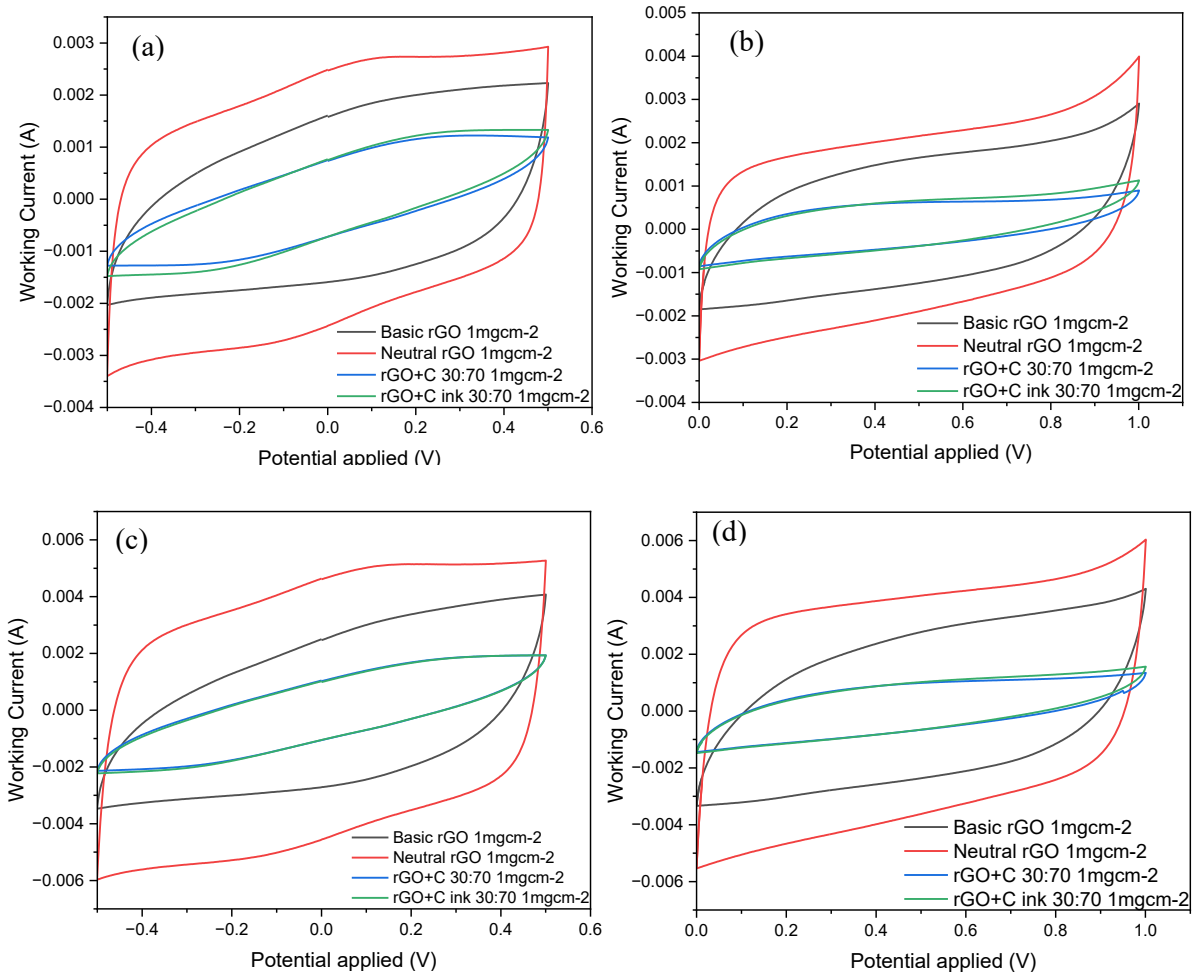

Figure. S21. Comparison of CVs of (alkaline & non-alkaline) 007 rGO on graphite & non-alkaline 007 rGO: CNF (30:70) on graphite (Nafion covering & Nafion ink)) a) 50 mV/s, -0.5 to +0.5 V b) 50 mV/s, 0 to 1 V c) 100 mV/s, -0.5 to +0.5 V d) 100 mV/s, 0 to 1 V

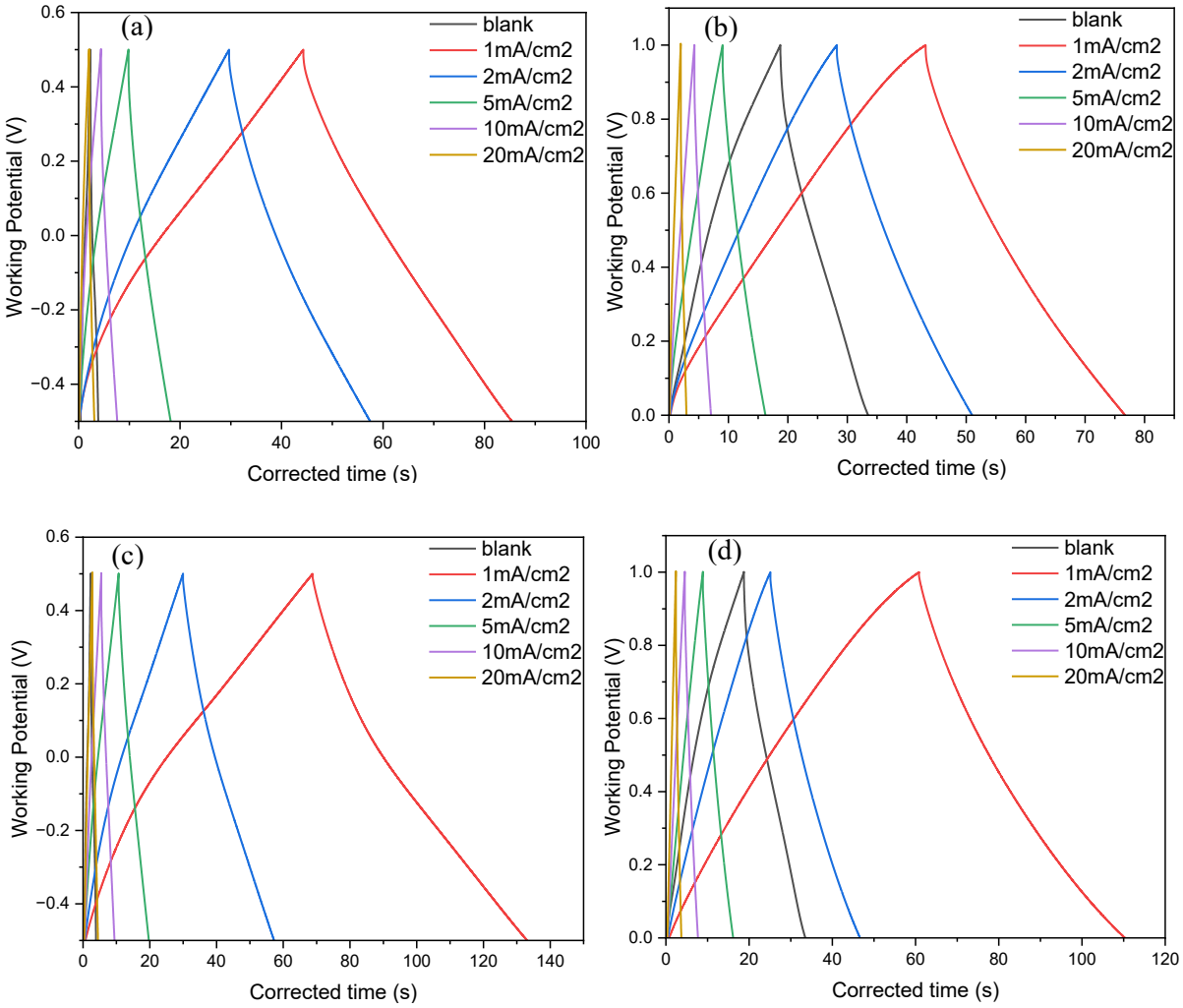

Figure. S22. GCDs at different current densities: for alkaline 007 rGO on graphite a) -0.5 to +0.5 V b) 0 to 1 V; for non-alkaline 007 rGO on graphite c) -0.5 to +0.5 V d) 0 to 1 V

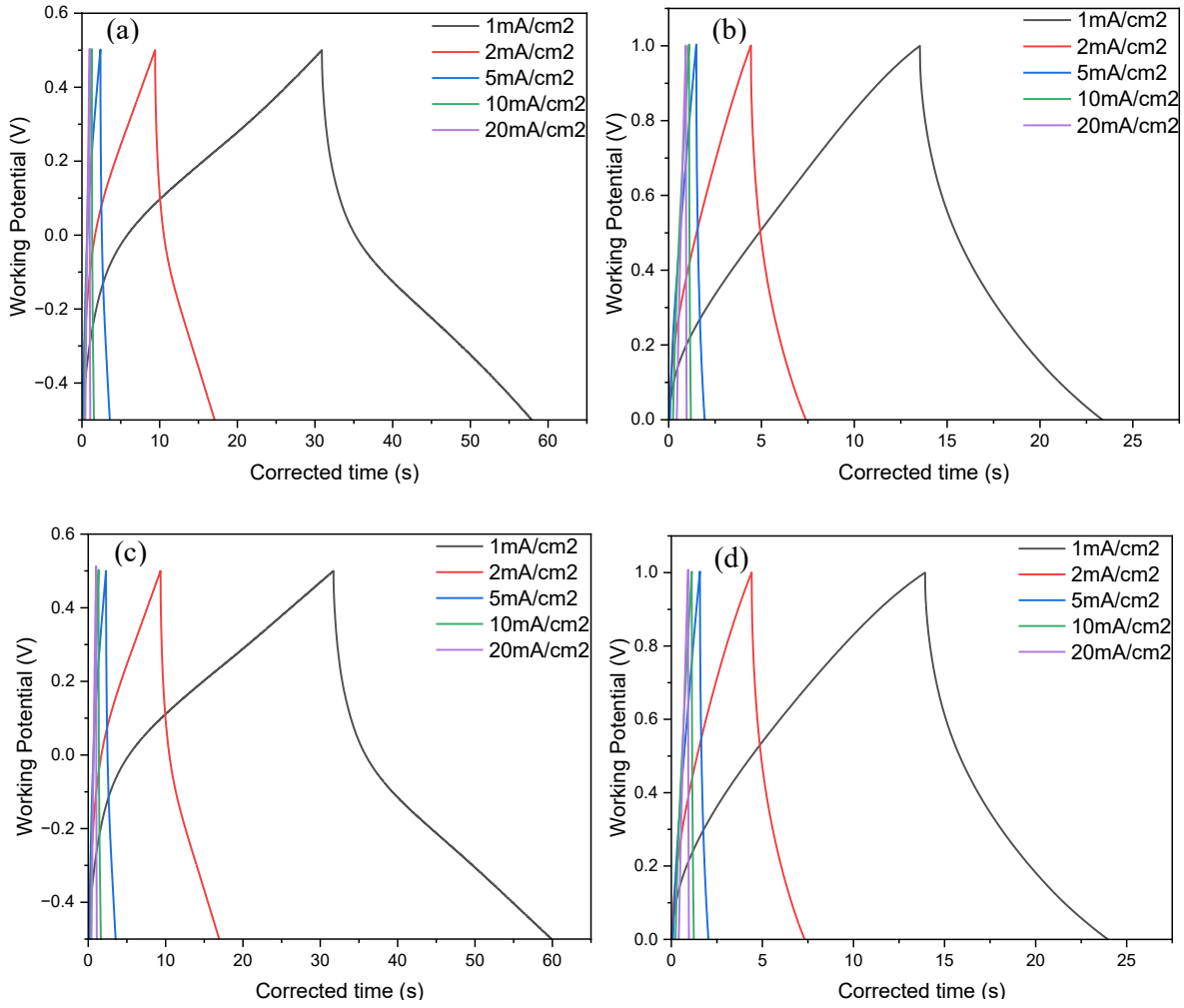

Figure. S23. GCDs at different current densities for non-alkaline 007 rGO: CNF (30:70) on graphite: Nafion covering a) -0.5 to +0.5 V b) 0 to 1 V; Nafion ink c) -0.5 to +0.5 V d) 0 to 1 V

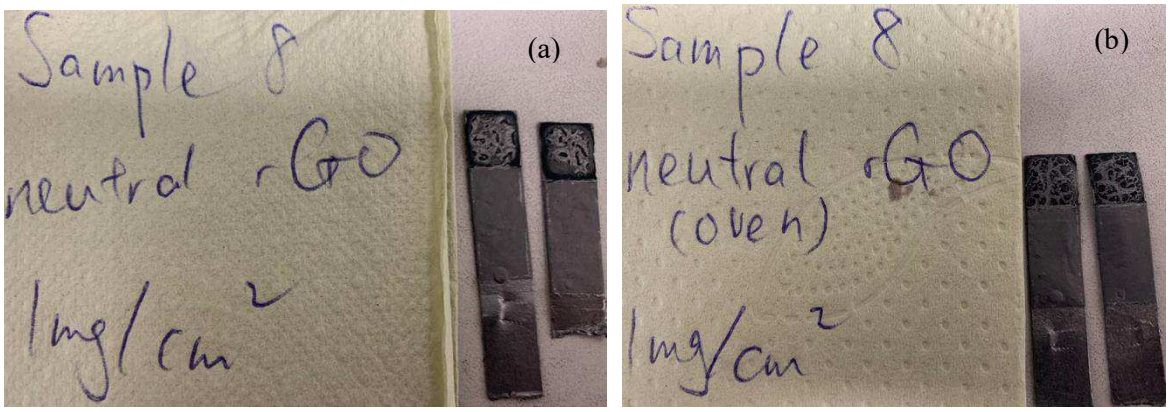

Figure. S24. 008 rGO on graphite: a) dried at RT b) dried in Oven at 120 °C 1h (a, b have Nafion covering)

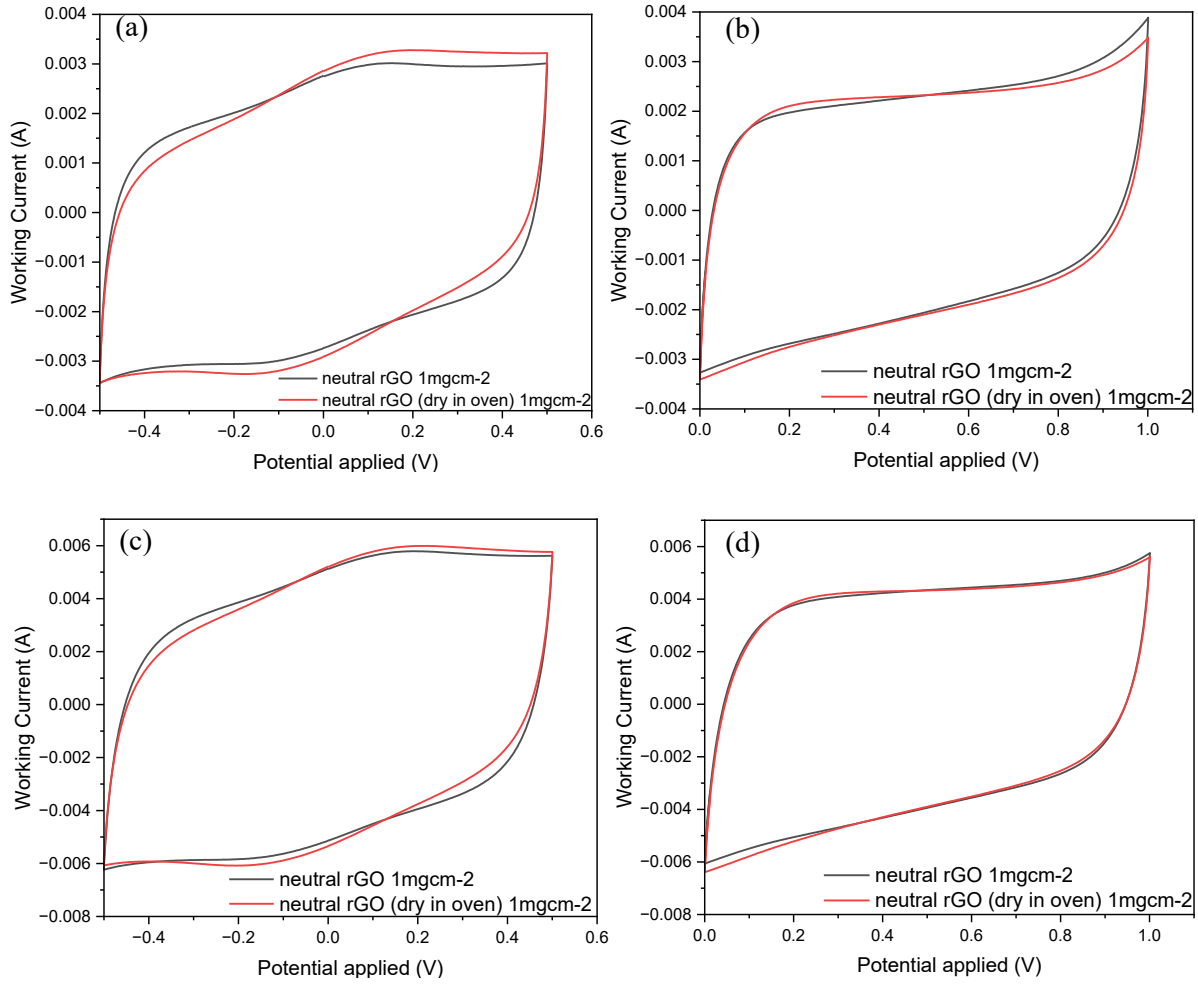

Figure. S25. Comparison of CVs of 008 rGO on graphite (RT & Oven) a) 50 mV/s, -0.5 to +0.5 V b) 50 mV/s, 0 to 1 V c) 100 mV/s, -0.5 to +0.5 V d) 100 mV/s, 0 to 1 V

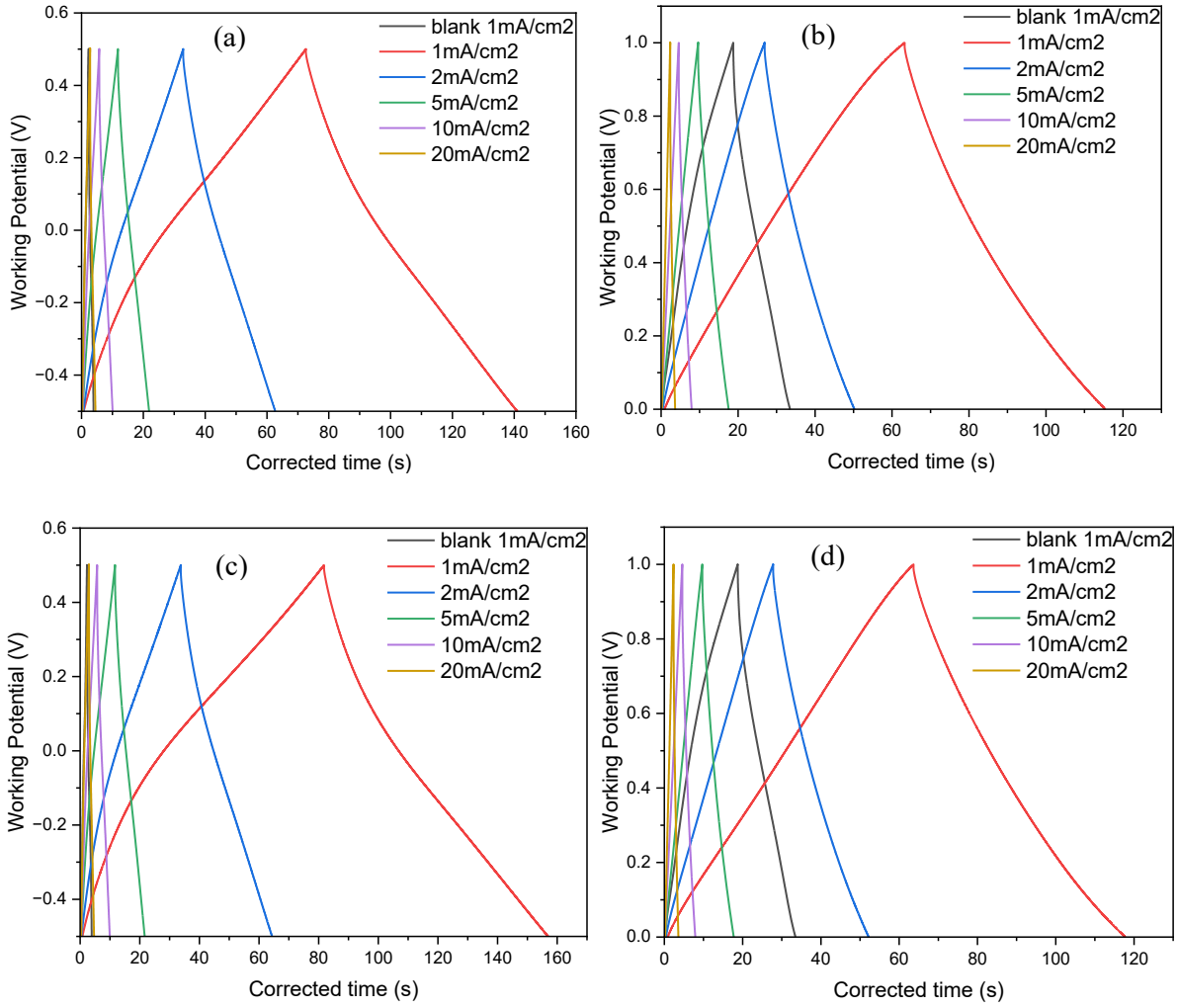

Figure. S26. GCDs at different current densities for 008 rGO on graphite: for RT dried a) -0.5 to +0.5 V b) 0 to 1 V; for Oven dried c) -0.5 to +0.5 V d) 0 to 1 V

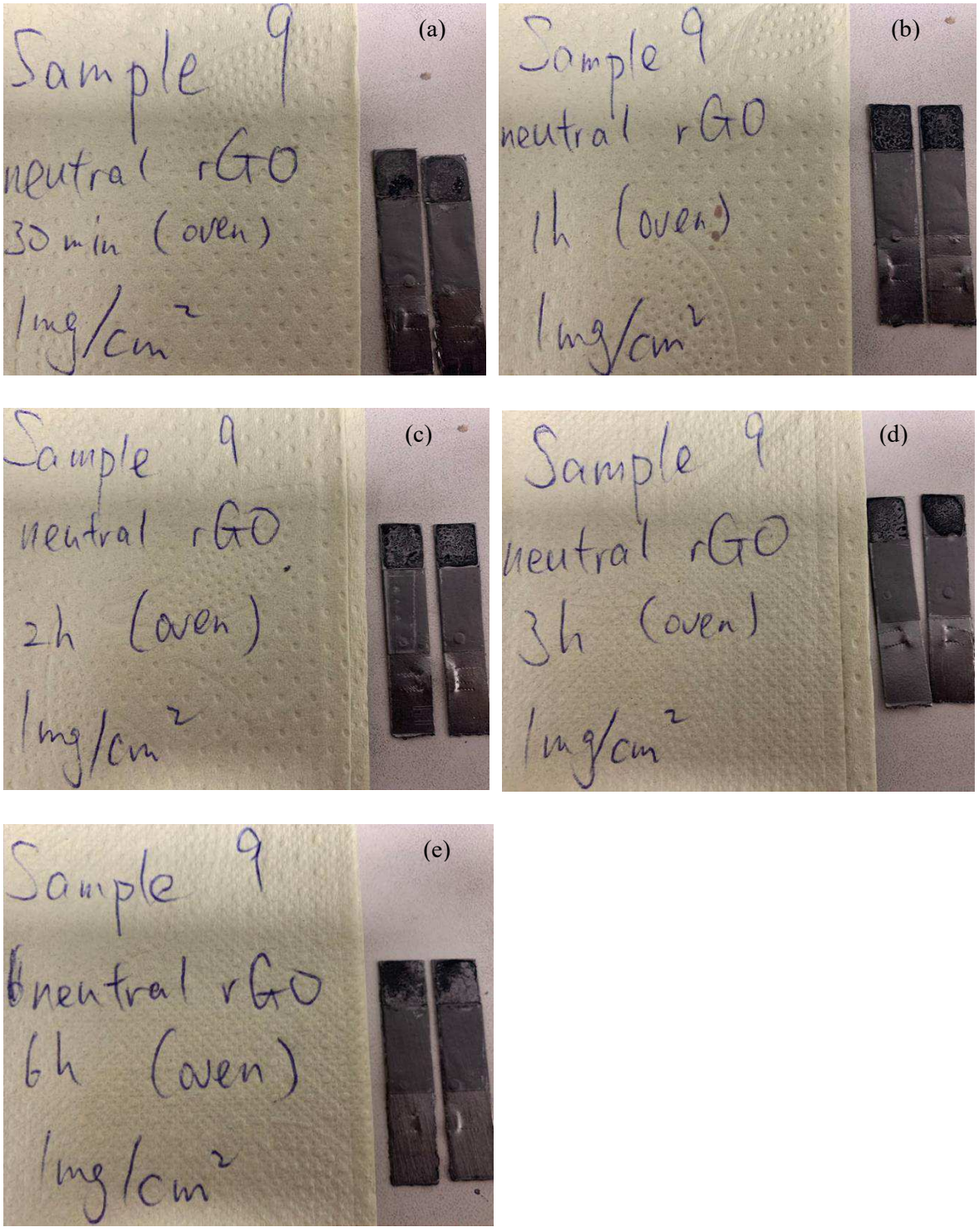

Figure. S27. 009 rGO on graphite dried in Oven: reduced for a) 30 min b) 1 h c) 2h d) 3h e) 6h (All having Nafion covering)

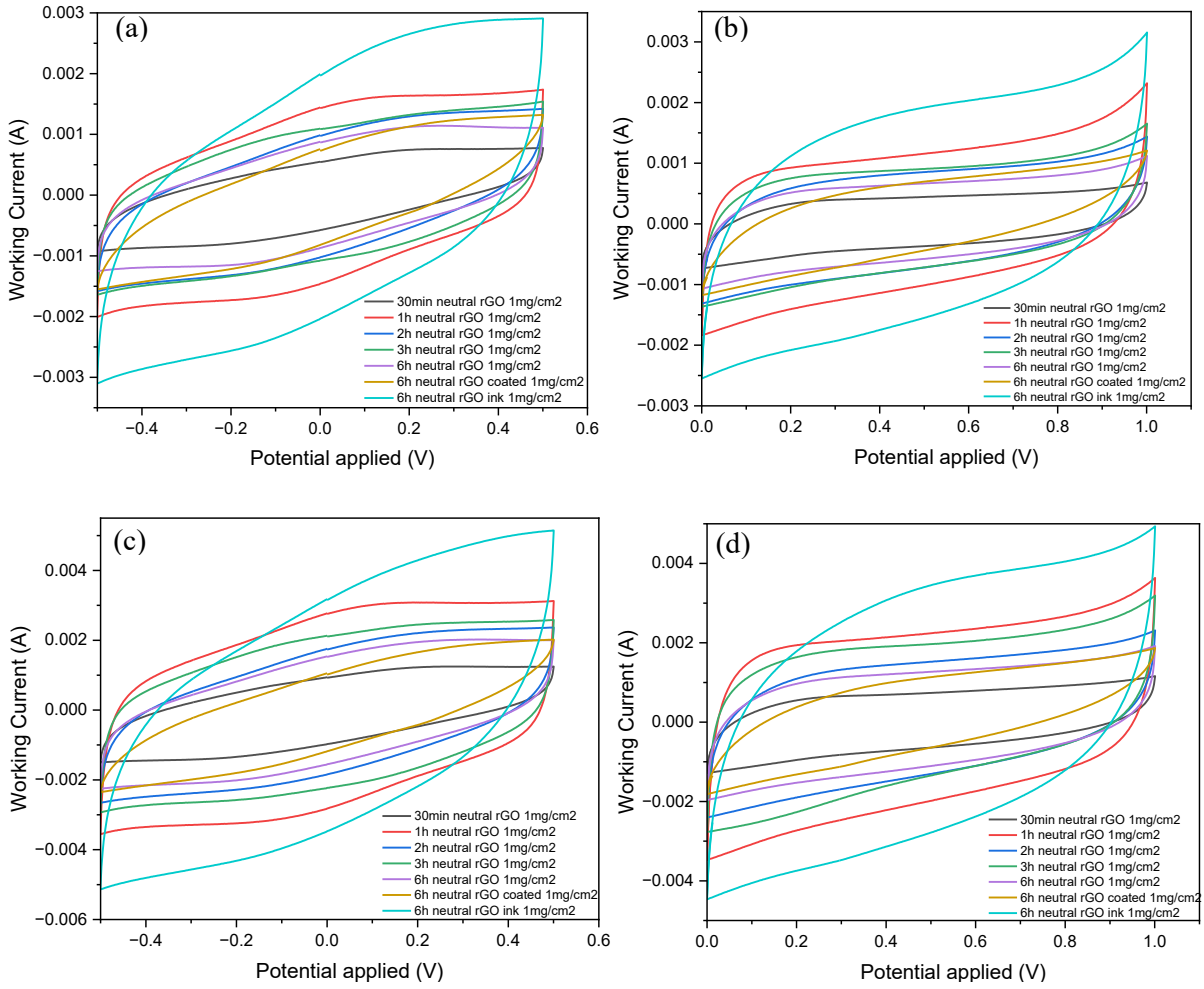

Figure. S28. Comparison of CVs of 009 rGO on graphite reduced for different time periods a) 50 mV/s, -0.5 to +0.5 V b) 50 mV/s, 0 to 1 V c) 100 mV/s, -0.5 to +0.5 V d) 100 mV/s, 0 to 1 V

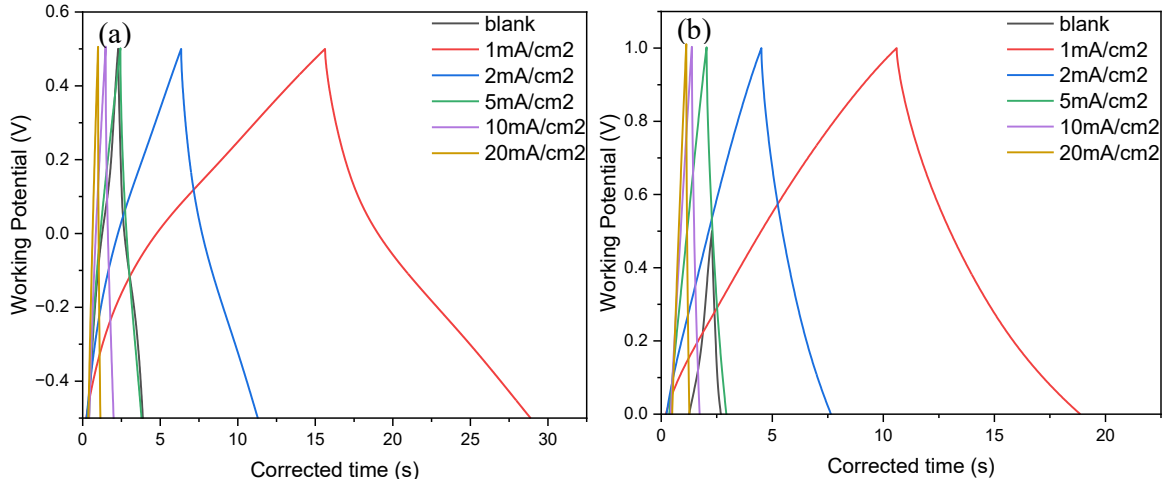

Figure. S29. GCDs at different current densities for 009 rGO on graphite (30 min reduced): a) -0.5 to +0.5 V b) 0 to 1 V

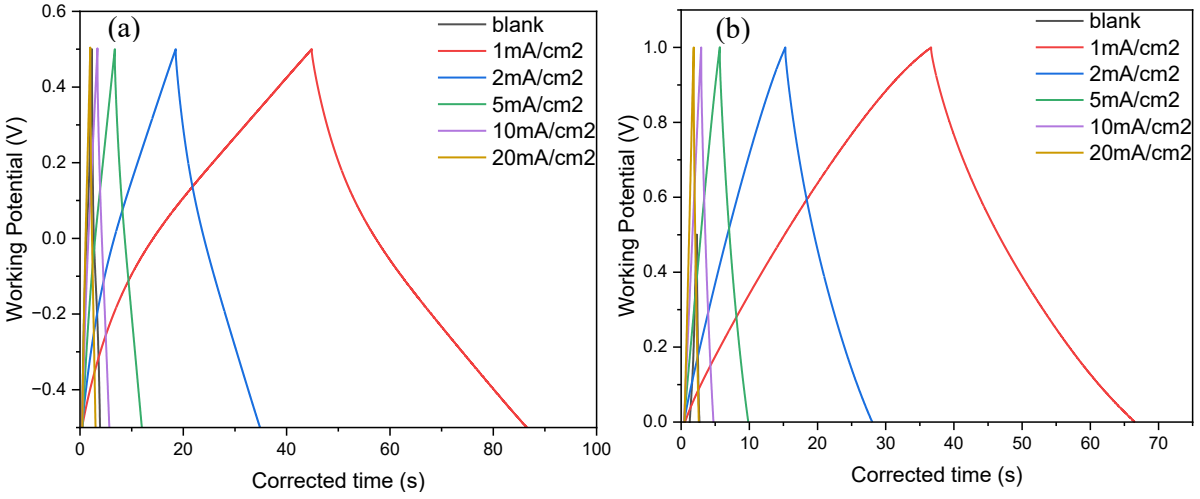

Figure. S30. GCDs at different current densities for 009 rGO on graphite (1 h reduced): a) -0.5 to +0.5 V b) 0 to 1 V

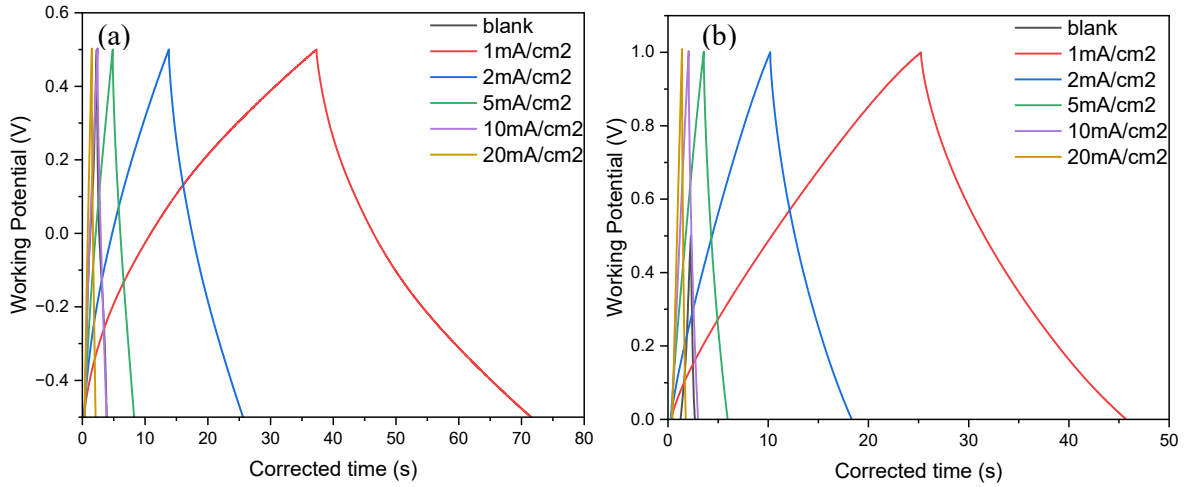

Figure. S31. GCDs at different current densities for 009 rGO on graphite (2 h reduced): a) -0.5 to +0.5 V b) 0 to 1 V

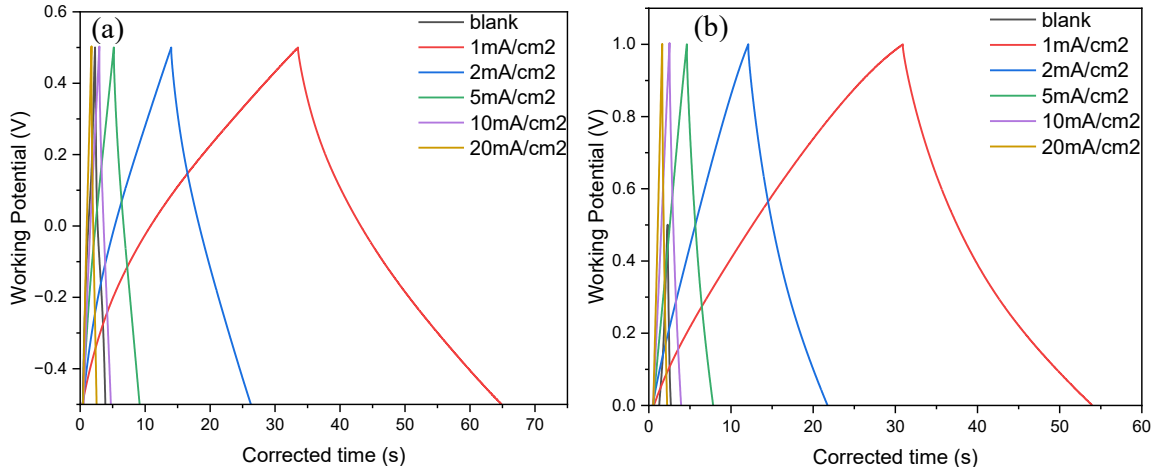

Figure. S32. GCDs at different current densities for 009 rGO on graphite (3 h reduced): a) -0.5 to +0.5 V b) 0 to 1 V

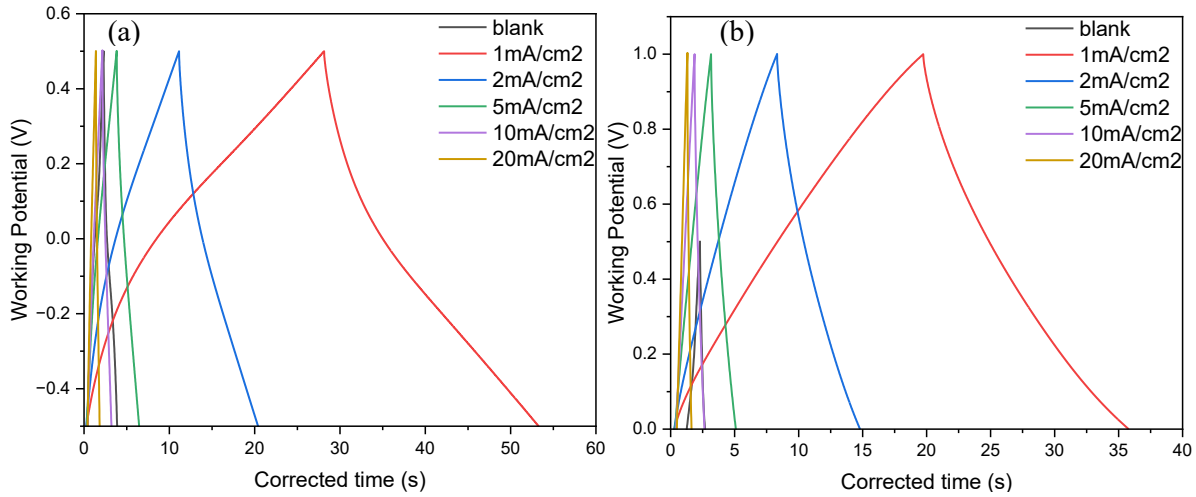

Figure. S33. GCDs at different current densities for 009 rGO on graphite (6 h reduced): a) -0.5 to +0.5 V b) 0 to 1 V

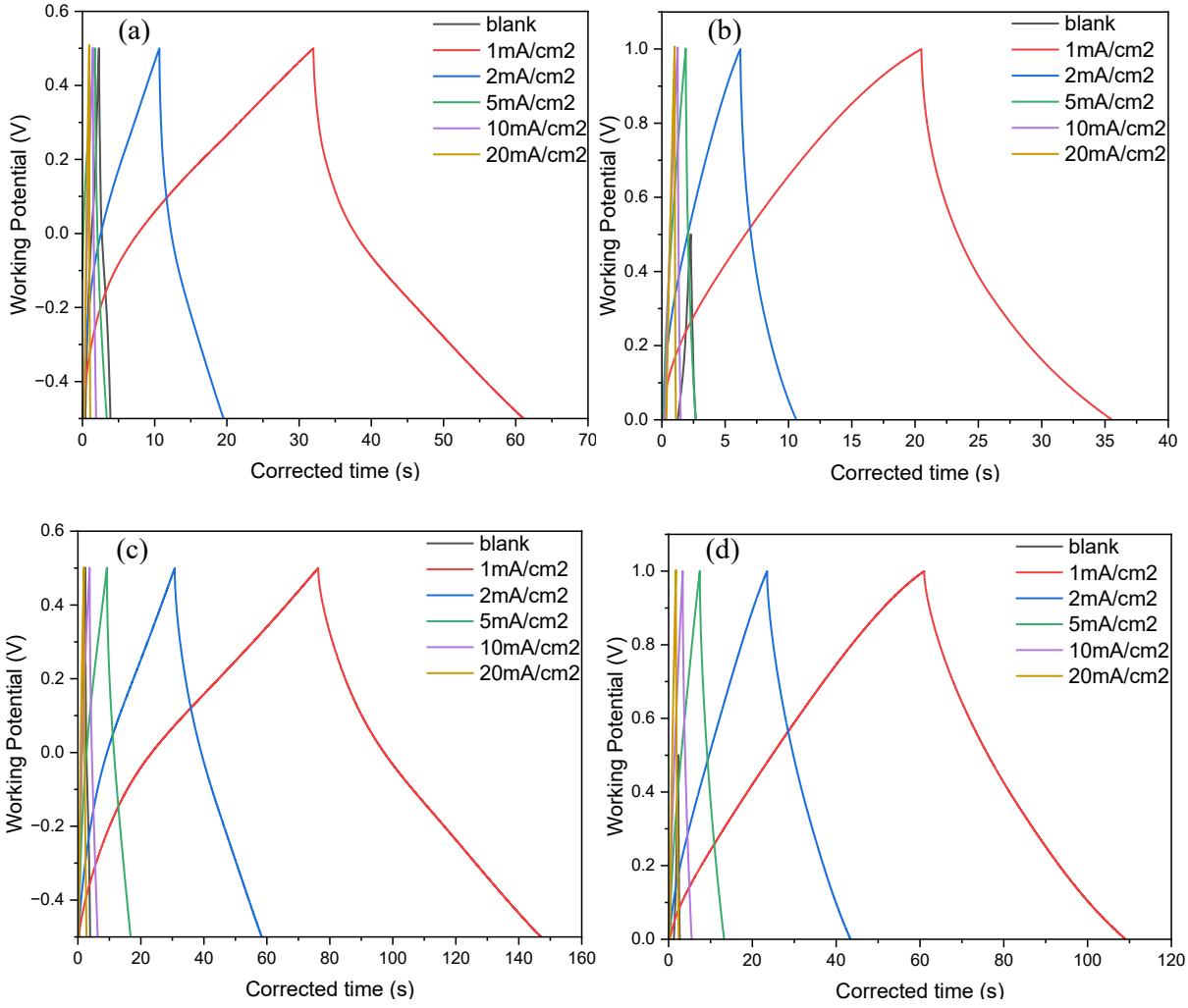

Figure. S34. GCDs at different current densities for 009 rGO on graphite (6 h reduced): Nafion covering a) -0.5 to +0.5 V b) 0 to 1 V; Nafion ink c) -0.5 to +0.5 V d) 0 to 1 V

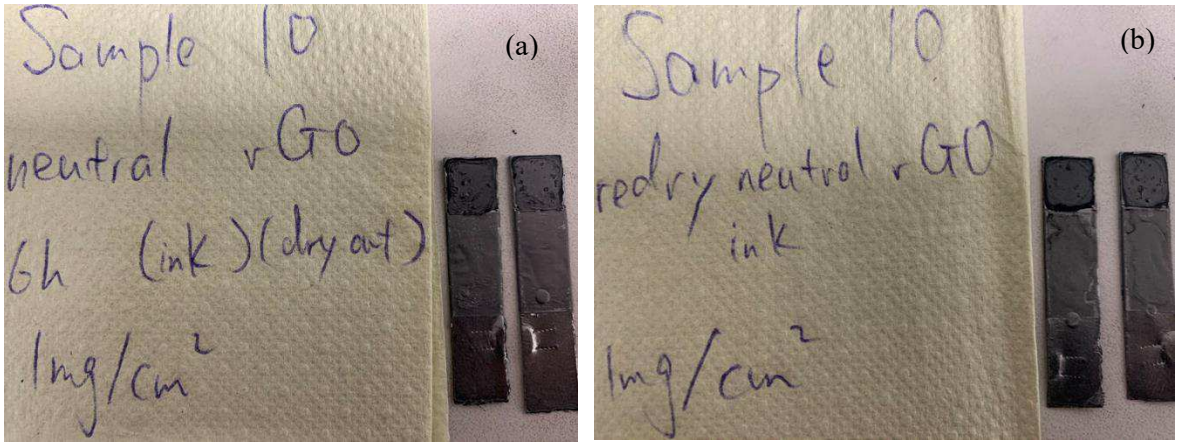

Figure. S35. 6h reduced 010 rGO on graphite a) RT dried b) Oven dried at 120 °C 1h (a, b, have Nafion ink)

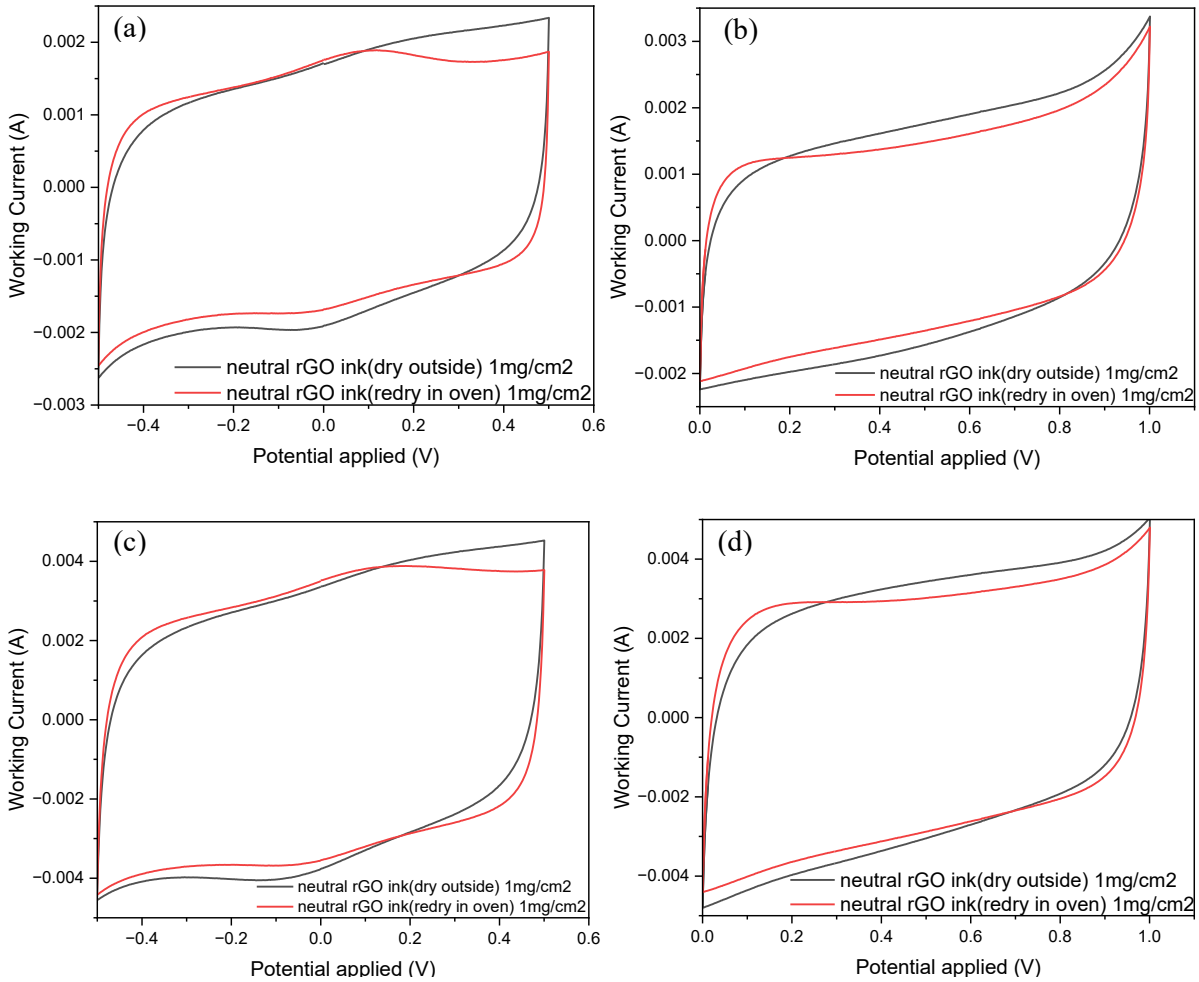

Figure. S36. Comparison of CVs of 6h reduced 010 rGO on graphite/Nafion ink (RT & Oven dried) a) 50 mV/s, -0.5 to +0.5 V b) 50 mV/s, 0 to 1 V c) 100 mV/s, -0.5 to +0.5 V d) 100 mV/s, 0 to 1 V

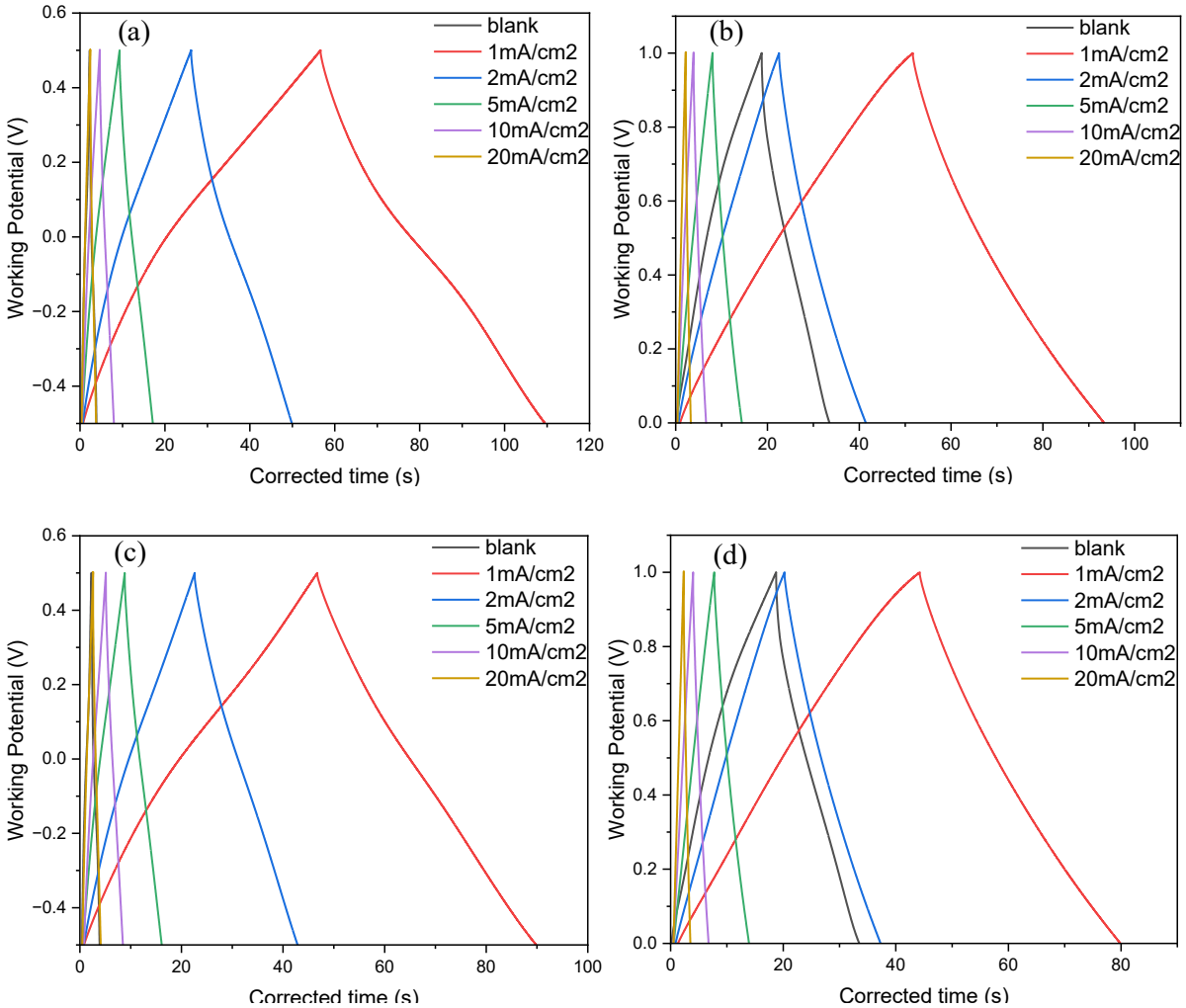

Figure. S37. GCDs at different current densities for 6h reduced 010 rGO on graphite / Nafion ink: RT dried a) -0.5 to +0.5 V b) 0 to 1 V; Oven dried c) -0.5 to +0.5 V d) 0 to 1 V

Comparison of electrochemical performance of synthesized rGOs (CV)

All rGO samples (001-010) were investigated for their electrochemical response under cyclic voltammetric (CV) conditions. This way, the conducting behaviors of plain rGOs can be checked first.

Based on the area under the curve (current density) from CV graphs, the capacitance behavior of the rGO samples can be understood. Table S3 shows the area values of all rGO samples in comparison.

rGO sample IDs	**50 mV/s -0.5 V to 0.5 V ($\times 10^{-3}$ mA.cm^{-2})**	**50 mV/s 0 V to 1 V ($\times 10^{-3}$ mA.cm^{-2})**	**100 mV/s -0.5 V to 0.5 V ($\times 10^{-3}$ mA.cm^{-2})**	**100 mV/s 0 V to 1 V ($\times 10^{-3}$ mA.cm^{-2})**
Blank	1.57	1.20	2.17	1.87
002	4.68	4.75	8.79	7.88
004	4.91	4.39	9.29	8.27
005	4.23	4.04	8.41	7.99
006	3.27	3.15	6.55	6.37
007	4.31	3.83	8.06	7.16
008	4.70	4.09	8.74	7.53
008 (oven)	4.73	4.14	8.65	7.53
009 1 h	2.38	2.09	4.65	4.07
009 6 h	3.34	2.95	5.52	5.24
010 ink	3.21	3.07	6.31	5.97
010 ink (redried)	3.04	2.80	6.26	5.74

Table S3. Area under the curve (current density) in CV for all rGO samples

Scan rate Scan range	Order of rGO sample IDs in terms of high to low current densities
50 mV/s -0.5 V to +0.5 V	004 > 008O > 008 > 002 > 007 > 005 > 009(6h) > 006> 010(6h) > 010(redried) > 009 > blank
50 mV/s 0 V to 1 V	002 > 004 > 008O > 008 > 005 > 007 > 006 > 010(6h) > 009(6h) > 010(redried) > 009 > blank
100 mV/s -0.5 V to +0.5 V	004 > 002 > 008 > 008O > 005 > 007 > 006 > 010(6h) > 010(redried) > 009(6h) > 009 > blank
100 mV/s 0 V to 1 V	004 > 002 > 008 > 008O > 005 > 007 > 006 > 010(6h) > 010(redried) > 009(6h) > 009 > blank

Table S4. Order of rGO sample IDs in terms of high to low current densities

Table S4 shows the order of rGO sample IDs in terms of high to low current densities (left to right). The bank graphite flakes' electrodes showed a very feeble current response than the rGO modified electrodes. This table shows a trend similar to what we saw in UV-Vis absorbance intensities. rGO samples 002, 004, 005, 006, 007, and 008 (1- 3h) have shown higher current densities than samples 009, and 010 (6h) comparatively, reiterating the fact that the longer reduction time could result in poor quality of rGO in terms of particles sizes, hence the current response was poor. However, in sample 009, the 6 h sample showed a better current response than the 1 h sample contrary to the UV-Vis absorbance trend.

Comparison of electrochemical performance of synthesized rGO: CNF composites (CV)

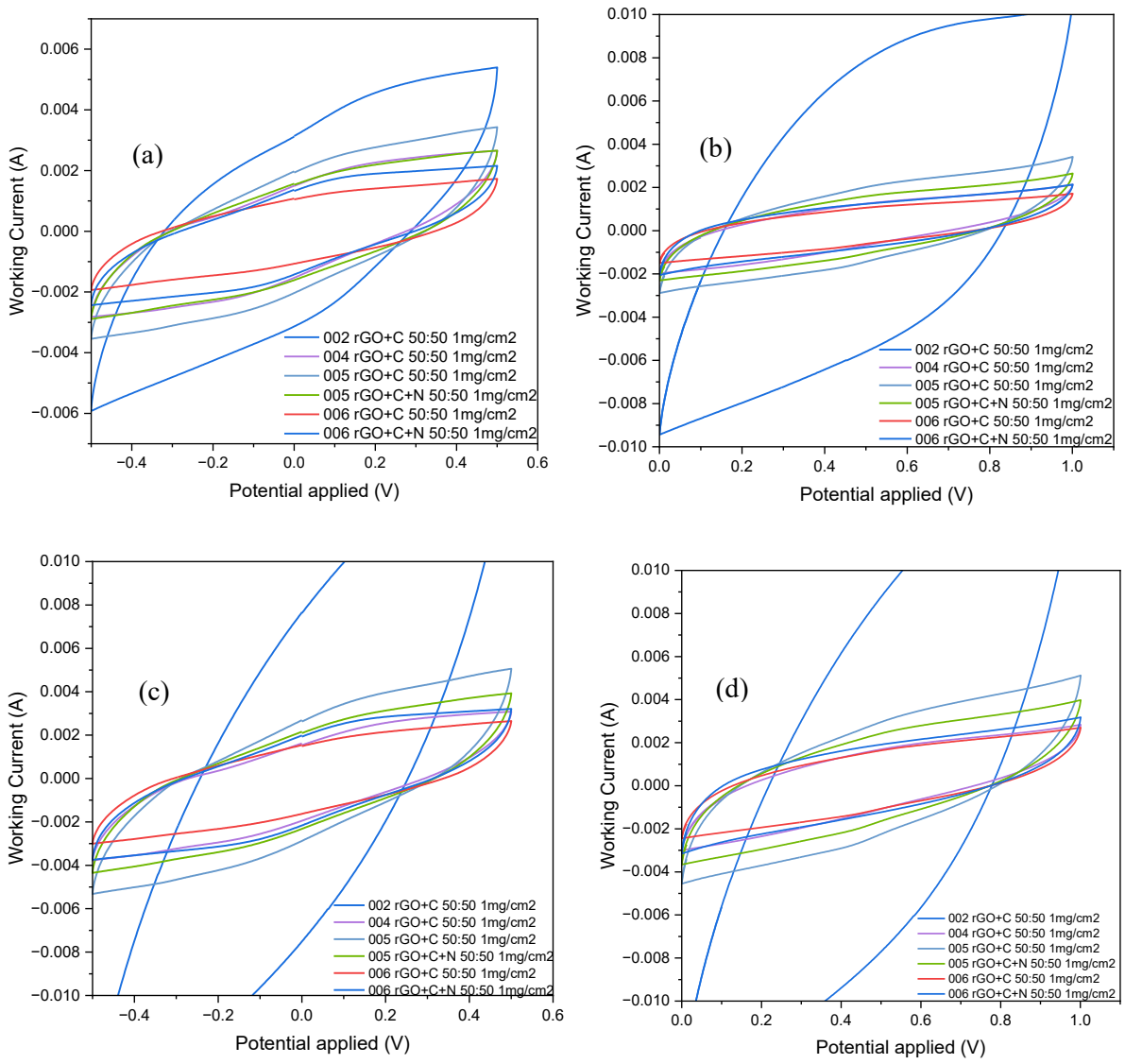

Figure. S38. Cyclic voltammograms of rGO: CNF 50:50 a) 50 mV/s, -0.5 to +0.5 V b) 50 mV/s, 0 to 1 V c) 100 mV/s, -0.5 to +0.5 V d) 100 mV/s, 0 to 1 V

rGO: CNF (50:50) composite sample IDs	50mV/s -0.5 V to 0.5 V ($\times 10^{-3}$ mA.cm^{-2})	50mV/s 0 V to 1 V ($\times 10^{-3}$ mA.cm^{-2})	100mV/s -0.5 V to 0.5 V ($\times 10^{-3}$ mA.cm^{-2})	100mV/s 0 V to 1 V ($\times 10^{-3}$ mA.cm^{-2})
002	4.87	10.05	11.16	12.23
004	2.35	1.57	2.78	2.27
005	3.10	2.72	4.35	4.15
005	2.45	2.11	3.50	3.24
006 cover	1.69	1.39	2.51	2.20
006 ink	2.05	1.69	3.14	2.63

Table. S5. Area under the curve (current density) in CV for all rGO: CNF 50:50 samples

Scan rate Scan range	Order of rGO: CNF 50:50 sample IDs in terms of high to low current densities
50 mV/s -0.5 V to +0.5 V	002>005>005N>004>006N>006
50 mV/s 0 V to 1 V	002>005>005N>006N>004>006
100 mV/s -0.5 V to +0.5 V	002>005>005N>006N>004>006
100 mV/s 0 V to 1 V	002>005>005N>006N>004>006

Table. S6. Order of rGO: CNF (50:50) composite sample IDs in terms of high to low current densities

Table S5 shows the area under the curve (current density) in CV (Fig. S38) for selected rGO: CNF 50:50 composite samples. Table S6 shows the order of selected rGO: CNF 50:50 composite samples in terms of high to low current densities (left to right). As we infer from Table S6, these selected composites were prepared from the best rGO samples (002, 004, 005, 006).

The above trend reflects that the rGO: CNF 50:50 composite made from rGO sample 002 was the most active followed by samples 005, 006, 004. The reason might be the longer sonication

time applied for composite 002, before drop casting on Grafoil sheets. The was caused by an accidental delay that the composite was sonicated for 1 hour and then left undisturbed for overnight. The next day, the composite hydrogel looked like inhomogeneous lumps due to phase separation between rGO and cellulose, hence it was sonicated again for another hour before drop casting.

Here, in 006N, N refers to 'Composite + Nafion mixed thoroughly as an ink' that the drop-casted on the electrode as against usual 'Composite drop casting followed by Nafion addition at the end as a covering'. With sample 006, Nafion ink proved to improve the performance, whereas in sample 005 it was the other way around. This suggests that if the rGO particle size is smaller enough (as in sample 005), Nafion ink procedure is not required.

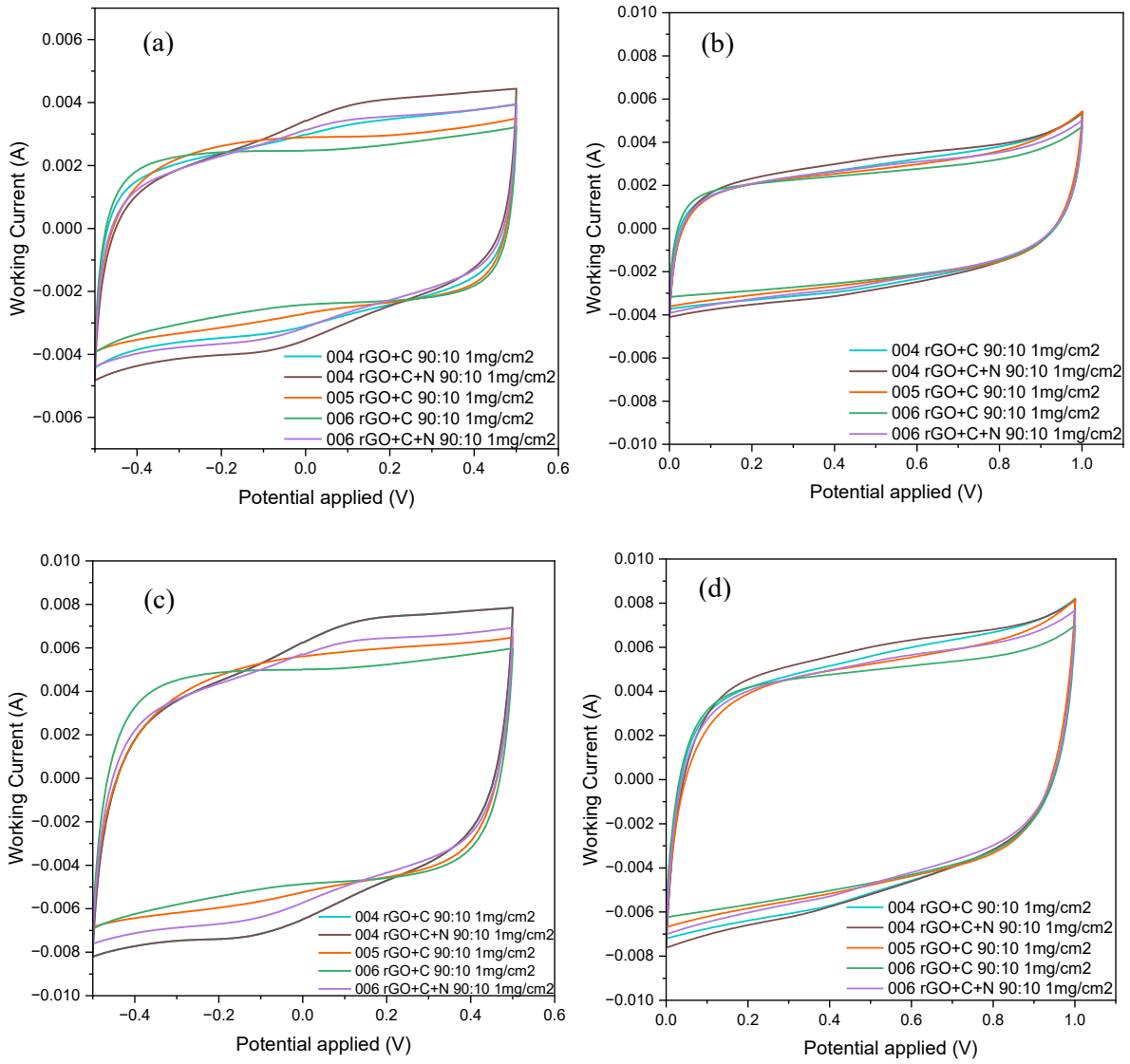

Figure. S39. Cyclic voltammograms of rGO: CNF 50:50 a) 50 mV/s, -0.5 to +0.5 V b) 50 mV/s, 0 to 1 V c) 100 mV/s, -0.5 to +0.5 V d) 100 mV/s, 0 to 1 V

rGO: CNF (90:10) composite sample IDs	50mV/s -0.5 V to 0.5 V ($\times 10^{-3}$ mA.cm^{-2})	50mV/s 0 V to 1 V ($\times 10^{-3}$ mA.cm^{-2})	100mV/s -0.5 V to 0.5 V ($\times 10^{-3}$ mA.cm^{-2})	100mV/s 0 V to 1 V ($\times 10^{-3}$ mA.cm^{-2})
004 1h composite	5.53	5.14	10.85	9.72
004 1h ink	5.99	5.46	10.85	9.99
005 1h composite	5.13	4.85	9.51	9.02
006 1h composite	4.84	4.59	9.29	8.77
006 1h ink	5.49	4.95	9.98	9.09

Table. S7. Area under the curve (current density) in CV for all rGO: CNF 90:10 samples

Scan rate Scan range	Order of rGO: CNF 90:10 sample IDs in terms of high to low current densities
50 mV/s -0.5 V to +0.5 V	004N>004>006N>005>006
50 mV/s 0 V to 1 V	004N>004>006N>005>006
100 mV/s -0.5 V to +0.5 V	004N>004>006N>005>006
100 mV/s 0 V to 1 V	004N>004>006N>005>006

Table. S8. Order of rGO: CNF (90:10) composite sample IDs in terms of high to low current densities

Table S7 shows the area under the curve (current density) in CV (Fig. S39) for selected rGO: CNF 90:10 composite samples. Table. S8 shows the order of selected rGO: CNF 90:10 composite samples in terms of high to low current densities (left to right). As we infer from the Table. S8, these selected composites were prepared from the best rGO samples (004, 005, 006). The above trend reflects that the rGO: CNF 90:10 composite, made from rGO sample 004 was most active followed by rGO samples 006, 005. Here, 004N, and 006N, both composite samples proved that Nafion ink procedure was advantageous as they were more active than composite samples 004, and 006 which have Nafion covering after the drop casting.

REFERENCES

1. What is the difference between graphene oxide and reduced graphene oxide https://nanografi.com/blog/what-is-the-difference-between-graphene-oxide-and-reduced-graphene-oxide/

2. Mousavi, S. M., Hashemi, S. A., Kalashgrani, M. Y., Gholami, A., Binazadeh, M., Chiang, W. H., & Rahman, M. M. Recent advances in energy storage with graphene oxide-for supercapacitor technology. Sustainable Energy & Fuels, 2023, 7, 5176-5197.

3. Moud, A. A. Advanced cellulose nanocrystals (CNC) and cellulose nanofibrils (CNF) aerogels: Bottom-up assembly perspective for production of adsorbents. International Journal of Biological Macromolecules, 2022, 222, 1-29.

4. Xu, W., Xin, B., & Yang, X. Carbonization of electrospun polyacrylonitrile (PAN)/cellulose nanofibril (CNF) hybrid membranes and its mechanism. Cellulose, 2020, 27, 3789-3804.

5. Wang, Z., Tammela, P., Strømme, M., & Nyholm, L. Cellulose-based supercapacitors: material and performance considerations. Advanced Energy Materials, 2017, 7(18), 1700130.

6. Sun, Z., Qu, K., You, Y., Huang, Z., Liu, S., Li, J., Hu, Q., & Guo, Z. Overview of cellulose-based flexible materials for supercapacitors. Journal of Materials Chemistry A, 2021, 9(12), 6989-7008

7. Zhang, L. L., Zhao, X. S., & Wu, J. Graphene-based materials as supercapacitor electrodes. Journal of Materials Chemistry, 2010, 20(30), 5983-5992

8. Chen, Y., Pötschke, P., Pionteck, J., Voit, B., & Qi, H. Aerogels Based on Reduced Graphene Oxide/Cellulose Composites: Preparation and Vapour Sensing Abilities. Nanomaterials, 2020, 10(9), 1729

9. Wang, H., Hao, Q., Yang, X., Lu, L., & Wang, X. Graphene oxide doped polyaniline for supercapacitors. Electrochimica Acta, 2012, 74, 245-251

10. Li, Y., Zhao, Y., Cheng, H., Hu, Y., Shi, G., Dai, L., & Qu, L. Nitrogen-doped graphene and its application in electrochemical biosensing. ACS Nano, 2012, 6(10), 8904-8913

11. Energy storage technologies: Supercapacitors. FOM TECHNOLOGY. https://www.fomtechnologies.com/insights-blog/energy-storage-technologies-supercapacitors

12. Pandolfo, A. G., & Hollenkamp, A. F. Carbon properties and their role in supercapacitors. Journal of Power Sources, 157(1), 2006, 11-27

13. O'Mullane A.P., Reference Module in Chemistry, Molecular Science and Chemical Engineering. Electrochemistry, 2013.

14. Bard, A. J., & Faulkner, L. R. Electrochemical methods: fundamentals and applications. John Wiley & Sons, 2001.

15. Pandolfo, A. G., & Hollenkamp, A. F. Carbon properties and their role in supercapacitors. Journal of Power Sources, 2006, 157(1), 11-27

16. Shukla, S. K., Joshi, G. M., & Hussain, C. M. (Eds.). Functionalized nanomaterials based devices for environmental applications. Elsevier, 2021, 199-218.

17. Wang, G., Zhang, L., & Zhang, J. A review of electrode materials for electrochemical supercapacitors. Chemical Society Reviews, 2012, 41(2), 797-828